Identification of Molecular Targets Specific to Pediatric Astrocytomas

Takrima Haque, BSc, MSc.

Supervisor
Dr. Nada Jabado

April 2012
McGill University
Montreal, Quebec, Canada

A thesis submitted to McGill in partial fulfillment of the requirements of the degree of Doctor of Philosophy

Abstract

Brain tumours are currently the leading cause of cancer related mortality and morbidity in the pediatric years and astrocytomas are the most common type of central nervous system tumours. High grade astrocytomas in children are rare; however, they have a high rate of morbidity and mortality. Our first focus was to identify gene expression profiles specific to grade IV pediatric astrocytomas also known as glioblastomas (GBM). We demonstrated that pGBM is distinct from adult GBM in their gene expression profile and also showed that there are at least two subsets of pGBM that can be distinguished based on their association or lack of association with an aberrantly active Ras and Akt pathway in a sample. These results were further confirmed using an independent data set consisting of formalin-fixed paraffin embedded (FFPE) pGBM samples. We further aimed to characterize whether grade III and IV pediatric astrocytomas had distinct gene expression profiles. Our results indicate that Grade III astrocytomas have unique gene expression signatures when compared to pGBM, including upregulation of the mTOR pathway, which was found to be the most differentially regulated between the two tumour grades. Analysis of our microarray results to identify genes differentially regulated specifically in pGBM and accounting for gliomagenesis led us to focus on sorting nexin 3 (SNX3), a protein involved in endosomal trafficking, based on its role in modulating EGFR, Ras and PI3K/Akt activation; which are major targets and signaling pathways in GBM. We showed that SNX3 is upregulated specifically in primary GBM tumours, and that this upregulation correlates with increased EGFR and MET expression in samples. Overexpression of SNX3 in pGBM cell lines, delayed EGFR degradation, sustained EGFR and MET signaling, increased cell proliferation, and induced tumorigenesis *in vivo*. Our work indicate that there are specific targets in gliomagenesis in children and identify the mTOR pathway and deregulation of endosomal recycling as potential drivers of gliomagenesis in respectively pediatric grade III and IV astrocytomas.

RESUME

Les tumeurs cérébrales sont actuellement la principale cause de mortalité et de morbidité liée au cancer chez l'enfant. Parmi elles, les astrocytomes sont le type de tumeur le plus fréquent. Les astrocytomes de haut grade sont rares à l'âge pédiatrique, avec cependant, un taux de morbidité et de mortalité particulièrement élevé. Durant ma thèse, le principal objectif a initialement été d'identifier les profils d'expression génétique spécifiques aux astrocytomes de grade IV ou glioblastomes pédiatriques (pGBM). Nous avons montré que les pGBM diffèrent des GBM adultes par leur profil d'expression génique et nous avons également identifié deux sous-ensembles de pGBM, distincts par l'activation ou non des voies de signalisation Ras et Akt. Ces résultats ont été validés sur un échantillon indépendant de pGBM fixés dans du formol et inclus dans la paraffine. Cette thèse a eu également pour but de caractériser les profils d'expression génique des astrocytomes pédiatriques de grade III et IV. L'analyse des données obtenues par microarray a identifié une signature unique aux astrocytomes de grade III par rapport aux pGBM, notamment par une suractivation de la voie mTOR. . Parmi les gènes spécifiquement dérégulés dans le groupe des pGBM, nous avons identifié Sorting Nexin 3 (SNX3) comme potentiellement impliqué dans l'oncogénèse des pGBM avec une activation des voies Ras et Akt. SNX3 est une protéine jouant un rôle dans le trafic endosomal des plusieurs récepteurs membranaires, dont EGFR. Par immunohistochimie, nous avons confirmé la surexpression de SNX3 et sa corrélation avec celle de récepteur tyrosine kinases telles que EGFR et MET. *In vitro*, la surexpression de SNX3 dans des lignées cellulaires de GBM entraine un retard de la dégradation d'EGFR, augmentant la signalisation de la voie Ras. Les cellules acquièrent ainsi un avantage de prolifération *in vitro* et de tumorigenèse *in vivo*. Nos travaux ont identifié de nouvelles cibles potentielles impliquées dans l'oncogenèse de ces tumeurs, telles que la voie mTOR dans les astrocytomes de grade III et SNX3 et la dérégulation du trafic endosomal dans les pGBM.

Acknowledgments

First of all I would like to thank my supervisor, **Dr. Nada Jabado**, for her patience, supervision and all the knowledge she gave me throughout the years. I would like to thank my committee members, Dr. Janusz Rak, Dr. Peter Seigel, and Dr. Cindy Goodyer for all their valuable time, support and input throughout all my committee meetings. I would also thank Andre Nantel for all the help with microarray analysis and Stephen Albrecht for the time he spent in classification of tumors.

I would like to thank all my lab members who have made this a very memorable and enjoyable journey. These long years would not have been so pleasant without Damien Faury, Karine Jacob, Caroline Sollier, Dong Anh Khuong Quang, Noha Gerges, Xiaoyang Liu, Margret Shirinian, and Adam Fontebasso.

I would like to thank all the staff and people in Place Toulon who have been very generous throughout my PhD.

I wouldn't be able to come this far without the support of my family. To my two children, despite keeping my very busy, thank you for allowing me to forget my PhD stress at the end of each day. I would like thank my husband for bearing with me through this long journey. Most of all I want to thank my Mom, whom I would like to dedicate this thesis to, for the all the unconditional love and support she gave me throughout all these years.

Table of Contents

List of Figures

CHAPTER 1

CHAPTER 2

CHAPTER 3

CHAPTER 4

CHAPTER 5

List of Tables

List of Abbreviations

AA	Anaplastic Astrocytoma
aGBM	Adult Glioblastoma
CB	Control Brain
CDK	Cyclin-Dependent Kinase
EEA1	Early Endosomal Marker
EGF	Epidermal Growth Factor
EGFR	Epidermal Growth Factor Receptor
EGF-Rh	Rhodamine tagged EGF
EV	Empty Vector
FF	Fresh Frozen
FFPE	Formalin Fixed Paraffin-Embedded
GBM	Glioblastoma
GFAP	Glial Fibrillary Acidic Protein
GO	Gene Ontology
HGA	High Grade Astrocytoma
HGF	Hepatocyte Growth Factor
HGG	High Grade Gliomas
IDH	Isocitrate Dehydrogenase
LAMP	Late Endosomal Marker
LCM	Laser Capture Microdissection
MAPK	Mitogen Activated Kinase
mTOR	Mammalian Target of Rapamycin
MVB	Multivesicular Body
PCA	Principal Component Analysis
PDGF	Platelet-derived Growth Factor
PDGFR	Platelet-derived Growth Factor Receptor
pGBM	Pediatric Glioblastoma
PI3K	Phosphoinositide 3'-kinase
PIP_2	Phosporylatidylinositol-4,5-biphosphate
PIP_3	Phosporylatidylinositol-3,4,5-triphosphate
PTEN	Phosphatease and Tensin Homology
PX	Phox Homology
Rb	Retinablastoma Protein
RTK	Receptor Tyrosine Kinase
SCID	Severe Combined Immunodeficiency
SNX	Sorting Nexin
SNX3	Sorting Nexin 3
TfR	Transferrin Receptor
TGFα	Transforming Growth Factor α
TMA	Tissue Microarray
VEGFR	Vascular Endothelial Growth Factor Receptor
WHO	World Health Organization
YB-1	Y-Box Binding Protein 1

Contributions of Authors

Chapter 2: Molecular Profiling Identifies Prognostic Subgroups of Pediatric Glioblastoma and Shows Increased YB-1 Expression in Tumors. (Published manuscript)
J Clin Oncol, 2007. 25(10): p. 1196-208

Damien Faury, André Nantel, Sandra E Dunn**,** Marie-Christine Guiot, **Takrima Haque**, Péter Hauser, Miklós Garami, László Bognár, Zoltán Hanzély, Pawel P. Liberski, Enrique Lopez-Aguilar, Elvis T. Valera, Luis G. Tone, Anne-Sophie Carret, Rolando F. Del Maestro, Martin Gleave **,** Jose-Luis Montes **,** Torsten Pietsch**,** Stephen Albrecht, and Nada Jabado

Damien Faury performed most of the experimental procedures. The candidate aided in the experiments and sample preparations. Andre Nantel did the microarray analysis. Marie-Christine Guiot did the immunohistochemical procedures. Stephen Albrecht classified the tumors. Nada Jabado was responsible for the study design

Chapter 3: Gene expression profiling from formalin-fixed paraffin embedded tumors of pediatric glioblastoma (Published manuscript)
Clin Cancer Res 13(21): 6284-6292

Takrima Haque, Damien Faury, Steffen Albrecht, Enrique Lopez-Aguilar, Péter Hauser, Miklós Garami, Zoltán Hanzély, László Bognár, Rolando F Del Maestro, Jeffrey Atkinson, Andre Nantel, Nada Jabado

The candidate was responsible for most of the experimental procedures and analysis. Damien Faury aided in the experiments. Andre Nantel did the microarray analysis. Stephen Albrecht classified the tumors. Nada Jabado was responsible for the study design.

Chapter 4: Pediatric grade III anaplastic astrocytomas are distinct from pediatric Grade IV glioblastomas (Manuscript in preparation)

Takrima Haque and Noha Gerges, Damien Faury, Andre Nantel, Nada Jabado

The candidate and Noha Gerges did experimental analysis. Damien Faury did the microarrays. Andre Nantel did the Microarray analysis. Nada Jabado was responsible for the study design.

Chapter 5: Determination of the Role of SNX3 in the endosomal trafficking of Receptor Tyrosine Kinases (RTKs) including the Epidermal Growth Factor Receptor (EGFR). (Manuscript in preparation)

Takrima Haque, Dongh-Anh Khuong-Quang, Damien Faury, Brian Meehan, Janusz Rak, Cynthia Hawkins, Nada Jabado

The candidate did most of the experimental procedures. Dongh-Anh Khuong-Quang with the collaboration of Brian Meehan and Janusz Rak was responsible for the mice work. She was also responsible for results with U251 and U87 cell lines. Damien Faury also aided in the mouse work. Cynthia Hawkins did the tissue microarrays. Nada Jabado was responsible for the study design.

Chapter 1

Introduction

1.1 Astrocytomas: General introduction and brief background on the distinct nature of pediatric astrocytoma

Brain tumors are the leading cause of cancer-related mortality and morbidity in the pediatric years [1-4]. Pediatric astrocytomas account for 50% of all brain tumors. Because of the similar histology, current treatments in children are driven by adult studies and as in adults, with little therapeutic success, but potentially for very different reasons. The impediment to treatment is the invasive capacity of astrocytomas within the brain and their inherent resistance to adjuvant therapies. In addition, permanent damage inflicted to a developing brain by current life-saving therapies severely impacts the quality of life of surviving children [5-8]. Consequently, an improved understanding to identify relevant therapeutic targets is essential as little is known about molecular mechanisms underlying their development.

Astrocytomas grading and clinical considerations in pediatric astrocytoma:

The World Health Organization (WHO) grading system classifies gliomas according to their predominant line of differentiation. Astrocytomas possibly arise from the astrocytic lineage, the most abundant of all glial cells and are commonly regrouped into low-grade (WHO grade I and II) or high-grade (WHO grade III or anaplastic astrocytoma and IV or glioblastoma (GBM)) tumors. Low grade tumours are less aggressive and more responsive to treatment than high grade tumours. Anaplastic astrocytomas (AA) and GBM share similar morphological characteristics; however, GBMs show more microvascular proliferation and necrosis. The frequency, anatomic

location, progression mode and pathologic spectrum of astrocytomas differ in children and in adults. This is of importance as the cell of origin, the microenvironment and chromatin conformation will differ based on age, cell type, and anatomical localization and may be relevant in pathogenesis. Astrocytomas are highly invasive and infiltrate nearby tissue making complete surgical removal difficult and leading to relapse in most cases. Grade IV tumors (GBM, highest grade and the most biologically aggressive form of cancer) account for up to 15% of all brain tumors in children, and close to 90% of them die within 2 years of diagnosis [2, 9, 10]. Grade II and III astrocytomas are rare in children (less than 5%) and grade I (pilocytic astrocytomas) account for 23% of all brain tumors and constitute a contrasting biological and therapeutic paradigm. Tumor grade, age at diagnosis, and degree of surgical resection are regarded as the most important prognostic factors for astrocytomas across the lifespan [9, 11, 12], but a deeper molecular understanding of the disease has already begun changing this perspective.

Pediatric and adult GBM – the molecular landscape:

GBM are the most common central nervous system (CNS) tumours in adults and are generally associated with a poor prognosis. The life expectancy for adult GBM is ~12 months, for patients with AA ~3 years, and for patients with grade II > 5 years. Although substantial information is available on adult GBM, little is known about the cytogenic and molecular changes in their pediatric counterpart. Presently, the therapeutic options available for pediatric GBM are based on knowledge acquired through studies on adult GBM. As advances are made in new genomic tools, a better understanding of pediatric tumours is revealed every year [13, 14].

1.2. Adult GBM

According to the literature and findings from our lab, there are significant molecular differences between pediatric and adult GBM. The presence of unique oncogenesis pathways is seen in the pediatric setting [15, 16]. Some of the differences among the two high grades, adult and pediatric astrocytomas are outlined in **table 1.1.**

1.2.1 Molecular pathways affected in adult GBM

GBMs are one of the most aggressive forms of human cancer. Tumors usually do not respond to chemotherapy or radiotherapy. In adults, they occur as *de novo* tumors (primary GBM) or from a progression of a lower grade glioma (secondary GBM). Primary and secondary GBMs are clinically and morphologically indistinguishable; however increasing evidence shows different genetic alterations between the two types that will be further detailed herein. Secondary GBMs are less frequent accounting for around 10% of all adult GBMs. Also the median age of patients developing secondary GBMs is lower (~45 years old) than that of primary GBMs (~60 years). Most patients with primary GBMs have a clinical history of less than 3 months. In secondary GBMs, progression from grade 3 astrocytomas occurs after ~2 years and from grade II tumours after ~5years [17-19].

1.2.2 Genetic alterations identified in Primary and Secondary GBM

Primary GBMs are often characterized by loss of heterozygosity of 10q in 70% of cases, EGFR amplification in 36% of the patients, PTEN mutations in about 25%, and $p16^{ink4a}$ deletion in 31% of cases. These genetic alterations are less frequent in secondary GBMs. Mutations/deletions in TP53, a tumor suppressor gene, are commonly found in secondary GBMs

and less in primary GBMs. However, in primary GBMs MDM2 is often overexpressed or amplified which targets p53 for ubiquitin-mediated degradation [1, 20]. P53 mutations occur early in the progression of astrocytomas and loss or mutations of PTEN and amplification of EGFR are characteristic of higher grade tumors. Recently, recurrent somatic mutations of isocitrate dehydrogenase 1(IDH1) and its related gene, IDH2 were identified in approximately 12% of all grade IV gliomas, and were preponderant secondary GBM where they were present in the vast majority of samples (~90%). These mutations were shown to be present in at the start of gliomagenesis in lower-grade gliomas (astrocytomas and oligodendrogliomas) and were identified in the majority of grade II (~70%) and III (80%) gliomas. These mutations are rare in primary GBMs. Importantly, patients with mutations in IDH1 and its related gene, IDH2 have a better outcome than those who are wild-type for IDH genes. It was also found that most of the patients with anaplastic astrocytomas with IDH1 or IDH2 mutations also had a TP53 mutation. However, PTEN, EGFR, or CDKN2A/CDKN2B alterations were rare in these tumors. On the other hand, patients with wild type IDH1/2 had fewer TP53 alterations and showed very frequent PTEN, EGFR, or CDKN2A/CDKN2B alterations [21, 22].

1.2.3 Alteration of tumor suppressor in aGBM

One of the key features about high grade astrocytomas is that they are highly mitotic, therefore, frequent mutations of cell cycle regulatory genes are seen in gliomas. Absence of cell cycle control renders HGAs susceptible to inappropriate cell division driven by constitutively active mitogenic signaling effectors such as phosphoinositide 3'-kinase (PI3K) and mitogen-activated kinase (MAPK) [18, 23].

1.2.3.1 RB pathway

The RB-CDK-CKI (cyclin-dependent kinase inhibitor) regulatory circuit which regulated cell cycle by governing the G1 to S phase is commonly disrupted in GBM. RB blocks proliferation by binding and sequestering the E2F family of transcription factors, thus preventing transactivation of genes that are essential for progression through cell cycle. Activation of the MAPK cascade leads to the induction of cyclin D1 and its association with cyclin-dependent kinases CDK4 and CDK6. Activated CDK complex phosphorylates RB, enabling E2F transactivation of its transcriptional targets to enable cell cycle progression. The RB-CDK-CKI circuit can be disrupted by many factors, including, loss of RB negative regulators, ($P16^{INK4A}$), amplification of CDK4 and/or CDK6, or mutation of the *RB1* gene. Loss of $P16^{INK4A}$, encoded by the CDKN2A gene, is detected in 40-57% of GBMs. CDK4 amplification is found in 12-14% of GBMs while mutation of the RB1 gene is seen in 14-33% of GBMs [20, 23, 24].

1.2.3.2 P53

Alterations of p53 are commonly found in GBMs. Loss of P53 is often due to point mutations that prevent DNA binding, or chromosomal deletion with loss of 17p. The p53 tumor suppressor prevents the propagation of cells with unstable genomes by either stopping the cell cycle in the G1 phase or starting an apoptosis pathway [23]. In the past it was believed that p53 inactivation was predominant in low grade asrocytomas and secondary GBMS. However, increasing evidence shows that a number of primary GBMs also carry TP53 mutations. Furthermore this pathway is deregulated in primary GBM through amplifications of *MDM2*, which encodes a protein that targets p53 for degradation [25-28].

1.2.3.3 PTEN

Another tumor suppressor gene, PTEN located at 10q23.3 is frequently deleted in many tumors and is also inactivated in 50% of high grade adult gliomas. PTEN loss is often seen in GBM but rarely seen lower-grade astrocytic tumors. Mutations in PTEN often occur in combination with mutations or deletions of TP53, CDKN2A, EGFR or PDGFR. PTEN is a phosphatase that acts as a key negative regulator of PI3K signaling and its loss causes resistance to apoptosis and increases proliferation [26]. The PI3K pathway is involved in processes such as cell growth, survival, proliferation, and migration. PI3K is responsible for phosporylating phosporylatidylinositol-4,5-biphosphate (PIP_2) on the 3' position to generate phosporylatidylinositol-3,4,5-triphosphate (PIP_3) which activates many downstream signaling pathways including AKT. PTEN acts as a phosphatase removing the phosphate from the three position ring of PIP_3 to create PIP_2, reversing the effects of PI3K [26, 29-31].

1.2.4 Mitogenic signaling pathways aberrantly activated in aGBMs

Proliferation of normal cells requires activation of mitogenic signaling pathways by diffusible growth factor binding, cell to cell adhesion, and/or contact with extracellular matrix components. GBM typically have constitutive activation of the PI3K and MAPK pathway to overcome the dependence of exogenous growth stimulation, enabling inappropriate cell division, survival, and motility [28, 32].

1.2.4.1 PI3K/Akt

The PI3K/Akt is one of the major cell survival pathways that are activated by receptor tyrosine kinases, such as EGFR which is overexpressed in a large number of GBMs [26].

Activation of PI3K/Akt pathway has been implicated in malignant transformation of many tumor cells and is frequently overexpressed in GBM tumors. This pathway is upregulated in GBM due to mutation or loss of PTEN, as mentioned earlier. Amplification of PI3KCA is detected in 30% of primary GBM and more recently amplification of Akt isoforms has also been described [31, 33].

Mammalian target of rapamycin (mTOR) is a serine/threonine kinase and it functions downstream of the PI3K/Akt pathway. In response to PI3K activation, Akt activates mTOR which leads to synthesis of many proteins involved in the regulation of cell growth, proliferation, metabolism, and apoptosis. The mTOR pathway is known to regulate cell proliferation, growth, and survival by translation initiation. MTOR regulates translation initiation by two pathways, 4EBP1 (eukaryotic translation initiation factor binding proteins) and p70S6K (ribosomal p70 S6 kinase) [33-35].

1.2.4.2 MAPK pathway

The MAPK pathway is another signaling pathway that is aberrantly activated in GBM, leading to the deregulation of many metabolic processes such as proliferation. Receptor tyrosine kinase activation results in receptor dimerization and cross-phosphorylation, creating binding sites for adaptor proteins such as Grb2/SOS and which in turn activates Ras. Ras undergoes a series of phosphorylation steps to activate in sequence Raf kinase, Mek, and finally ERK which enters the nucleus and phosphorylates nuclear transcription factors that induces expression of genes causing cell cycle proliferation, such as cyclin D1 [18, 23, 33].

1.2.5 Receptor Tyrosine Kinases in adult GBM

Receptor Tyrosine Kinases (RTKs) are a large family of cell surface receptors that have intrinsic protein kinase activity. They are activated by a wide variety of ligands and regulate important cellular functions such as cell cycle, cell migration, metabolism, survival, proliferation and differentiation. Deregulation of several RTKs such as MET, EGFR, PDGFR, and VEGFR have been implicated in a number of cancers, including GBMs. Frequently, RTKs are co-expressed in many cancers. For instance, EGFR and MET are frequently overexpressed in astrocytomas [23, 36].

1.2.5.1 Epidermal Growth Factor Receptor (EGFR)

EGFR is an important RTK and a well-documented proto-oncogene that has been shown to be overexpressed in a number of epithelial cancers including lung cancer, GBM and adenocarcinoma causing increased tumor survival and angiogenesis [37]. There are 3 major mechanisms leading to deregulation of EGFR signaling in GBM: 1.overexpression or amplification of EGFR, 2. activation of autocrine loops, i.e secretion of increased amounts of ligands, and 3. through mutant forms of EGFR [38]. EGFR is a 170kDa transmembrane cell surface receptor and is part of the ErbB/EGFR family and is also known as ErbB1 or HER1. Other members of this family include, ErbB2, ErbB3, and ErbB4. This family shares a similar extracellular ligand-binding domain that is linked to a hydrophobic transmembrane domain down to a cytoplasmic domain which contains both tyrosine kinase domain and C-terminal tail. Upon ligand binding, these receptors dimerize and cause trans-phosphorylation on multiple tyrosine residues. After ligand binding to EGFR, complex signaling pathways are activated and result in increased cell proliferation and survival. EGFR undue activation can initiate tumorigenesis,

metastasis, or proliferation through several potential downstream mediators. In normal physiological conditions, EGFR signaling is tightly regulated at the gene, transcript and protein levels. Deregulation of EGFR expression and/or activation can be caused by a number of genetic events, including EGFR gene amplification, increased EGFR transcription or translation, increased secretion of EGFR ligands, or decreased protein degradation[37, 39-41].

EGFR becomes activated through the binding of different ligands, namely, EGF, transforming growth factor α (TGFα), heparin-binding EGF (HB-EGF), β-Cellulin, amphiregulin, epiregulin and epigen on its extracellular domain. Ligand binding results in the recruitment of PI3K to the cell membrane, which activates phophatidylinositol 4, 5 biphosphate to 3-Phophate (PIP3). This activates downstream effectors such as AKT, mTOR and ERK leading to a number of events such as cell proliferation and increased cell survival [42].

In adult primary GBM, EGFR amplification is frequently found (~40%). Also a mutant truncated form of EGFRvIII is commonly found in this setting in association with EGFR amplification. EGFRvIII is constitutively active and independent of ligand binding. In pGBM, EGFR gene amplification is a rare event (<10%) and EGFRvIII is almost never seen, however, EGFR is overexpressed at the mRNA and protein level in more than 70% of samples [37, 43, 44].

1.2.5.2 PDGFR

Elevated expression of RTK PDGFRA and B, along with its ligand PDGF is found in all grade astrocytomas, and is more frequent in HGAs. Overexpression of PDGF stimulates proliferation of nestin overexpressing cells and astrocytes. Proliferation of astrocytes is determined by GFAP expression, which is often used as a marker for astrocytic tumors. In

pediatric HGAs it has been shown that the PDGFR signaling cascade is a strong driver of proliferation and *PDGFRA* is an important target of focal amplification in pediatric HGA [45, 46].

1.2.5.3 MET Receptor

Another RTK that has been implicated in brain tumor growth is MET and its ligand hepatocyte growth factor (HGF) [47, 48]. The Met receptor regulates several distinct biological processes, including, cell scatter, cell survival, cell invasion, and epithelial remodeling. This receptor is genetically altered by several mechanisms in many cancers. The MET receptor is a disulfide –linked heterodimer consisting of α and β chains. Upon HGF binding, MET autophosphorylation and homodimerization occurs. Activation of MET causes the recruitment of scaffolding protein such as Gab1 and Grb2, which lead to the activation of RAS and ERK/MAPK. Active c-MET also leads to the activation of Akt. Like EGFR, activated MET gets internalized and degraded in normal physiological conditions [49].

1.2.5.4 VEGF Receptor

VEGFR is another RTK deregulated in cancer and is a key mediator of angiogenesis. The VEGF family is the most critically important receptor in the regulation of endothelial cell growth and function. GBMs are highly vascular and the VEGF pathway is important for its neovascularization [50, 51].

1.2.6 Crosstalk between receptors and pathways

Increasing research suggests that aberrant signal transduction in cancers can be mediated through crosstalk between RTKs. MET and EGFR are often co-expressed in cancers and in many cases transactivation of MET is dependent on overexpression of EGFR. VEGFR and EGFR are also overexpressed in cancers. Several cases have shown if one RTK is overexpressed, it stimulates overexpression of another. Other studies have shown inhibiting one RTK in cancer increases the activity of another RTK. In many cases, it has been found that MET is amplified in patients who develop resistance to EGFR inhibitors. For this reason, dual inhibition of MET and EGFR are required for effective growth inhibition [49, 52]. Other studies have also shown inhibition of both EGFR and VEGFR have more anti-tumor activity against many cancers [53].

In summary, several RTKs are amplified, mutated or rearranged in a large proportion of aGBM. RTK signaling drives the transformation process towards angiogenesis, and/or induces a marked increase of proliferation and resistance to cell death [54, 55]. It also activates pathways, including Ras, Akt and the cell cycle, which are further activated by amplification of oncogenic members (PI3KCA) or loss of tumor supressors (PTEN). These signals are amplified and permit incontrollable cell growth and survival based on altered cell cycle pathways (Rb and P53 pathways). RTKs may cooperate to provide a signaling threshold that prevents the inhibition of mitogenic and survival signals following the inactivation of any single RTK [23, 56]. The discovery of receptor co-activation or cooperation suggests that tumor RTK profiling in GBMs may be mandated for the design of successful personalized therapeutic regimen, and that the initially disappointing clinical trials using RTK-targeted agents in GBMs [57] should be

reanalyzed with respect to the RTKs profiles of the responders and non-responders. Premises of these therapeutic changes based on the tumor biology are starting to change the dismal prognosis seen with current therapies in aGBM [58-61].

1.2.7 Integrated genomics in GBM

Many studies have shown that molecular categorization of tumors may be better for predicting prognosis than histological grading. In the case of GBMs it is very difficult to predict patient outcomes on the basis of histological features. Therefore, many studies have done gene expression profiling in aGBMs and as a result different molecular subtypes have been identified [24, 46, 62-68]. Since HGAs are very heterogeneous, gene expression profiling helps in finding prognostic markers or signature genes specific to different subgroups that will facilitate better targeted therapeutic strategies. The study done by Phillip *et al* identified 3 subgroups in adult HGA, designated as proneural, proliferative, and mesenchymal [64]. Verhaak *et al* also further classified aGBM into four subtypes: Proneural, neural, classical, and mesenchymal based on gene expression and integrated copy number and mutational analysis from the TCGA (Tumour Cancer Genome Atlas) group results for each tumour. These results indicated that classical subtypes had EGFR amplification and RB pathway alteration through CDKN2 deletion. Neural stem cell markers were also highly expressed in the classical subtype. The mesenchymal subtype had NF1 abnormalities, displayed expression of mesenchymal markers including CHI3L1 and MET, and tumors had an overall higher necrosis. The proneural class had *PDGFRA* alterations (amplification and mutation) and point mutations in IDH1 or 2. The Neural subtype had mainly increased neuronal markers. TP53 mutations or copy number alteration were

mainly identified in the Proneural subgroup and at lower level in other subgroups. The proneural subgroups had a slightly better survival advantage [24].

1.2.8 Stem cells in GBM

GBMs are extremely resistant to conventional radiation and chemotherapies and it has been hypothesized that a highly tumorigenic subpopulation of GBM stem cells may be promoting therapeutic resistance [69]. Cancer stem cells share important characteristics with normal stem cells such as, self-renewal capacity, multi-lineage differentiation and sustained proliferation and have been characterized in GBM by several groups [69, 70]. These cells have shown to stimulate tumor angiogenesis, promote metastasis, and cause an aggressive invasive phenotype [71, 72]. Stem cell resides within stem cell niches that are responsible for regulating their self renewal and fate. It has been shown that the development of abnormal stem cell niches contributes to tumorigeneisis. In the case of GBMs, vascular stem cell niches were found. Since the niches seem important in survival of cancer cells, further investigations are ongoing on understanding the molecular drivers, cellular components and therapeutic measures to disrupt these stem cell niches [73].

1.3 Pediatric GBM

Astrocytomas are the most common type of pediatric brain tumors. Contrary to adults, low grade astrocytic tumors are the most common astrocytomas in children. GBM is less frequent, representing 15% of all brain tumours in children. As such, very few studies had been done on this tumor when I started my PhD in 2004 and most of the current therapeutic strategies are still based on adult studies, including the use of the chemotherapeutic agent Temozolomide

and anti-angiogenic inhibitor bevacuzimab [59, 74]. However, increasing evidence shows that pediatric astrocytomas follow different genetic pathways from adult tumors. One of the major differences is that pGBMs almost always occurs *de novo*, and do not progress from lower grades, like primary GBMs. PGBMs show similarities with secondary adult GBMs that include rare EGFR amplifications/mutation (EGFRvIII is rarely seen in pediatric GBM) and common P53 mutations (43%) [13], IDH mutations are extremely rare in pediatric GBM with only a fraction of tumors carrying these mutations (~5%) and in mainly older children, above 14years [75]. PTEN mutations are also less frequent [76-78]. Interestingly, EGFR and PDGFR overexpression are seen in a vast number of pGBM (60-80% based on the study) in the absence of genetic amplification.

In summary, a number of comprehensive studies integrating genomic epigenetic and gene expression analyses helped identify in aGBM common regions of genomic gain and/or loss, gene expression signatures, and epigenetic changes capable of predicting the outcome[24, 64, 65, 68, 79-92]. They allowed molecular sub-classification of tumours while further indicating that all GBM have disrupted the p53, PI3K and RB pathways through various genetic mechanisms. Whole tumour genome sequencing through the TCGA consortium (Cancer Atlas Genome Project) also revealed, among other targets, crucial role for metabolic pathways in the genesis of subgroups of adult gliomas as mutations in *IDH1* and *2*, were identified in up to 80% of grade II and III gliomas and secondary GBM and are thought to be initiating events in these tumours [24, 85, 93]. By comparison, pGBM are largely understudied at the molecular level [2, 13, 15, 77, 94]. They are morphologically indistinguishable from adult GBM, which prompted investigators to view them as the same disease. Only a handful of studies, including from our group demonstrate the prognostic importance of the analysis of the unique biology of pGBM [67, 95,

96]. This work suggests that the ***assumptions*** as to the similarities between pediatric and adult GBM were not borne out in analyses directed at genes mutated in adult [59] patients. Indeed, while mutations in *TP53**,*** *CDKN2A**,*** and *PIK3CA* are common to both age groups; *PTEN* mutations and *EGFR* amplifications, frequent in adult primary GBM, occur in less than 10% of paediatric GBM while *IDH* mutations are rare in children. One of the major goals of this thesis is to see whether childhood HGAs can be classified into genetic subgroups similar to adult HGA and identify molecular targets relevant in gliomagenesis. Data I helped gather have shown them to be different at the molecular level and identified sorting nexin 3 (see below) as one potential target helping drive genesis of pGBM.

1.4 Anaplastic Astrocytoma (AA)

Anaplastic astrocytomas are grade III tumors and constitute 4% of all malignant nervous system tumors [97]. They arise from a low-grade astrocytoma or as *de novo* tumours without a malignant precursor identified [98]. They have more anaplasia and proliferation compared to grade II tumors and are usually characterized by pleomorphic cells, nuclear atypia, and mitosis [50]. They show no necrosis or vascular proliferation compared to grade IVs. They have a survival of 2-3 years and can progress to grade IV in adults within 2-3 years [23]. Some of the key differences between adult AA and adult GBM are: 1. GBMs have EGFR amplification while AA have EGFR overexpressed, 2. PTEN is mutated or deleted in GBM and this genetic event is less frequent in AA, and 3. AA have IDH mutations while most GBMs do not (except secondary GBMs that arise from these AA) [97]. No studies targeting directly AA are available in children. Most data is based on general studies that included a majority of GBM and few AA where no specific distinction regarding grade has been made. Limited data regarding progression

from AA to GBM is available, even if the general understanding is that AA neither will nor progress to GBM in children even if they carry similar poor prognosis. In order to investigate whether they constitute a distinct entity, I investigated during my PhD the molecular signatures of pediatric AA and compared them to pediatric GBM and adult AA.

1.5 Sorting Nexins

The candidate gene Sorting Nexin 3 (SNX3) was selected for further investigations based on its involvement in membrane receptor trafficking including RTKs, and the role of RTKs in gliomagenesis including in children. Very limited documentation is available on this target gene, however, in a paper published by Xu et al. (2001a), it was shown that overexpression of SNX3 in cells causes delayed EGFR targeting to the lysosomes for degradation [99]. The sorting nexin (SNXs) family of proteins has been recently characterized and consists of 33 mammalian members [100]. It was initially discovered in yeast where they were shown to function to transport cargo from endosomes to the golgi. SNXs are a group of cytoplasmic and membrane-associated proteins involved in endocytosis and protein trafficking. They are characterized by a phox homology (PX) domain, with limited conservation between the SNXs [101]. The PX domain has different binding affinities for phosphatidylinositol phosphates (PtdInsPs). PtdIns's are known to regulate many biological processes, including cell proliferation, cell survival, membrane trafficking and signal transduction [102]. SNXs are sub-grouped into 3 categories: SNX-BAR, these SNXs contain a PX domain and a BAR domain which can induce or sense membrane curvature, SNX-PX are those that only have a PX domain, SNX3 falls in this category, and SNX-other, which are the rest of the SNXs that have different structural motifs along with the PX domain. [103-105]. The PX domain of SNX3 binds directly to PtdIns3 and it

has been shown that this interaction is needed for SNX3 function [99]. PtdIns3 is produced by phosphorylation by the PI3K, a kinase whose activation is initiated by growth factor receptors including EGFR [102]. Review of the literature shows that SNXs are involved in regulating endosomal EGFR trafficking. SNX1 was the first mammalian SNX characterized. It was found that when SNX1 was overexpressed, it increased EGFR degradation [106]. SNX 1 and 2 were later found to be part of a complex involved in endosome to golgi transport [107]. SNX16 showed an increase in the rate of EGFR degradation and decreased EGFR signaling [108]. SNX2 and SNX4 also have shown to increase the rate of EGFR degradation. Overexpressing SNX5 has shown to delay EGFR degradation however, in the same cells if SNX1 is overexpressed it attenuates the effect of SNX5. This shows that SNXs can interact with each other and act as antagonists [109]. **Table 1.2** summarizes some of the roles known to different SNXs. [109-111]. From the table, we can easily deduce that SNXs are involved in trafficking of a wide variety of membrane receptors. Many of the SNXs are not specific to one receptor but are involved in endosomal trafficking of several entities. **Figure 1.1** depicts the different mammalian SNXs.

1.5.1 Sorting Nexin 3 (SNX3)

SNX3 only has a PX domain and binds to PtdIns3. It is associated with early endosomes, as shown by its co-localization with the early endocytic marker, EEA1. It was found that adding wortmannin (a drug that inhibits PI3K) causes an inhibition of membrane recruitment of SNX3. The first studies done on SNX3 revealed that it is involved in the recycling of transferrin receptor (TfR) and delays EGFR degradation [99]. In another paper, published by Pons et al, 2008, also found that SNX3 overexpression delayed EGFR degradation; however silencing SNX3 did not

have an effect on EGFR degradation. This study concluded that SNX3 is required for the multivesicular body (MVB) formation, which serves as an intermediate to endosomal carrier vesicle (ECV), referred to as ECV/MVB. This is the complex that is eventually leading to late endosomes or lysosomes. Overexpressing SNX3 causes its accumulation in early endosomes and delays the maturation into late endosomes and EGFR remains trapped within this compartment. However, from SNX3 knockdown results, the authors concluded that SNX3 does not interfere with lysosomal targeting of EGFR, thus lysosomal targeting is not linked to the formation of ECV/MVBs [112]. In another study, SNX3 was also found to be upregulated by lithium and to regulate neurite formation. This paper also found that not only the PX domain but the C-terminal is required for PtdIns3 binding [113].

These studies show that SNXs are involved in membrane receptor trafficking and degradation. Their association with human disease is recent and has been shown for SNX1, a component of the retromer, whose expression has been found to be down regulated in a proportion of colon cancer, promoting tumorigenesis, and more recently for SNX3, which has been shown to promote delayed maturation of salmonella containing vacuoles, ultimately favoring intra-cellular persistence and virulence of the bug [114].

1.6 RTK degradation using EGFR as a paradigm of RTK endosomal trafficking

Proper endocytic uptake and endosomal sorting of signaling receptors are important for the regulation of signaling activity involved in cellular growth, development, and differentiation [42]. EGFR degradation is the best understood out of all the RTKs and hence it was used to initially study the effects of SNX3, our target gene for this thesis, on receptor trafficking (see below). Recent evidence suggests that an impaired or ineffective EGFR degradation pathway

plays a major role in increased cancer development. Prolonged signaling can lead to sustained proliferation and therefore it is crucial that activated receptors become internalized rapidly and targeted to lysosomes for degradation. In general, signaling and trafficking are very tightly linked cellular events. The rate of receptor degradation is much slower than that of internalization. Usually EGFR not bound by ligands is recycled back to the surface, and activated (ligand-bound) receptors are sorted into the lysosomal pathway [115]. EGFR degradation usually occurs via clathrin coated pits. When EGFR is activated, it recruits the E3 ligase c-Cbl, which mediates the ubiquitination of the receptor. This initiates the receptor to go through endocytosis and eventually leading to its degradation. EGFR which is initially internalized via clathrin coated pits fuses with early endosomes (after shedding off their clathrin coat) resulting in a cascade of events, that triggers the formation of a multivesicular body (MVB). The sorting for lysosomal degradation is mediated by Hrs/STAM and endosomal sorting complex which is required for transport (ESCRT) complexes. The formation of this late endosomal compartment eventually leads to fusion with lysosomes, leading to receptor degradation [38, 42]. **Figure 1.2** depicts an overview of EGFR degradation.

1.7 Implications of delayed receptor degradation and cancer

Impaired endocytic downregulation of signaling receptors is often associated with many cancers, since it can lead to uncontrolled and increased receptor signaling. Recently, increasing research is being done on targeting endocytosis as a crucial process driving cancer initiation and progression [116]. There are several mechanisms by which cancer cells can obtain uncontrolled EGFR signaling, including increased receptor expression, activating mutations, and escape from endocytic receptor downregulation. Acquired mutations in RTKs, which evade sorting to

degradation, are widespread in cancer. For example the mutant form EGFRvIV, in GBM, escapes degradation by lacking the direct Cbl binding sites, which mediates degradation. Another example is EGFRvIII which has hypophosphorylation of the Cbl docking site and this delays receptor internalization and increases receptor recycling [116-119]. Aside from RTK mutations, there may be overexpression or mutations within the mediators involved in sorting that can also contribute to endosomal sorting dysfunction. Interestingly, when the receptor is internalized EGF-EGFR complexes still have the ability to generate cell signaling from within the endosomes. Therefore, a delay in the degradation of RTKs can prolong its effect on proliferation, angiogenesis, growth, etc. Thus, it is important to determine the different sorting steps involved in endosomal trafficking leading to the cessation of signaling [42, 108, 115, 120].

1.8 Hypothesises and Objectives of the thesis

There are two major hypotheses and objectives of my work:

1. Our first hypothesis was that pediatric HGA are distinct from adult HGA and pediatric HGA can be further sub grouped based on grade and molecular profile. Thus, the first aim was to identify a molecular signature specific to pediatric high grade astrocytomas, and will be described within the next three chapters: we aimed to characterize grade IV astrocytomas using gene expression profiling and assess in pediatric tumours activation of the Ras and Akt pathways. The next part of this objective is to characterize grade III astrocytoma in children and compare molecular and genetic profiles to adult AA and pediatric GBM, in order to identify whether this is a distinct entity with a specific molecular signature.

2. The second hypothesis of this thesis was that high levels of SNX3 delays RTK degradation and induce or sustain signaling leading to growth advantage in pGBMs. The second aim of this work was to study the functional role of a target gene overexpressed in a sub-group of pediatric HGA. Through extensive investigation of hundreds of genes identified in the first part of the thesis, we focused on one gene: SNX3 in the sub-group showing abnormal Ras and Akt activation, based on its role in RTK trafficking including EGFR. The last chapter depicts the role of SNX3 in pGBM.

1.9 Tables and Figures

	EGFR	PTEN loss	P53 Mutation	IDH Mutation	PDGFR O/E and amplification	Progression from lower grades
aPrimary GBM	amplified	Yes	No	No	< secondary	No
aSecondary GBM	O/E	<primary	Yes	Yes	Yes	Yes
pGBM	O/E	No	Yes	Rare	Yes	No
Adult AA	O/E	No	< secondary	Yes	Yes	Yes
Pediatric AA		No	Yes	> pGBM	Yes	Yes

Table 1.1: A summary of important differences between high grade astrocytomas**.**

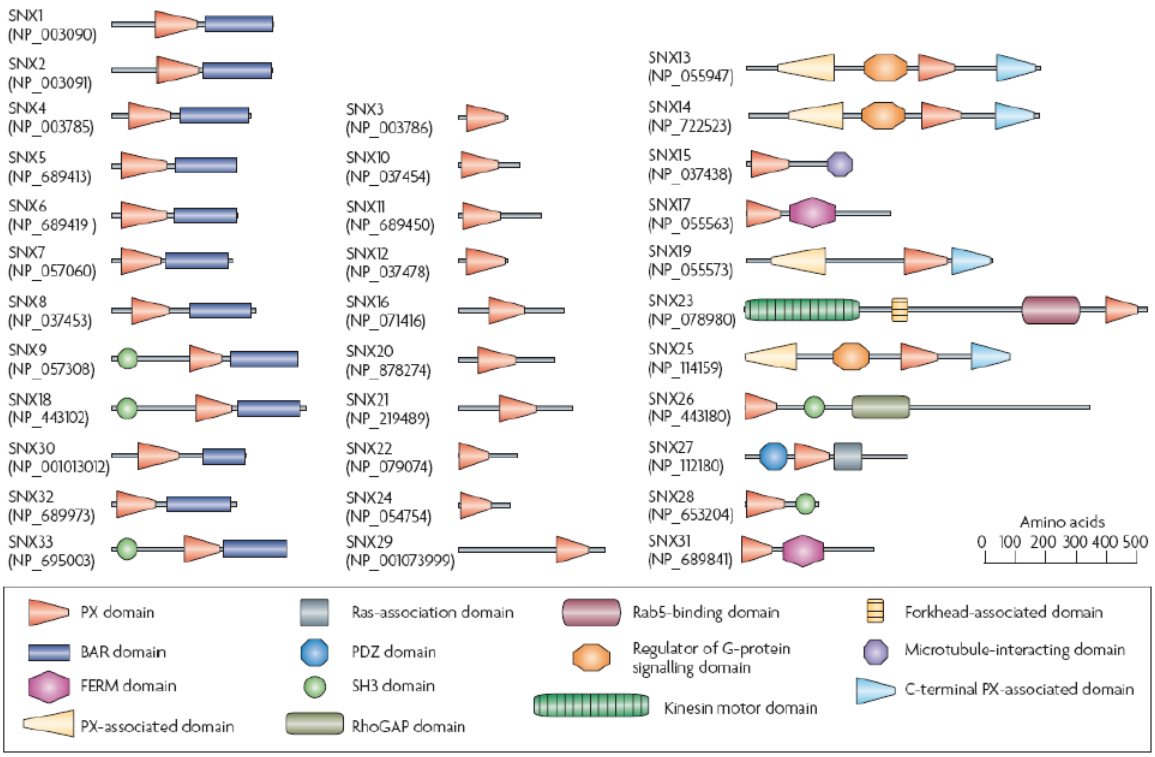

Figure 1.1: Members of the SNX family. From Cullen P. J., Nature Reviews Molecular Cell Biology, 2008 [121].

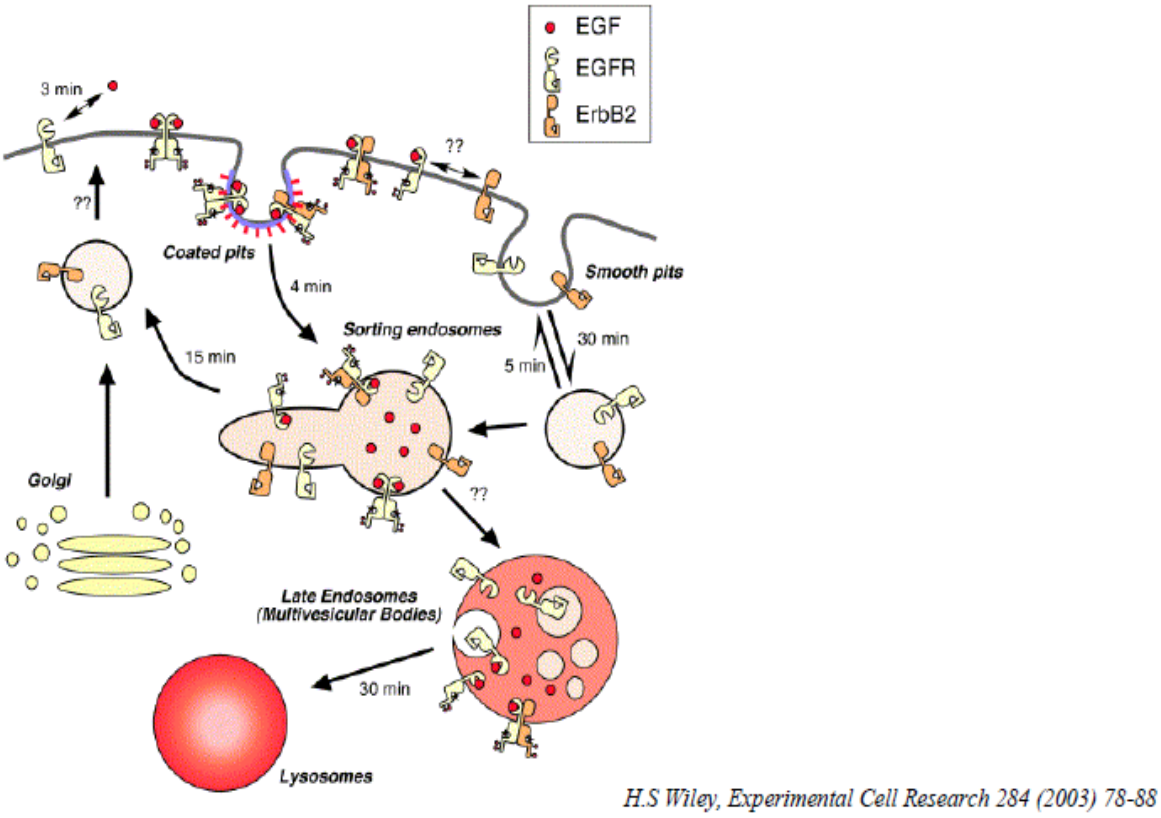

Figure 1.2: Endosomal trafficking of EGFR leading to its degradation. [115]

SNX	*LIPID BINDING PREFERENCE*	*PROTEIN-PROTEIN INTERACTIONS/COMPLEXES*	*POTENTIAL PROTEINS SORTED*	*LOCATED IN CELL*
SNX1	PtdIns(3,4,5)P_3>PtdIns(3,5)P_2>PtdIns(3)P	HRS, VPS35, VPS29, VPS35, SNX1, SNX2, SNX4, SNX4, SNX6, SNX15	ALK4, EGFR, IR, Leptin, Shiga toxin	Cytosol, endosomes
SNX2	PtdIns(3)P> PtdIns(4)P> PtdIns(5)P	FBP17, VPS26, VPS29, VPS35, SNX1, SNX2, SNX4, SNX6	ALK4, EGFR, IR, LeptinPDGFR, TFR	Cytosol, endosomes
SNX3	PtdIns(3)P	N/D	TFR, EGFR	Cytosol, endosomes
SNX4	N/D	SNX1, SNX2, SNX6	N/D	Cytosol, endosomes
SNX5	PtdIns(3,5)P_2>PtdIns(4)P	FANCA, SNX1	EGFR	Cytosol, endosomes
SNX6	N/D	PIM1, SNX1, SNX2, SNX4, SNX5	ALK1, ALK5, ALK6, EGFR, IR, leptin, PDGFR, TβRII KD	Cytosol, endosomes
SNX 8	N/D	N/D	Shiga toxin	Endosomes
SNX9	N/D	ACK2, AP-50, MDC9, MDC15, WASP	EGFR	N/D
SNX10	PtdIns(3)P	N/D	EGFR, , MT-MMP	endosomes
SNX13	PtdIns(3)P= PtdIns(5)P> PtdIns(3,5)P_2= PtdIns(3,5)P_2= PtdIns(4)P	N/D	EGFR, GPCR	endosomes
SNX15			Furin, PDGFR, TGN38, TFR	
SNX16	PtdIns(3)P> PtdIns(3,4)P_2	N/D	EGFR	Cytosol, endosomes
SNX17 SNX 27	PtdIns(3)P	P-selectin Diacylglycerol kinase ζ	LDLR Kir3 channels, 5-HT_4R	endosomes

Adapted from Nature Reviews Molecular Cell Biology **3**, 919-931 (2002)

Table 1.2: Summary of different SNX functions

1.10 References

1. Ohgaki, H. and P. Kleihues, *Genetic pathways to primary and secondary glioblastoma.* Am J Pathol, 2007. **170**(5): p. 1445-53.
2. Merchant, T.E., I.F. Pollack, and J.S. Loeffler, *Brain tumors across the age spectrum: biology, therapy, and late effects.* Semin Radiat Oncol, 2010. **20**(1): p. 58-66.
3. Pollack, I.F., *Pediatric brain tumors.* Semin Surg Oncol, 1999. **16**(2): p. 73-90.
4. Saran, F., *Recent advances in paediatric neuro-oncology.* Curr Opin Neurol, 2002. **15**(6): p. 671-7.
5. Broniscer, A., et al., *Clinical and molecular characteristics of malignant transformation of low-grade glioma in children.* J Clin Oncol, 2007. **25**(6): p. 682-9.
6. Broniscer, A., *Past, present, and future strategies in the treatment of high-grade glioma in children.* Cancer Invest, 2006. **24**(1): p. 77-81.
7. Fisher, P.G., et al., *Outcome analysis of childhood low-grade astrocytomas.* Pediatr Blood Cancer, 2008. **51**(2): p. 245-50.
8. Gajjar, A., et al., *Low-grade astrocytoma: a decade of experience at St. Jude Children's Research Hospital.* J Clin Oncol, 1997. **15**(8): p. 2792-9.
9. Rutka, J.T., et al., *Advances in the treatment of pediatric brain tumors.* Expert Rev Neurother, 2004. **4**(5): p. 879-93.
10. Bouffet, E., et al., *Possibilities of new therapeutic strategies in brain tumors.* Cancer Treat Rev, 2010. **36**(4): p. 335-41.
11. Finlay, J.L., et al., *Randomized phase III trial in childhood high-grade astrocytoma comparing vincristine, lomustine, and prednisone with the eight-drugs-in-1-day regimen. Childrens Cancer Group.* J Clin Oncol, 1995. **13**(1): p. 112-23.
12. Pollack, I.F., *The role of surgery in pediatric gliomas.* J Neurooncol, 1999. **42**(3): p. 271-88.
13. Pollack, I.F., et al., *Expression of p53 and prognosis in children with malignant gliomas.* N Engl J Med, 2002. **346**(6): p. 420-7.
14. Louis, D.N., et al., *The 2007 WHO classification of tumours of the central nervous system.* Acta Neuropathol, 2007. **114**(2): p. 97-109.
15. Rood, B.R. and T.J. Macdonald, *Pediatric high-grade glioma: molecular genetic clues for innovative therapeutic approaches.* J Neurooncol, 2005.
16. Faury, D., et al., *Molecular profiling identifies prognostic subgroups of pediatric glioblastoma.* J Clin Oncol, 2006. **In press**.
17. Maher, E.A., et al., *Malignant glioma: genetics and biology of a grave matter.* Genes Dev, 2001. **15**(11): p. 1311-33.
18. Huang, P.H., et al., *Uncovering therapeutic targets for glioblastoma: a systems biology approach.* Cell Cycle, 2007. **6**(22): p. 2750-4.
19. Rickman, D.S., et al., *Distinctive molecular profiles of high-grade and low-grade gliomas based on oligonucleotide microarray analysis.* Cancer Res, 2001. **61**(18): p. 6885-91.
20. Zhu, Y. and L.F. Parada, *The molecular and genetic basis of neurological tumours.* Nat Rev Cancer, 2002. **2**(8): p. 616-26.
21. Yan, H., et al., *IDH1 and IDH2 mutations in gliomas.* N Engl J Med, 2009. **360**(8): p. 765-73.

22. Nobusawa, S., et al., *IDH1 mutations as molecular signature and predictive factor of secondary glioblastomas.* Clin Cancer Res, 2009. **15**(19): p. 6002-7.
23. Furnari, F.B., et al., *Malignant astrocytic glioma: genetics, biology, and paths to treatment.* Genes Dev, 2007. **21**(21): p. 2683-710.
24. Verhaak, R.G., et al., *Integrated genomic analysis identifies clinically relevant subtypes of glioblastoma characterized by abnormalities in PDGFRA, IDH1, EGFR, and NF1.* Cancer Cell, 2010. **17**(1): p. 98-110.
25. Ishii, N., et al., *Cells with TP53 mutations in low grade astrocytic tumors evolve clonally to malignancy and are an unfavorable prognostic factor.* Oncogene, 1999. **18**(43): p. 5870-8.
26. Zheng, H., et al., *p53 and Pten control neural and glioma stem/progenitor cell renewal and differentiation.* Nature, 2008. **455**(7216): p. 1129-33.
27. Huang, H., et al., *Gene expression profiling of low-grade diffuse astrocytomas by cDNA arrays.* Cancer Res, 2000. **60**(24): p. 6868-74.
28. Kato, H., et al., *Functional evaluation of p53 and PTEN gene mutations in gliomas.* Clin Cancer Res, 2000. **6**(10): p. 3937-43.
29. Baker, S.J. and P.J. McKinnon, *Tumour-suppressor function in the nervous system.* Nat Rev Cancer, 2004. **4**(3): p. 184-96.
30. Sansal, I. and W.R. Sellers, *The biology and clinical relevance of the PTEN tumor suppressor pathway.* J Clin Oncol, 2004. **22**(14): p. 2954-63.
31. Endersby, R. and S.J. Baker, *PTEN signaling in brain: neuropathology and tumorigenesis.* Oncogene, 2008. **27**(41): p. 5416-30.
32. Hu, X., et al., *mTOR promotes survival and astrocytic characteristics induced by Pten/AKT signaling in glioblastoma.* Neoplasia, 2005. **7**(4): p. 356-68.
33. Puli, S., et al., *Effect of combination treatment of rapamycin and isoflavones on mTOR pathway in human glioblastoma (U87) cells.* Neurochem Res, 2010. **35**(7): p. 986-93.
34. McBride, S.M., et al., *Activation of PI3K/mTOR pathway occurs in most adult low-grade gliomas and predicts patient survival.* J Neurooncol, 2010. **97**(1): p. 33-40.
35. Gulati, N., et al., *Involvement of mTORC1 and mTORC2 in regulation of glioblastoma multiforme growth and motility.* Int J Oncol, 2009. **35**(4): p. 731-40.
36. Reznik, T.E., et al., *Transcription-dependent epidermal growth factor receptor activation by hepatocyte growth factor.* Mol Cancer Res, 2008. **6**(1): p. 139-50.
37. Layfield, L.J., et al., *Epidermal growth factor receptor gene amplification and protein expression in glioblastoma multiforme: prognostic significance and relationship to other prognostic factors.* Appl Immunohistochem Mol Morphol, 2006. **14**(1): p. 91-6.
38. Huang, P.H., A.M. Xu, and F.M. White, *Oncogenic EGFR signaling networks in glioma.* Sci Signal, 2009. **2**(87): p. re6.
39. Roepstorff, K., et al., *Differential effects of EGFR ligands on endocytic sorting of the receptor.* Traffic, 2009. **10**(8): p. 1115-27.
40. Baldys, A. and J.R. Raymond, *Critical role of ESCRT machinery in EGFR recycling.* Biochemistry, 2009. **48**(40): p. 9321-3.
41. Madshus, I.H. and E. Stang, *Internalization and intracellular sorting of the EGF receptor: a model for understanding the mechanisms of receptor trafficking.* J Cell Sci, 2009. **122**(Pt 19): p. 3433-9.
42. Roepstorff, K., et al., *Endocytic downregulation of ErbB receptors: mechanisms and relevance in cancer.* Histochem Cell Biol, 2008. **129**(5): p. 563-78.

43. Hargrave, D., *Paediatric high and low grade glioma: the impact of tumour biology on current and future therapy.* Br J Neurosurg, 2009. **23**(4): p. 351-63.
44. Smith, J.S., et al., *PTEN mutation, EGFR amplification, and outcome in patients with anaplastic astrocytoma and glioblastoma multiforme.* J Natl Cancer Inst, 2001. **93**(16): p. 1246-56.
45. Paugh, B.S., et al., *Integrated molecular genetic profiling of pediatric high-grade gliomas reveals key differences with the adult disease.* J Clin Oncol, 2010. **28**(18): p. 3061-8.
46. Brennan, C., et al., *Glioblastoma subclasses can be defined by activity among signal transduction pathways and associated genomic alterations.* PLoS One, 2009. **4**(11): p. e7752.
47. Abounader, R., *Interactions between PTEN and receptor tyrosine kinase pathways and their implications for glioma therapy.* Expert Rev Anticancer Ther, 2009. **9**(2): p. 235-45.
48. Li, Y., et al., *Interactions between PTEN and the c-Met pathway in glioblastoma and implications for therapy.* Mol Cancer Ther, 2009. **8**(2): p. 376-85.
49. Lai, A.Z., J.V. Abella, and M. Park, *Crosstalk in Met receptor oncogenesis.* Trends Cell Biol, 2009. **19**(10): p. 542-51.
50. Sul, J. and H.A. Fine, *Malignant gliomas: new translational therapies.* Mt Sinai J Med, 2010. **77**(6): p. 655-66.
51. Grau, S.J., et al., *Expression of VEGFR3 in glioma endothelium correlates with tumor grade.* J Neurooncol, 2007. **82**(2): p. 141-50.
52. Mueller, K.L., et al., *Met and c-Src cooperate to compensate for loss of epidermal growth factor receptor kinase activity in breast cancer cells.* Cancer Res, 2008. **68**(9): p. 3314-22.
53. Hoffmann, S., et al., *Differential effects of cetuximab and AEE 788 on epidermal growth factor receptor (EGF-R) and vascular endothelial growth factor receptor (VEGF-R) in thyroid cancer cell lines.* Endocrine, 2007. **31**(2): p. 105-13.
54. Mischel, P.S., et al., *Identification of molecular subtypes of glioblastoma by gene expression profiling.* Oncogene, 2003. **22**(15): p. 2361-73.
55. Halatsch, M.E., et al., *EGFR but not PDGFR-beta expression correlates to the antiproliferative effect of growth factor withdrawal in glioblastoma multiforme cell lines.* Anticancer Res, 2003. **23**(3B): p. 2315-20.
56. Stommel, J.M., et al., *Coactivation of receptor tyrosine kinases affects the response of tumor cells to targeted therapies.* Science, 2007. **318**(5848): p. 287-90.
57. Mellinghoff, I.K., et al., *Molecular determinants of the response of glioblastomas to EGFR kinase inhibitors.* N Engl J Med, 2005. **353**(19): p. 2012-24.
58. Mischel, P.S. and T.F. Cloughesy, *Targeted molecular therapy of GBM.* Brain Pathol, 2003. **13**(1): p. 52-61.
59. Hegi, M.E., et al., *MGMT gene silencing and benefit from temozolomide in glioblastoma.* N Engl J Med, 2005. **352**(10): p. 997-1003.
60. Donson, A.M., et al., *MGMT promoter methylation correlates with survival benefit and sensitivity to temozolomide in pediatric glioblastoma.* Pediatr Blood Cancer, 2006.
61. Nicholas, M.K., *Glioblastoma multiforme: evidence-based approach to therapy.* Expert Rev Anticancer Ther, 2007. **7**(12 Suppl): p. S23-7.
62. Freije, W.A., et al., *Gene expression profiling of gliomas strongly predicts survival.* Cancer Res, 2004. **64**(18): p. 6503-10.

63. Tso, C.L., et al., *Distinct transcription profiles of primary and secondary glioblastoma subgroups.* Cancer Res, 2006. **66**(1): p. 159-67.
64. Phillips, H.S., et al., *Molecular subclasses of high-grade glioma predict prognosis, delineate a pattern of disease progression, and resemble stages in neurogenesis.* Cancer Cell, 2006. **9**(3): p. 157-73.
65. Liang, Y., et al., *Gene expression profiling reveals molecularly and clinically distinct subtypes of glioblastoma multiforme.* Proc Natl Acad Sci U S A, 2005. **102**(16): p. 5814-9.
66. Godard, S., et al., *Classification of human astrocytic gliomas on the basis of gene expression: a correlated group of genes with angiogenic activity emerges as a strong predictor of subtypes.* Cancer Res, 2003. **63**(20): p. 6613-25.
67. Faury, D., et al., *Molecular profiling identifies prognostic subgroups of pediatric glioblastoma and shows increased YB-1 expression in tumors.* J Clin Oncol, 2007. **25**(10): p. 1196-208.
68. Dreyfuss, J.M., M.D. Johnson, and P.J. Park, *Meta-analysis of glioblastoma multiforme versus anaplastic astrocytoma identifies robust gene markers.* Mol Cancer, 2009. **8**: p. 71.
69. Dirks, P.B., *Cancer: stem cells and brain tumours.* Nature, 2006. **444**(7120): p. 687-8.
70. Sanai, N., A. Alvarez-Buylla, and M.S. Berger, *Neural stem cells and the origin of gliomas.* N Engl J Med, 2005. **353**(8): p. 811-22.
71. Huang, Z., et al., *Cancer stem cells in glioblastoma--molecular signaling and therapeutic targeting.* Protein Cell, 2010. **1**(7): p. 638-55.
72. Sunayama, J., et al., *Dual blocking of mTor and PI3K elicits a prodifferentiation effect on glioblastoma stem-like cells.* Neuro Oncol, 2010. **12**(12): p. 1205-19.
73. Gilbertson, R.J. and J.N. Rich, *Making a tumour's bed: glioblastoma stem cells and the vascular niche.* Nat Rev Cancer, 2007. **7**(10): p. 733-6.
74. Fountzilas, G., et al., *Post-operative combined radiation and chemotherapy with temozolomide and irinotecan in patients with high-grade astrocytic tumors. A phase II study with biomarker evaluation.* Anticancer Res, 2006. **26**(6C): p. 4675-86.
75. Pollack, I.F., et al., *IDH1 mutations are common in malignant gliomas arising in adolescents: a report from the Children's Oncology Group.* Childs Nerv Syst, 2011. **27**(1): p. 87-94.
76. Nakamura, M., et al., *Molecular pathogenesis of pediatric astrocytic tumors.* Neuro Oncol, 2007. **9**(2): p. 113-23.
77. Pytel, P., *Spectrum of pediatric gliomas: implications for the development of future therapies.* Expert Rev Anticancer Ther, 2007. **7**(12 Suppl): p. S51-60.
78. Mueller, S. and S. Chang, *Pediatric brain tumors: current treatment strategies and future therapeutic approaches.* Neurotherapeutics, 2009. **6**(3): p. 570-86.
79. Bredel, M., et al., *High-resolution genome-wide mapping of genetic alterations in human glial brain tumors.* Cancer Res, 2005. **65**(10): p. 4088-96.
80. Kotliarov, Y., et al., *High-resolution Global Genomic Survey of 178 Gliomas Reveals Novel Regions of Copy Number Alteration and Allelic Imbalances.* Cancer Res, 2006. **66**(19): p. 9428-36.
81. Maher, E.A., et al., *Marked genomic differences characterize primary and secondary glioblastoma subtypes and identify two distinct molecular and clinical secondary glioblastoma entities.* Cancer Res, 2006. **66**(23): p. 11502-13.

82. Rich, J.N., et al., *Gene expression profiling and genetic markers in glioblastoma survival.* Cancer Res, 2005. **65**(10): p. 4051-8.
83. *Comprehensive genomic characterization defines human glioblastoma genes and core pathways.* Nature, 2008. **455**(7216): p. 1061-8.
84. Bredel, M., et al., *A network model of a cooperative genetic landscape in brain tumors.* Jama, 2009. **302**(3): p. 261-75.
85. Parsons, D.W., et al., *An integrated genomic analysis of human glioblastoma multiforme.* Science, 2008. **321**(5897): p. 1807-12.
86. Carro, M.S., et al., *The transcriptional network for mesenchymal transformation of brain tumours.* Nature. **463**(7279): p. 318-25.
87. Fischer, I. and K. Aldape, *Molecular tools: biology, prognosis, and therapeutic triage.* Neuroimaging Clin N Am. **20**(3): p. 273-82.
88. Noushmehr, H., et al., *Identification of a CpG island methylator phenotype that defines a distinct subgroup of glioma.* Cancer Cell. **17**(5): p. 510-22.
89. Feng, J., et al., *An integrated analysis of germline and somatic, genetic and epigenetic alterations at 9p21.3 in glioblastoma.* Cancer, 2011.
90. Wang, R., et al., *Glioblastoma stem-like cells give rise to tumour endothelium.* Nature, 2010. **468**(7325): p. 829-33.
91. Cerami, E., et al., *Automated network analysis identifies core pathways in glioblastoma.* PLoS One, 2010. **5**(2): p. e8918.
92. Purow, B. and D. Schiff, *Advances in the genetics of glioblastoma: are we reaching critical mass?* Nat Rev Neurol, 2009. **5**(8): p. 419-26.
93. Weller, M., et al., *Molecular predictors of progression-free and overall survival in patients with newly diagnosed glioblastoma: a prospective translational study of the German Glioma Network.* J Clin Oncol, 2009. **27**(34): p. 5743-50.
94. Pollack, I.F., et al., *Rarity of PTEN deletions and EGFR amplification in malignant gliomas of childhood: results from the Children's Cancer Group 945 cohort.* J Neurosurg, 2006. **105**(5 Suppl): p. 418-24.
95. Qu, H., et al., *Genome–wide profiling using Single Nucleotide Polymorphism Arrays identifies distinct chromosomal imbalances in Pediatric and Adult High-Grade Astrocytomas.* . Cancer research, 2008. **submitted**.
96. Haque, T., et al., *Gene expression profiling from formalin-fixed paraffin-embedded tumors of pediatric glioblastoma.* Clin Cancer Res, 2007. **13**(21): p. 6284-92.
97. Gulati, S., et al., *Overexpression of c-erbB2 is a negative prognostic factor in anaplastic astrocytomas.* Diagn Pathol, 2010. **5**: p. 18.
98. Holland, H., et al., *WHO grade-specific comparative genomic hybridization pattern of astrocytoma - a meta-analysis.* Pathol Res Pract, 2010. **206**(10): p. 663-8.
99. Xu, Y., et al., *SNX3 regulates endosomal function through its PX-domain-mediated interaction with PtdIns(3)P.* Nat Cell Biol, 2001. **3**(7): p. 658-66.
100. van Weering, J.R., P. Verkade, and P.J. Cullen, *SNX-BAR proteins in phosphoinositide-mediated, tubular-based endosomal sorting.* Semin Cell Dev Biol, 2010. **21**(4): p. 371-80.
101. Worby, C.A. and J.E. Dixon, *Sorting out the cellular functions of sorting nexins.* Nat Rev Mol Cell Biol, 2002. **3**(12): p. 919-31.
102. Xu, Y., et al., *The Phox homology (PX) domain, a new player in phosphoinositide signalling.* Biochem J, 2001. **360**(Pt 3): p. 513-30.

103. Bonifacino, J.S. and J.H. Hurley, *Retromer.* Curr Opin Cell Biol, 2008. **20**(4): p. 427-36.
104. Seet, L.F. and W. Hong, *The Phox (PX) domain proteins and membrane traffic.* Biochim Biophys Acta, 2006. **1761**(8): p. 878-96.
105. Carlton, J., et al., *Sorting nexins--unifying trends and new perspectives.* Traffic, 2005. **6**(2): p. 75-82.
106. Kurten, R.C., *Sorting motifs in receptor trafficking.* Adv Drug Deliv Rev, 2003. **55**(11): p. 1405-19.
107. Griffin, C.T., J. Trejo, and T. Magnuson, *Genetic evidence for a mammalian retromer complex containing sorting nexins 1 and 2.* Proc Natl Acad Sci U S A, 2005. **102**(42): p. 15173-7.
108. Choi, J.H., et al., *Sorting nexin 16 regulates EGF receptor trafficking by phosphatidylinositol-3-phosphate interaction with the Phox domain.* J Cell Sci, 2004. **117**(Pt 18): p. 4209-18.
109. Liu, H., et al., *Inhibitory regulation of EGF receptor degradation by sorting nexin 5.* Biochem Biophys Res Commun, 2006. **342**(2): p. 537-46.
110. Zhong, Q., et al., *Endosomal localization and function of sorting nexin 1.* Proc Natl Acad Sci U S A, 2002. **99**(10): p. 6767-72.
111. Haft, C.R., et al., *Identification of a family of sorting nexin molecules and characterization of their association with receptors.* Mol Cell Biol, 1998. **18**(12): p. 7278-87.
112. Pons, V., et al., *Hrs and SNX3 functions in sorting and membrane invagination within multivesicular bodies.* PLoS Biol, 2008. **6**(9): p. e214.
113. Mizutani, R., et al., *Sorting nexin 3, a protein upregulated by lithium, contains a novel phosphatidylinositol-binding sequence and mediates neurite outgrowth in N1E-115 cells.* Cell Signal, 2009. **21**(11): p. 1586-94.
114. Braun, V., et al., *Sorting nexin 3 (SNX3) is a component of a tubular endosomal network induced by Salmonella and involved in maturation of the Salmonella-containing vacuole.* Cell Microbiol, 2010. **12**(9): p. 1352-67.
115. Wiley, H.S. and P.M. Burke, *Regulation of receptor tyrosine kinase signaling by endocytic trafficking.* Traffic, 2001. **2**(1): p. 12-8.
116. Mosesson, Y., G.B. Mills, and Y. Yarden, *Derailed endocytosis: an emerging feature of cancer.* Nat Rev Cancer, 2008. **8**(11): p. 835-50.
117. Pochampalli, M.R., R.M. el Bejjani, and J.A. Schroeder, *MUC1 is a novel regulator of ErbB1 receptor trafficking.* Oncogene, 2007. **26**(12): p. 1693-701.
118. Dikic, I., *Mechanisms controlling EGF receptor endocytosis and degradation.* Biochem Soc Trans, 2003. **31**(Pt 6): p. 1178-81.
119. Haglund, K., P.P. Di Fiore, and I. Dikic, *Distinct monoubiquitin signals in receptor endocytosis.* Trends Biochem Sci, 2003. **28**(11): p. 598-603.
120. Kirisits, A., D. Pils, and M. Krainer, *Epidermal growth factor receptor degradation: an alternative view of oncogenic pathways.* Int J Biochem Cell Biol, 2007. **39**(12): p. 2173-82.
121. Cullen, P.J., *Endosomal sorting and signalling: an emerging role for sorting nexins.* Nat Rev Mol Cell Biol, 2008. **9**(7): p. 574-82.

Preface to thesis chapters

Preface to Chapter 2:

In this chapter I am only a co-author, not the first author of the paper, However I performed several of the protein work described in the paper and this chapter builds the foundation of my thesis as many of the results obtained serve as basis of the following chapters.

In our lab, 32 pGBM (frozen and paraffin embedded) were studied by microarray analysis. We demonstrated that pGBM is distinct from adult GBM in their gene expression profile. Using a Method of data reduction called Principal Component Analysis (PCA), we also showed that there are at least two subsets of pGBM that can be distinguished based on their association or lack of association with an aberrantly active Ras and Akt pathway in a sample. PGBM associated with an aberrantly active Ras pathway (Ras+ samples) showed a higher level of angiogenesis and had a poor survival compared to the other subset of pGBM showing no activation of either pathways. In this paper a target gene YB-1 was described, this was continued by other members in the lab, and hence there will be no mention of YB-1 throughout the rest of the thesis.

Preface to Chapter 3

This chapter serves as a continuation of the previous chapter, also a published paper. GBM are rare and frozen raw material is scarce. In order to validate our results on a larger dataset we obtained additional FFPE samples. I extracted RNA, performed microarray experiments and analyzed data sets generated from these FFPE samples that were a separate set from the frozen ones. Despite the high levels of RNA degradation in these samples, I was able to validate our previous findings and also showed that pGBM are a heterogenous disease and could

be divided in at least two distinct subgroups. Gene expression profiles of both of these groups were further analyzed and separate gene lists identifying differentially regulated genes were compiled. They validated our results on frozen samples, and further helped our determination of specific drivers of oncogenesis in pGBM. Importantly they also helped me identify SNX3 as a potential target in pediatric GBM that I further investigated *in vivo* and *in vitro* during my PhD.

Preface to Chapter 4

High grade astrocytomas are composed of anaplastic astrocytomas and glioblastoma which are heterogenous tumours. In the adult setting, multiple studies have been done to further stratify patients using integrated genomics and according to the tumour molecular profiles and clinical data especially survival. This ultimately may provide a better understanding to enable more precise drug targeting. In comparison, limited numbers of studies exist for pediatric HGA and importantly no further molecular stratification beside tumour grade. We know from the analysis of adult data sets that significant differences are found among grade III or anaplastic astrocytomas (AA) and grade IV (GBM) and that IDH and P53 mutations are major drivers of AA and secondary GBM. We also know that, in contrast to adults where patients with grade III tumours will progress to grade IV, pediatric GBM do not result from the progression of a grade III astrocytoma and occur as *de novo* tumours in the vast majority of cases. In that sense, it is important to establish the molecular differences between the grades III and IV astrocytomas, which are often compiled together and are treated similarly in studies available in the literature. Based on these observations AA and GBM may have potentially different molecular signatures across grades and the lifespan and molecular events amenable to therapeutic targeting may be identified by further analysis. Thus, we need a better understanding at the molecular level as to

what genes are being differentially expressed between the two grades and between pediatric and adult HGA. Microarrays on 10 AA samples were performed and gene expression profiles were compared to data set generated on pediatric GBM. We identified differences in gene expression profiles using hierarchical clustering, Anova testing ($p<0.5$) and PCA. Grade III astrocytomas clustered separately from grade IV tumours. Using the Ingenuity software for microarray data analysis, we identified the most significantly differentially regulated signaling pathways between the two grades. Importantly, grade III astrocytomas did not carry driver mutations recently identified by my lab in the H3F3A gene nor in IDH and TP53 genes. They showed increased activation of the mTOR pathway which may be amenable to therapeutic targeting in this setting.

Preface to Chapter 5

One of the differences between adult and pediatric GBM is that in adult GBM, EGFR is amplified while in children it is overexpressed without genetic amplification. Therefore, EGFR is being regulated at either the protein or RNA level in the pediatric setting and not on the genomic level. Our goal was to identify genes that were differentially regulated in the samples associated with Ras activation compared to the group with no Ras activation and not differentially expressed in adult GBM, and are potential targets involved in EGFR regulation. Through extensive investigation of hundreds of genes, the list was reduced to a handful of transcripts namely most differentially regulated genes, genes not identified in adult HGA, genes relevant to receptor tyrosine kinase expression and signaling, and genes which function is modulated by Akt. We chose to focus on a target gene based on its relevance to EGFR and Ras and PI3K/Akt activation; sorting nexin 3 (SNX3). We were able to show that SNX3 was overexpressed mainly in high grade primary pediatric GBM and that increased expression

correlated with increased EGFR, PDGFR and MET expression in a tumor. We also showed that overexpression of SNX3 in GBM cell lines, delays EGFR and MET degradation, sustains their signaling, increases cell proliferation, and causes tumors in vivo in nude mice.

CHAPTER 2

Molecular profiling identifies prognostic subgroups of pediatric glioblastoma and shows increased YB-1 expression in tumors.

Damien Faury[1$], André Nantel[2$], Sandra E Dunn[3], Marie-Christine Guiot[4], **Takrima Haque[1]**, Péter Hauser[5], Miklós Garami[5], László Bognár[6], Zoltán Hanzély[6], Pawel P. Liberski[7], Enrique Lopez-Aguilar[8], Elvis T. Valera[9], Luis G. Tone[9], Anne-Sophie Carret[1], Rolando F. Del Maestro[10], Martin Gleave [11], Jose-Luis Montes [12], Torsten Pietsch[13], Stephen Albrecht[14], and Nada Jabado[1*].

(Published Manuscript)

Faury, D., et al., *Molecular profiling identifies prognostic subgroups of pediatric glioblastoma and shows increased YB-1 expression in tumors.* J Clin Oncol, 2007. 25(10): p. 1196-208.

[1]Division of Hemato-Oncology, Department of Pediatrics, Montreal Children's Hospital Research Institute, McGill University Health Center, Montreal, Canada.
[2] Biotechnology Research institute, National Research Council of Canada, Montreal, Canada
[3]Laboratory for Oncogenomic Research, Department of Pediatrics, British Columbia Research Institute for Children's and Women's Health, Vancouver, British Columbia, Canada.
[4]Department of Pathology, Montreal Neurological Institute, McGill University Health Center, Montreal, Canada.
[5]2nd Department of Pediatrics, Faculty of Medicine, Semmelweis University, Budapest, Hungary
[6] Division of Neuro-surgery, Division of Pathology, National Institute of Neurosurgery, Budapest, Hungary.
[7] Department of Neuropathology, Medical University of Lodz, Lodz, Poland.
[8] Oncology Department, Pediatrics Hospital, Centro Medico Nacional Siglo XXI, Mexico City, Mexico
[9]Department of Pediatrics, University Hospital, Faculdade de Medicina de Ribeirão Preto, Universidade de São Paulo, Ribeirão Preto, São Paulo, Brazil.
[10]Division of Neuro-Surgery and the Brain Tumor Research Center, Montreal Neurological Institute, McGill University Health Center, Montreal, Canada.
[11] Department of Surgery, Prostate Cancer Center, Jack Bell Research Laboratories, Vancouver BC, Canada.
[12] Division of Neuro-Surgery, Montreal Children's Hospital, McGill University Health Center, Montreal, Canada.
[13]Department of Pathology, University of Bonn, Bonn, Germany.
[14]Department of Pathology, Montreal Children's Hospital, McGill University Health Center, Montreal, Canada.

[$] Contributed equally to the manuscript
* Corresponding author:
Nada Jabado, MD PhD, Montreal Children's Hospital Research Institute, 4060 Ste Catherine West, PT-239, Montreal, Qc, Canada, H3Z 2Z3. Tel: (514) 412 4400 ext 23270; Fax: (514) 412 4331; e-mail: nada.jabado@mcgill.ca

2.1 Abstract

Purpose: Pediatric glioblastoma (pGBM) is a rare, but devastating brain tumor. In contrast to GBM in adults (aGBM), little is known about the mechanisms underlying its development. Our aim is to gain insight into the molecular pathways of pGBM.

Material and Methods: Thirty-two pGBM and 7 aGBM samples were investigated using biochemical and transcriptional profiling. Ras and Akt pathway activation was assessed through the phosphorylation of downstream effectors, and gene expression profiles were generated using the UHN Human 19K cDNA arrays. Results were validated using real-time PCR and immunohistochemistry and compared to existing data sets on aGBM.

Results: There are at least two subsets of pGBM: One subset, associated with Ras and Akt pathway activation, has very poor prognosis and exhibits increased expression of genes related to proliferation and to a neural stem cell phenotype, similar to findings in aggressive aGBM. This subset was still molecularly distinguishable from aGBM after unsupervised and supervised analysis of expression profiles. A second subset, with better prognosis, is not associated with activation of Akt and Ras pathways, may originate from astroglial progenitors, and does not express gene signatures and markers shown to be associated with long-term survival in aGBM. Both subsets of pGBM show overexpression of Y-Box-Protein-1 that may help drive oncogenesis in this tumor.

Conclusion: Our work, the first study of gene expression profiles in pGBM, provides valuable insight into active pathways and targets in a cancer with minimal survival and suggests that these tumors cannot be understood exclusively through studies of aGBM.

2.2 Introduction

Brain tumors are the leading cause of cancer-related mortality in children. Pediatric grade-IV astrocytomas (glioblastomas, pGBM) are non-neuronal tumors originating from the astrocytic lineage [1-3], account for 15% of all pediatric brain tumors and have a 3-year survival of less than 20% and high morbidity [4]. Considerable information is available on adult GBM (aGBM), where this tumor is frequent and deadly and thought to arise by at least two molecular pathways. Secondary GBM occur in adults aged less than 40 years, evolve from low-grade astrocytomas, and have a high frequency of *p53* mutations and a low frequency of *Epidermal Growth Factor Receptor* (*EGFR)* amplification. Primary GBM (*de novo*) target older patients and exhibit gain of function mutations of *EGFR*. Both forms are indistinguishable to pathologists, and share aberrations of the p53 and RB pathways and similar prognosis[1-3, 5]. A number of gene expression profiling analyses performed in aGBM helped to identify molecular events leading to oncogenesis and provided more accurate means for classification of subtypes and outcomes[6-8]. Fewer molecular data exist on the mechanisms underlying the development and progression of pGBM, mainly because of the relative lack of frozen samples[9, 10]. PGBM are histologically indistinguishable from aGBM. Although they occur as *de novo* tumors, they exhibit *p53* mutations but only rarely *EGFR* amplification[11]. Moreover, the few cytogenetic studies show that pediatric and adult astrocytomas have different chromosomal imbalances[12, 13], and published data study pGBM in conjunction with other grade and lineage gliomas (grade III, mixed oligo-astrocytomas)[11]. A better understanding of the molecular pathogenesis of pGBM is required for the development of more effective therapies, particularly since most current treatments are based on molecular knowledge gained from aGBM.

Compelling data from human studies and animal models of GBM indicate a key role for the combined activation of the Ras and Akt pathways that control cell growth, differentiation and survival[11]. Activity of Ras is aberrantly increased in most aGBM and aGBM cell lines, and Akt activation is observed in ~70 % of aGBM[14, 15]. Activation of these pathways in pGBM has not been investigated.

To gain insight into the molecular pathways driving oncogenesis in pGBM, we investigated 32 pGBM and, in parallel, 7 aGBM tumors.

2.3 Materials and Methods

Characteristics of Samples and Central Pathological Review. A neuro-pathologist independently blindly reviewed all samples to ensure consistent classification based on contemporary guidelines from the World Health Organization[16]. Only grade IV astrocytomas (GBM) were used. Clinical findings of all patients with GBM and control brains are shown in **Tables 2.1** and **2.2**.

Cell line, Protein Extraction, SDS-PAGE, immunoblot and immunohistochemical analysis. U87 aGBM cells was grown as described[11]. Extracts were prepared from cell pellets or from human brain tissue and processed as previously described[15]. Immunohistochemical analyses for pErk, pAkt, GFAP, p53, YB1 were performed as described Pollack et al. and Sutherland et al. [16, 17].

Laser Capture Microdissection(LCM) RNA Extraction, and Linear Amplification(SupTable1)**.** Frozen sections (8μm) were cut and processed for hematoxylin-eosin staining as described[18].

The neuro-pathologist identified tumor cells for capture for each sample. The rest of the block was used for protein analysis. RNA was extracted from controls and tumor samples and subjected to 2 rounds of T7-RNA-polymerase amplification. Fidelity and reproducibility of RNA amplification has been shown[19] and was further validated.

Microarray Analyses. RNA from 14 pGBM and 7aGBM fresh frozen (FF) samples was compared to the same reference pooled RNA extracted from 3 normal brains from children aged 1, 7 and 15 years respectively. Cy3 or Cy5-labeled cDNA probes from samples and pooled controls were hybridized to Human 19K cDNA spotted arrays (19,008 human genes and ESTs, University Health Network, http://www.microarrays.ca). Slides were scanned and intensity quantified using QuantArray® software package. Inversion of fluors in distinct cDNA probes were performed (dye swap) to account for non-specific dye associated effects on hybridization and signal detection. The lowess scatter smoothing algorithm in the GeneSpring 7.0 software package (Agilent) normalized the raw fluorescence data. We analyzed 60 hybridizations consisting of dye-swap hybridizations of 30 biological replicates for 14 pediatric and 7 aGBM samples (analysis of several samples was duplicated to assess for reproducibility from 2 different RNA extractions and amplifications). "Filter on Confidence" and ANOVA statistical tools in GeneSpring were used to identify genes with reproducible changes in transcript abundance. The same software package was used to perform hierarchical clustering and PCA. Quantitative-RT-PCR was performed in to validate relative gene expression.

2.4 Results

Activation of Ras and Akt pathways occurs in only a subset of pGBM and is associated with poor outcome.

We investigated activation of the Ras and Akt pathways in 18 frozen pGBM tumors by western blot analysis using phosphorylation-specific antibodies against known effectors of these pathways. U87 aGBM cell-line and a pooled protein lysate from samples of 3 pediatric control brains (1, 7 and 15 years) were used as positive and negative controls respectively. Slides from the same blocks were stained with hematoxylin/eosin confirming that only lysates from pGBM tumor populations were being analyzed. Phosphorylation of Raf, Mek1/2 and Erk 1/2 was seen in 12/18 pGBM samples and in U87 cell-line indicating activation of the Ras pathway (Fig.2.1A, data not shown). Phosphorylation of these downstream effectors of Ras was not observed in 6/18 pGBM. Phosphorylation of Akt and GSK3 was observed in 10 samples (Fig.2.1A, data not shown), all of which were also active for Ras and had lower levels of PTEN, the dual-activity phosphatase known to participate in inactivating the Akt pathway[20].

We validated results obtained by western blot using an immunohistochemical approach on 18 formalin-fixed paraffin-embedded (FFPE) pGBM samples that included 4 samples previously tested by western blot on their frozen counterparts, and another new set of 14 pGBM for which no frozen counterparts were available. Sections from samples were tested for pErk (associated with Ras activation), pAkt (associated with Akt activation) and Glial Fibrillary Acidic Protein (GFAP, astrocytic marker) immunoreactivity. Five samples showed no staining for pErk, while showing normal staining for GFAP of adjacent sections, excluding problems related to tissue preservation. The remaining samples showed strong staining for pErk

(Fig.2.1B). pErk positive regions contained spindle-like tumor cells showing atypical elongated nuclei and a fibrillary staining typical of GBM and active Ras[21]. pAkt was present in 13/18 samples that were also positive for pErk (Fig. 2.1B). Where material for both technical approaches was available, the same results were obtained.

When investigating putative prognostic factors, striking results were obtained for Ras activation. Children with active Ras (21/32) had poor survival with only one survivor, whereas 5/11 with no Ras activation are alive and disease free, with a follow-up of at least 4 years (log rank of $p<0.009$). This result reflects Akt activation as most patients with active Ras also had active Akt (19/21). Gender, younger age, treatment, p53-expression were not associated with better survival with the limitation of sample size[22].

Availability of frozen tissue from pGBM is limited. To determine if the data obtained on Ras and Akt activation in pGBM has potential prognostic value, we performed immunohistochemistry for pErk and pAkt on an independent data set of 21 FFPE pGBM samples (Table 2.2). PErk and pAkt were highly immunoreactive in 13/21 samples, whereas both staining were negative in 8/21 samples (fig 2.1B). Survival data further validated our data on the association of Ras and Akt activation with poor survival in pGBM (Table 2.2). Our data suggest that there are at least 2 forms of pGBM: one form with poor survival, with only one patient alive, associated with an active Ras/Akt pathways (35 [66%] of 53 samples for Ras and 31[58.5%] of 53 for Akt), and a second form with a better prognosis (9 of 18 children alive and disease free), without activation of either Ras or Akt (18 [34% of 53; log-rank $P<.0001$; Fig 2.1C, Tables 2.1 and 2.2).

Transcriptional profiling distinguishes 2 subsets of pGBM based on their association with Ras/Akt activity and reveals a molecular signature for pGBM that is distinct from aGBM

To study gene expression changes, we selected an approach that allows us to compare changes between tumor and normal brain as well as changes between pGBM samples. RNA from 14 pGBM frozen samples was isolated and hybridized to Human 19K cDNA spotted arrays together with the same reference pooled RNA extracted from 3 control pediatric brains. LCM was used to selectively capture malignant astrocytes. RNA was subjected to 2 rounds of T7 linear amplification (aRNA) to circumvent the limited amount of frozen material[23-25]. GeneSpring's "Filter on Confidence" tool identified 2593 transcripts with statistically significant changes in abundance in the 14 pGBM samples compared to the pooled control (Welsch t-test, p-value<0.0001, multiple testing correction: Benjamini and Hochsberg, false discovery rate of 3.4%). Two-dimensional hierarchical clustering organized and visualized the profiles of these transcripts (Y-axis) from each of the 14 samples (X-axis, Fig. 2.2A) and indicated a high degree of homogeneity in pGBM. Other statistical algorithms (the Wilcoxon-Mann-Whitney test of Significance Analysis of Microarrays) were tested with the same results. We analyzed the data set using a module-level view obtained from a 'cancer compendium'[26] and also organized the gene sets using GoMiner, a computer resource that incorporates the hierarchical structure of the Gene Ontology (GO) Consortium[27] to automate a functional categorization of gene lists based on biological processes. Both methods aim to distill a higher-order. They yielded similar results showing, as expected, that pGBM are actively proliferating tumors (Fig. 2.2B).

To visualize similarities within samples, we used Principal Component Analysis (PCA), a method of data reduction in which the high dimensionality of the data is reduced to 2-3 viewable dimensions representing linear combinations of genes that account for most of the variance of the

data set. PCA separated samples into 2 groups indicating the presence of at least two distinct populations of pGBM (Fig. 2.2C). These populations were associated with Ras/Akt activity in a sample (Ras active color coded in yellow, inactive in red) and not with other known markers for pGBM (necrosis, proliferation index, p53 expression, age)[22, 28]. ANOVA testing identified 1437 transcripts that could distinguish tumors associated with differing Ras activity (Welch t-test, p-value cutoff 0.0001, multiple testing correction: Benjamini and Hochsberg). Most transcripts were distinct from those that distinguished pGBM from control brain (Fig 2.2C). GO Terms analysis shows that transcripts associated with Ras/Akt active tumors exhibit enhanced rates of nucleic acid, protein synthesis, and metabolism. With the limitation of sample size, ANOVA testing of expression profiles did not reveal a difference based on treatment, necrosis, age, or p53-overexpression[10, 16].

To determine whether pGBM are molecularly distinguishable from aGBM, we performed microarray analysis on 7 aGBM samples, using the same LCM/RNA amplification approach and the same reference control aRNA. Using scatter plots, several of the changes in transcript abundance that distinguish tumors from control brain are maintained between aGBM and pGBM. Using PCA, components 2 and 3 showed that aGBM (coded in blue) cluster separately from both types of pGBM (Fig 2.2C). Furthermore, ANOVA testing, using the same stringency as before, identified a sharp signature of 1569 transcripts that distinguished pGBM from aGBM (Fig 2.2C). These transcripts combined with the 1437 genes that distinguished pGBM based on their association with Ras activity were separated by conditional hierarchical clustering (Fig 2.3A). A first tree-branching separated Ras-non-active pGBM samples from Ras-active samples. A second branching in samples associated with Ras activation separated pGBM from aGBM. One

long-term survivor aGBM clustered with Ras-non-active samples. Sample showed weak pErk staining.

Data from transcriptional profiling mirror data obtained on the protein level and indicate that there are at least 2 subgroups of pGBM and that both differ molecularly from aGBM.

Validation of the data set and identification of targets involved in pGBM gliomagenesis

There are no reports of gene expression profiling that specifically target pGBM. We compared our results to recent series on adult High-Grade-Gliomas(aHGG). Using the common gene name as a correspondence marker for an independent data set of 31 aHGG[8], we found an overlap between both data sets. Phillips et al. identified prognostic subgroups of aHGG[29]: tumors segregated into subclasses based on their preferential expression of genes characteristic of neural tissue(PN, favorable prognosis), proliferating cells(Prolif, poor risk disease), or mesenchymal tissues(Mes, poor risk disease). Authors likened Mes, Prolif, and PN signatures to those of neural stem cells, transit-amplifying cells, and immature neurons, respectively. We applied their classification scheme to our data set (Fig 2.3B-2.3C). PCA using their 108 probes also separated pGBM samples from aGBM samples and both subsets of pGBM. AGBM, as expected, had the Mes or Prolif signatures as did Ras-active pGBM(Fig 2.3B). However, this subset of pGBM could still be distinguished from aGBM. Conditional clustering with Pearson correlation using the Mes and Prolif probe sets separated aGBM from both subsets of pGBM(Fig 2.3C). PGBM associated with no Ras/Akt activation lacked the PN signature associated with better prognosis in aGBM. These data validate our data set and show that, aside from the lack of Akt activation, the pGBM subset associated with a better survival has a unique molecular profile that is distinct from known markers of long-term survivors in aGBM.

PGBM associated with no Ras/Akt activation express no neural stem cell markers and up-regulate apoptosis associated transcripts.

Recent evidence suggests that HGG may arise from stem-cell like cancer cells at multiple stages of differentiation[30]. Tumors associated with Ras/Akt activation and poor prognosis overexpressed markers associated with neural stem cells including CD133, nestin, Maternal Embryonic Leucine Zipper Kinase(MELK), vimentin, and Dlx2, whereas the subset of pGBM associated with no activation of Ras/Akt and better outcome only showed increased vimentin expression[30-32](Fig 2.4A). Expression levels were validated by qRT-PCR for all these transcripts (data not shown). Using Go-Miner, differentially modulated transcripts associated with Ras-non-active pGBM showed overexpression of gene sets involved in apoptosis. Conversely, aGBM and pGBM associated with a Ras-active pathway showed overexpression of gene sets involved in protein synthesis, translation, transcription, DNA repair and synthesis.

Y-Box protein 1(YB1) is overexpressed in pGBM and may increase EGFR expression in Akt active samples

YB-1 showed increased expression (3.8 fold relative to normal brain) in 12/14 pGBM samples, but not in aGBM (Fig 2.2D). YB-1 was further investigated as it is involved in brain embryogenesis and contributes to oncogenesis in a range of epithelial cancers potentially through Akt mediated phosphorylation[11]. We validated expression of YB-1 by qRT-PCR and by immunohistochemistry(Fig 2.4B-C, Tables 2.1-2.2). YB-1 was overexpressed in 26/32 samples with mostly nuclear localization in samples with active Akt, and cytoplasmic in samples with no active Akt. These data were corroborated by results obtained on the independent data set of 37 pGBM samples: 26/37 positive with nuclear staining for YB-1 in Akt active samples (Table 2.2).

Nuclear YB-1 increases expression of several genes including EGFR[11]. We found EGFR overexpression by qRT-PCR and immunohistochemistry mainly in Akt-active samples(Tables 2.1-2.2).

2.5 Discussion

This study is one of the first reports of gene expression profiling in pGBM that focuses exclusively on pGBM. Protein analysis and transcriptional profiling suggests that there are at least two subtypes of pGBM, one associated with Ras/Akt-activation and poor prognosis and the other with no obvious Ras/Akt activity and a better outcome (Fig 2.1). This is in contrast to aGBM, where Ras pathway is activated in most tumors[14, 33]. Even though they share, as expected, common gene sets that are mainly related to the general tumorigenic process, both subtypes of pGBM exhibit distinct profiles from aGBM (Figs 2.1-2.4).

Previous studies on pHGG reported that patients older than 3 years had increased p53 expression in tumors and both parameters correlated with worse outcome[16, 22, 28]. P53 overexpression in this study was not associated with differences in survival or in gene expression patterns, probably due to the sample size and the limited number of infants we tested. Established markers of better outcome in aHGG include a younger age, grade III and absence of necrosis on histology, no Akt activation, and, more recently molecular signatures associated with NOTCH signaling and pro-neural markers[7, 32, 34, 35]. In this study on grade IV tumors, we found Akt activation, expression of markers of neural stem cells (nestin, dlx2, CD133, vimentin, ELK), a proliferative and, to a lesser extent, a mesenchymal signature to be common prognostic factors between pGBM associated with Ras/Akt activation and aGBM. However, despite these similarities, we could still distinguish both subsets using unsupervised and supervised analysis

(Figs 2.2-2.3). The subset of pGBM showing a better outcome did not have neuronal lineage markers as seen in long-term aHGG survivors[32], whereas we observed up-regulation of genes associated with apoptosis and a phenotype consistent with immature astroglial cells [36, 37](CD133-, Dlx2-, nestin-, ELK-, vimentin+).

YB-1 was overexpressed in 52/69 (75%) of pGBM (Fig. 2.4-Tables1-2). YB-1 is involved in brain development[38] and nuclear localization of this transcription factor is associated with poorer outcome, increased *MDR* expression and tumor progression in several cancers, which did not previously include CNS tumors[36]. YB-1 was mainly expressed in the cytoplasm of pGBM samples not displaying Ras/Akt activation and may have contributed to general transcriptional repression through its binding to pro-mRNAs[37](Fig 2.4-Table 2.2). In breast cancer cell lines, Akt-mediated YB-1 phosphorylation leads to nuclear translocation, relieving the translational repression of YB1[17, 37] and promoting increased expression of genes including *EGFR*, a known oncogene in primary aGBM[39, 40]. YB-1 was mainly nuclear in pGBM associated with Ras/Akt activation (Fig. 2.4D, Tables 2.1-2.2), which displayed increased *EGFR* levels (Tables 2.1-2.2). These findings indicate that YB-1 may be one target of active Akt in pGBM contributing to gliomagenesis.

Ras and Akt cooperate in tumorigenesis and increase translation efficiency in tumor cells[14, 15, 41-43] as also shown in this study (Figs. 2.2-2.3), which may also account for differences in survival we see between both sub-groups of pGBM.

Our work suggests that pGBM cannot be understood exclusively through studies of aGBM. We have strong leads for mechanistic events including YB-1 expression that warrants additional work and provide insight into molecular profiles in a pediatric cancer where survival is minimal.

2.6 Tables and Figures

Table 2.1 Characteristics of all frozen samples included in study

Samples	Gender	Age	FFPE	Microarray	Akt (WB)	Ras (WB)	EGFR (qRT-PCR)	YB1 (qRT-PCR)	Survival from surgery
Pediatric GBM**									
P1	F	7	no	yes	neg	neg	0.6	1.8	**A, 4 Y**
P2	F	4	no	yes	neg	pos	1.5	3.7	D, 12 M
P3	F	10	no	yes	neg	neg	1.0	2	D, 5 M
P4	F	14	no	yes	neg	neg	1.1	0.5	**A, 6 Y**
P5	M	14	no	yes	neg	neg	1.9	2.6	**A, 6 Y**
P6	M	14	no	yes	pos	pos	10.0	13.7	D, 1 M
P7	F	9	no	yes	pos	pos	4.6	6.7	D, 2 M
P8	M	1	no	yes	pos	pos	7.5	10.6	D, 7 M
P9	F	11	no	yes	pos	pos	2.2	4	D, 9 M
P10	F	13	no	yes	pos	pos	2.7	6.7	D, 14 M
P11	M	2	no	yes	neg	neg	1.9	4.6	**A, 5 Y**
P12	F	16	no	yes	pos	pos	3.9	6.5	D, 2 M
P13	M	16	no	yes	pos	pos	4.3	8.1	D, 36 M
P14	M	13	no	yes	pos	pos	3.0	4.5	D, 11 M
P15*	F	7	yes	no	neg	neg	1.2	1.6	**A, 4Y**
P16*	M	0.5	yes	no	pos	pos	4.7	5.3	D, 7 M
P17*	F	4	yes	no	neg	neg	1.6	1.2	D, 12 M
P18*	F	4	yes	no	pos	pos	3.9	4.5	**A, 6 Y**
Primary Adult GBM									
A1	M	52	no	yes	pos	pos	4.2	1.3	D, 10 M
A2	F	30	yes	yes	neg	pos	6.3	0.4	D, 26 M
A3	M	70	yes	yes	pos	pos	15.1	1.2	D, 5 M
A4	F	82	no	yes	pos	pos	4.2	0.9	D, 3 M
Secondary Adult GBM									
A5	M	52	no	yes	pos	pos	1.1	1.5	D, 9 M
A6	F	49	yes	yes	pos	pos	1.3	1.2	D, 13 M
A7	M	67	yes	yes	pos	pos	1.0	1.1	D, 5 M
Control Brain									
CB1	M	1	yes	yes	neg	neg	ND	ND	A
CB2	F	7	yes	yes	neg	neg	ND	ND	A
CB3	F	15	yes	yes	neg	neg	ND	ND	A

Table 2.2. Characteristics of all Formalin-Fixed Paraffin Embedded samples in the study.

GBM	Age (years)	pAkt (IHC)	pErk (IHC)	EGFR (IHC)	YB1 (IHC)	Survival from surgery
P15	7	neg	neg	neg	neg	**A, 4Y**
P16	0.5	pos	pos	pos	C, N	D, 7 M
P17	4	neg	neg	neg	neg	D, 12 M
P18	4	pos	pos	pos	C,N	**A, 6 Y**
P19	6	neg	neg	neg	neg	D, 15 M
P20	12	pos	pos	pos	C, N	D, 11 M
P21	8	pos	pos	pos	C, N	D, 14 M
P22	14	pos	pos	pos	C,N	D, 2.5Y
P23	8	pos	pos	pos	C, N	D, 9 M
P24	8	pos	pos	pos	C, N	D, 14 M
P25	12	pos	pos	pos	C, N	D, 3 Y
P26	7	pos	pos	pos	C, N	D, 2 M
P27	9	pos	pos	pos	C, N	D, 36 M
P28	12	neg	neg	neg	neg	D, 3Y
P29	4	neg	pos	neg	C	D, 2Y
P30	16	neg	neg	neg	C	D, 2Y
P31	6	neg	neg	neg	neg	D, 2Y
P32	5	neg	pos	neg	C	D, 7 M
SP1	10	pos	pos	pos	C,N	D,6M
SP2	12	pos	pos	pos	C, N	D, 9 M
SP3	4	neg	neg	neg	neg	**A 3Y**
SP4	5	neg	neg	neg	neg	D, 15 M
SP5	6	neg	neg	neg	neg	**A, 5Y**
SP6	12	pos	pos	pos	C, N	D, 11 M
SP7	8	pos	pos	pos	C, N	D, 4 M
SP8	14	pos	pos	pos	C,N	D, 18M
SP9	8	pos	pos	pos	C, N	D, 9 M
SP10	8	pos	pos	pos	pos	D2M
SP11	12	neg	pos	neg	neg	D, 1 Y
SP12	7	pos	pos	pos	C, N	D, 5 M
SP13	10	pos	pos	pos	C, N	D, 36 M
SP14	12	neg	neg	neg	neg	D, 2Y
SP15	4	neg	neg	neg	neg	D, 2Y
SP16	5	neg	neg	neg	neg	**A, 4Y**
SP17	6	neg	neg	neg	neg	D, 6M
SP18	9	pos	pos	pos	C, N	D, 7 M
SP19	4	pos	pos	pos	C, N	D, 3M
SP20	7	pos	pos	pos	C, N	D, 10M
SP21	15	pos	pos	pos	C, N	D, 9M
CB1	1	neg	neg	neg	neg	A
CB2	7	neg	neg	neg	neg	A
CB3	15	neg	neg	neg	neg	A

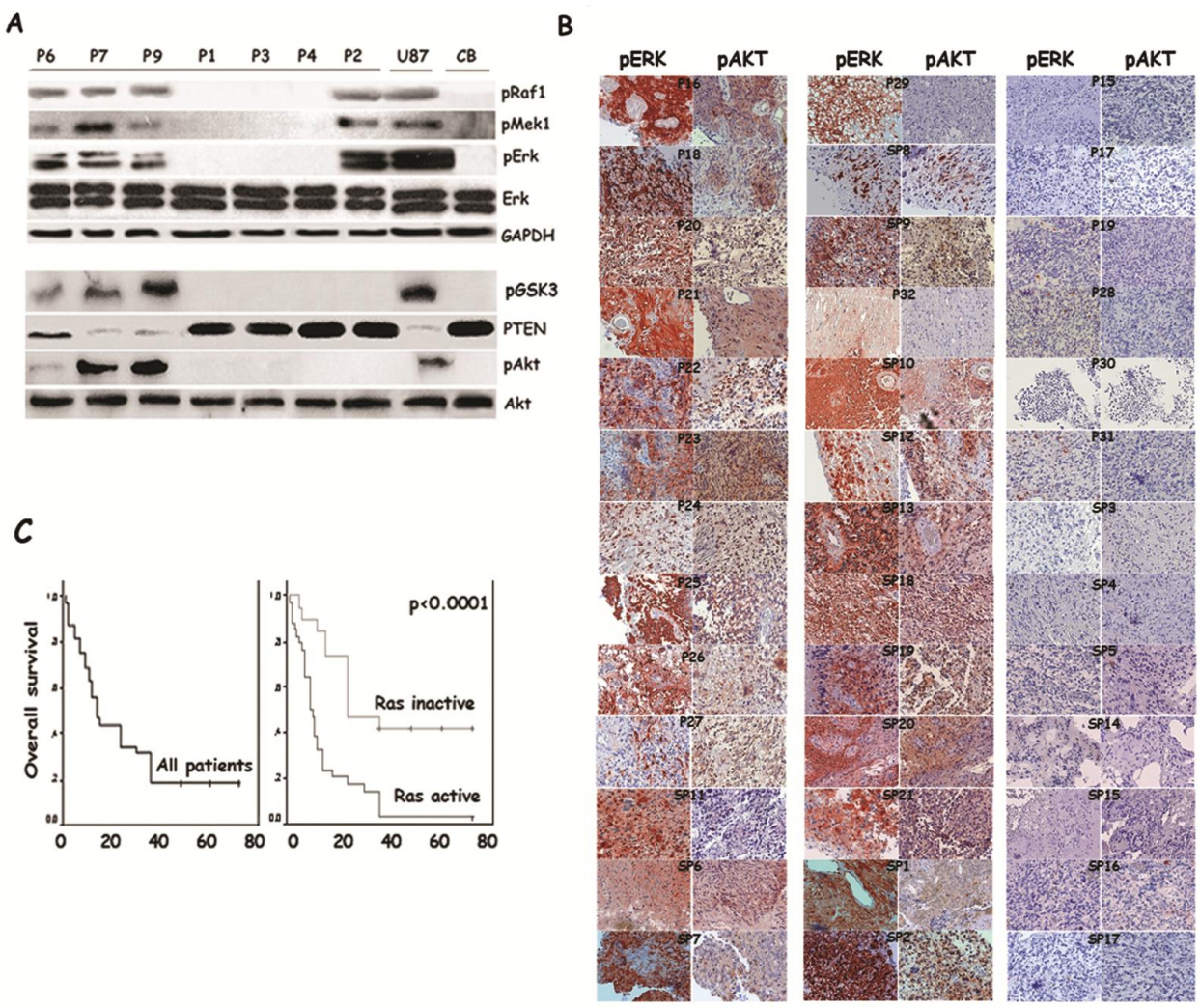
A
P6
P7
P9
P1
P3
P4
P2
U87
CB
pRaf1
pMek1
pErk
Erk
GAPDH
pGSK3
PTEN
pAkt
Akt
B
pERK
pAKT
pERK
pAKT
pERK
pAKT
C
Overall survival
All patients
p<0.0001
Ras inactive
Ras active
0
20
40
60
80
0
20
40
60
80

Figure 2.1

A.

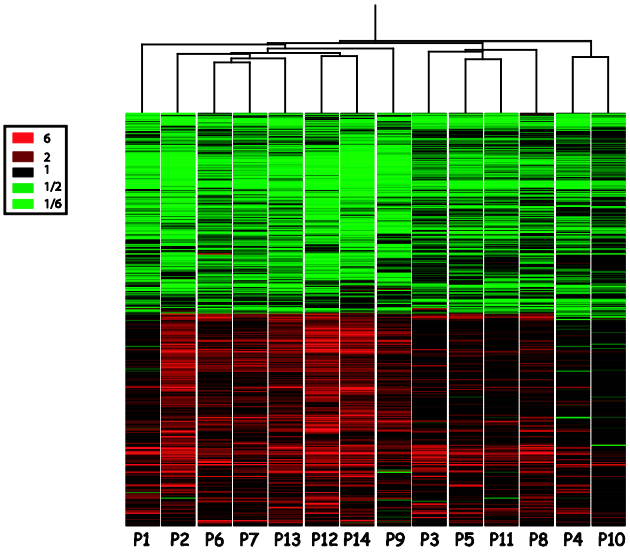

B.

Cancer gene expression module		p-value
UP		
83	Protein biosynthesis	1.26E-19
114	Ribosomes	4.96E-19
151	Ribosomes	5.13E-18
32	Nucleic acid binding	1.14E-16
98	Nucleus and transcription	2.06E-11
54	Cell cycle (expression clusters)	5.44E-11
252	TFs and nuclear	2.63E-10
198	Nucleus	6.14E-10
8	DNA metabolism	3.05E-09
3	Mitosis	4.35E-09
17	DNA replication	2.32E-07
105	Cell cycle	1.16E-06
47	ECM and collagens	1.39E-06
DOWN		
11	Neurogenesis	5.18E-25
100	Neurogenesis	4.86E-22
66	Neurogenesis	7.99E-22
137	CNS genes	1.77E-21
274	Vesicular transport/synapse genes	3.10E-08

C.

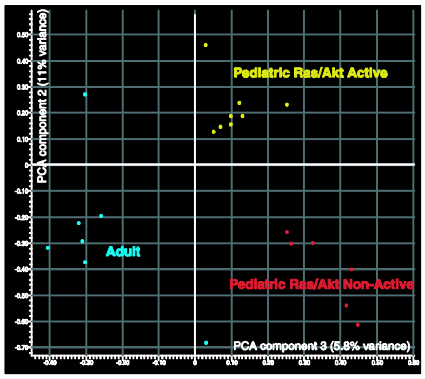

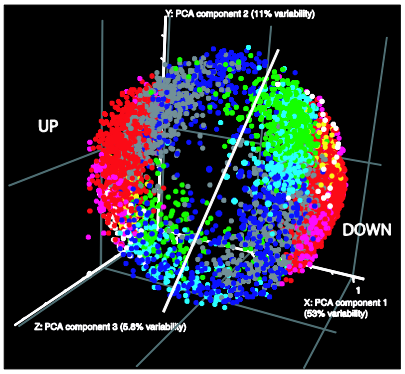

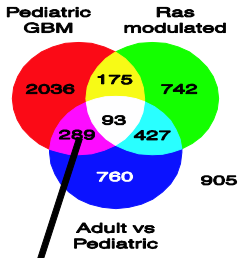

D.

Systematic	P-value	pGBM/CB	aGBM/CB	pGBM/aGBM	Common
AA114919	5.58E-14	3.861	1.564	2.443	YB-1
BF967458	6.59E-14	3.579	1.807	1.783	CD63
BQ028065	6.77E-14	2.799	1.684	1.663	RPN2
BM793706	2.86E-12	4.617	1.691	2.730	HLA-B
BM974828	2.74E-11	2.839	1.144	2.482	RPL18
N80187	1.90E-10	3.818	1.766	1.848	IGFBP7
AA116099	9.19E-10	2.161	1.273	1.698	MAGED2
BQ004942	4.16E-09	2.545	1.060	2.400	CCND1
N54628	1.16E-08	2.508	1.185	2.116	ARF4
BG398130	1.16E-08	2.584	1.194	2.165	RPL41
AL568322	6.83E-07	2.126	0.962	2.209	TUBA3

CB: control brain , systematic=chip ID, Common=common name

Figure 2.2

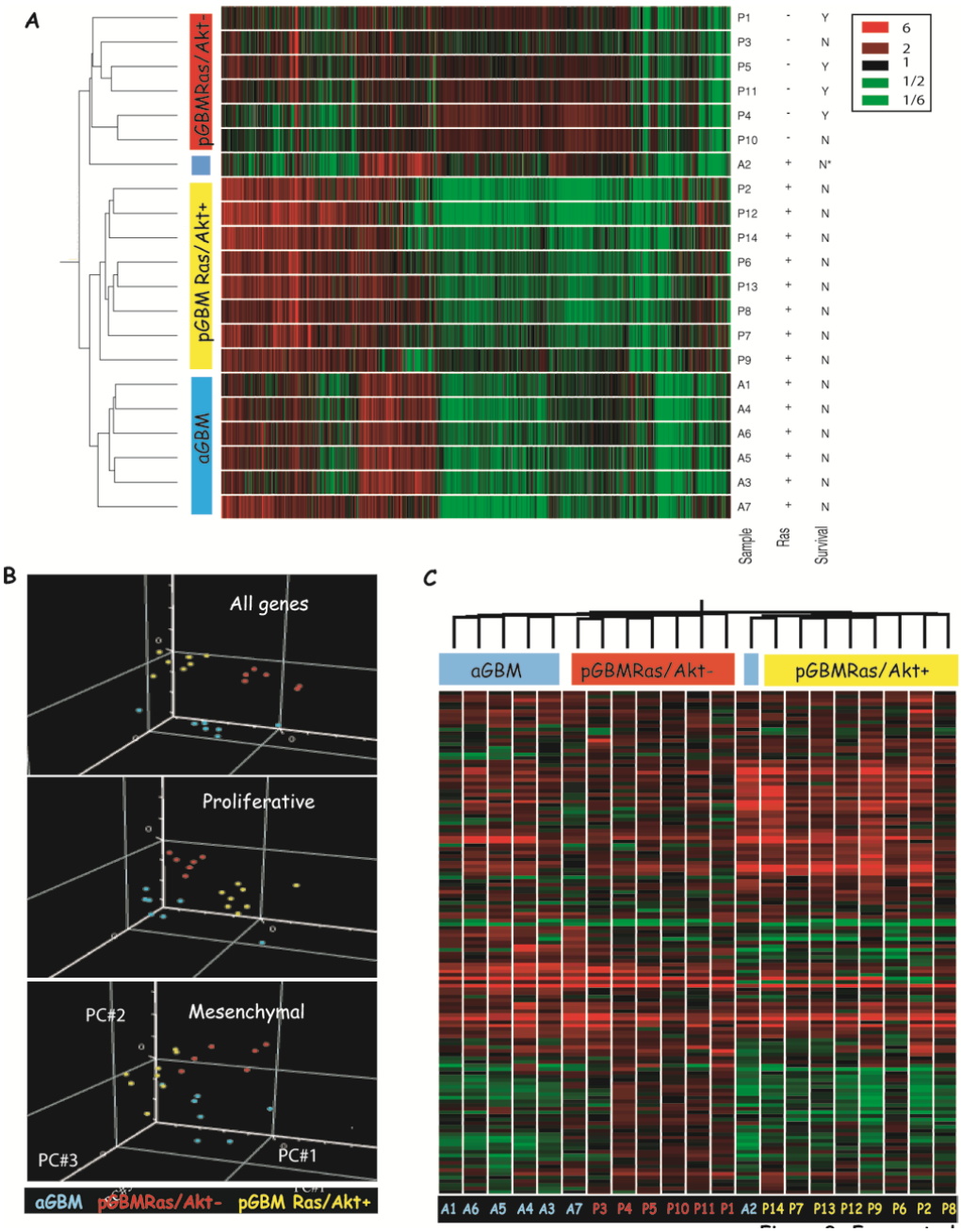
A
pGBMRas/Akt-
pGBM Ras/Akt+
aGBM
P1 - Y
P3 - N
P5 - Y
P11 - Y
P4 - Y
P10 - N
A2 + N*
P2 + N
P12 + N
P14 + N
P6 + N
P13 + N
P8 + N
P7 + N
P9 + N
A1 + N
A4 + N
A6 + N
A5 + N
A3 + N
A7 + N
Sample
Ras
Survival
6
2
1
1/2
1/6
B
All genes
Proliferative
Mesenchymal
PC#2
PC#3
PC#1
aGBM
pGBMRas/Akt-
pGBM Ras/Akt+
C
aGBM
pGBMRas/Akt-
pGBMRas/Akt+
A1 A6 A5 A4 A3 A7 P3 P4 P5 P10 P11 P1 A2 P14 P7 P13 P12 P9 P6 P2 P8

Figure 2.3

A

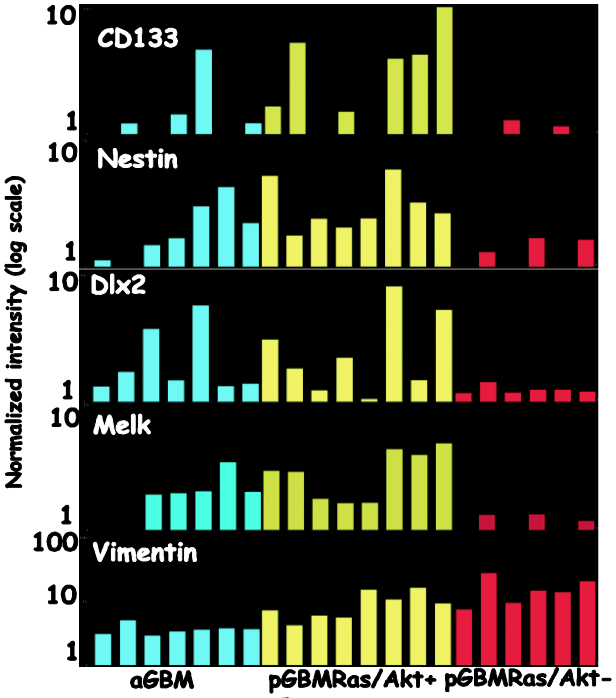

B

GBM	YB-1		Arha	
	Genespring	qRT-PCR	Genespring	qRT-PCR
P1	1.65	1.8+/- 0.22	1.25	1.5+/- 0.36
P2	3.22	3.7 +/- 0.39	1.89	1.6+/- 0.52
P3	3.07	2 +/- 0.31	1.75	2.6 +/- 0.72
P4	1.54	0.5 +/- 0.13	0.95	0.3 +/- 0.07
P5	3.61	2.6+/- 0.16	1.31	0.7+/- 0.34
P6	7.37	13.7+/- 0.62	1.94	3.3+/- 1.10
P7	4.04	6.7+/- 0.15	1.16	0.6+/- 0.19
P8	5.28	10.6 +/- 0.32	2.35	4.2 +/- 1.34
P9	1.76	4 +/- 0.31	2.18	3.1 +/- 1.32
P10	4.48	4.6 +/- 1.01	0.91	0.8+/- 0.10
P11	2.62	6.7 +/- 0.49	1.19	1.1 +/- 0.24
P12	3.2	6.5+/- 0.49	3.24	3.1+/- 1.73
P13	4.5	8.1 +/- 0.21	3	6.4+/- 1.50
P14	3.68	4.5+/- 1.33	2.98	3+/- 1.23

C

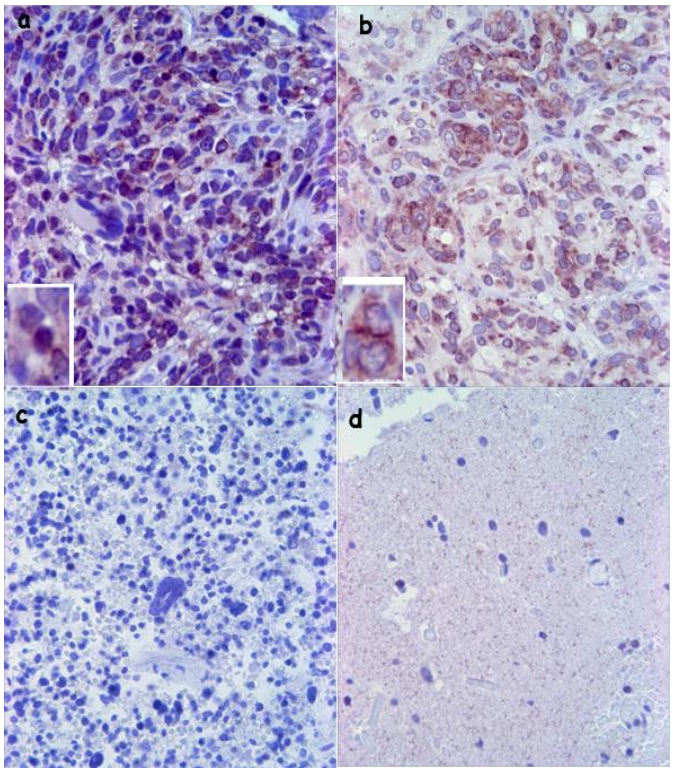

Figure 2.4

Figure Legends

Fig. 2.1: Phosphorylation of Ras and Akt effectors in Pediatric GBM and effect on survival. **(A)** Total cell extracts of pooled control brains, the U87 cell line and 18 pediatric GBM were separated by electrophoresis and immunoblotted using antibodies against GAPDH and signaling proteins representing Ras (ERK, MEK, Raf) and Akt (Akt, PTEN, GSK3) pathways. Control brain (CB) represents pooled lysates from 3 pediatric normal brains; Results from 7 pGBM, the U87 cell line treated with sorbitol for optimal activation of the Ras pathway (positive control) and the pooled lysate from normal brains (negative control) are shown. Characteristics of the pGBM samples are detailed in Table 1. Phospho-specific antibodies are denoted with a prefix "p". Unphosphorylated proteins and GAPDH account for protein loading. **(B)** Immunohistochemistry for pErk and GFAP on sections from 18 FFPE samples from pGBM (prefix P, full characteristics provided in Table 2). Sections were stained using anti-pERK (left panel) and anti-GFAP (right panel) followed by detection using the DAKO kit (red accounts for positive staining) and hematoxylin counterstaining. Staining intensity was scored as in [44]. Representative staining from 7pGBM samples and a control brain are shown. **(C).** Kaplan-Meier overall survival curve for all patients (left panel, 18.75%) and for patients with and without Ras activation in their GBM tumor (right panel) showing that aberrant signaling through Ras in pGBM is associated with a poorer outcome (Log Rank $p<0.009$).

Fig. 2.2: Tumor samples show distinct expression profiles that correlate with the age of the patient and Ras activation. (A). Unsupervised hierarchical clustering of the 12593 probes with a statistically significant (Welsch t-test, p-value cutoff 0.0001, multiple testing correction: Benjamini and Hochsberg) change in transcript abundance between 14 pediatric GBM and the

pool of normal brain tissue shows homogeneity in transcript profiles. Experimental samples are on the X axis and the probes on the Y axis. Each experimental data point is colored according to the change in fluorescence ratio (more abundant in pGBM colored in red, less abundant colored in green, color scale provided). **(B)** The differentially expressed gene set in pGBM was compared to a module map showing conditional activity of expression of groups of genes (modules) in cancer [26]. Modules where gene sets were up-regulated (up, red) and down-regulated (down, green) are listed. P-values represent the significance of the overlap between our gene lists and the cancer gene expression modules. **C)** The 14 pediatric and 7 aGBM samples were subjected to a Principal Components Analysis (PCA) based on the expression profile measured on 15,068 individual probes. ***Left panel:*** A two-dimensional plot of PCA (used to reduce the dimensionality of the gene expression profiles) components 2 and 3 resulted in a clear differentiation between the aGBM and pGBM and can also distinguish the Ras scores of the pediatric tumors (left panel). Although component 1 could explain 58% of the variability in the data set, most of it described variations in the amplitude of changes in transcript abundance between GBM and normal brain tissue, and did not produce a distinct separation between the different subtypes of GBM. ***Middle and right panels:*** Three-dimensional PCA on the 5427 most significant genes placed according to their respective profile in all of the tested tumors. In such a representation, transcripts with a similar profile across the entire dataset will find themselves closer to each other. Abundant transcripts in GBM clustered on the left of the distribution while the less abundant transcripts clustered on the right. Each spot is colored according to the Venn Diagram (right panel): **Red**: transcripts that distinguish pGBM from normal brain tissue; **Green**: those that distinguish the Ras scores of pGBM; **Blue**: those that distinguish pGBM from aGBM; **Grey**: those that distinguish aGBM from normal brain tissue. (middle panel). **D)** An example of

transcripts showing significant differential regulation between pGBM and aGBM and the normal brain are shown (complete gene list available in the Sup. gene lists at http://candida.bri.nrc.ca/papers/gbm/index.cfm.).

Fig. 2.3: A) Profiling of transcripts that distinguish patient age and Ras scores. Two dimensional hierarchical clustering of 2486 probes that exhibit a statistically significant change in transcript abundance between sample pairs from either Ras + pGBM, Ras - pGBM or from aGBM. Each sample is further classified according to age (A for Adult, P for Pediatric), activation of Ras and survival of the patient. **B)**- we used supervised analysis and PCA on the 108 probe sets that identified the prognostic subgroups established by Phillips at al [32]: 3D PCA: upper panel shows all 108 probes and middle panel probes associated with a proliferation signature (Proliferative). Both probe sets differentiate samples based on age and Ras activity as in our data set; lower panel shows that the signature probes associated with a Mesenchymal signature are partly shared by both subsets of pGBM. Samples are arbitrarily color coded for clarity reasons: blue, aGBM; yellow pGBM associated with Ras/Akt activation (Ras/Akt+); red pGBM not associated with Ras/Akt active pathways (Ras/Akt-) **C)-** Conditional hierarchical clustering with pearson correlation on probes associated with a mesenchymal (Mes) or a Proliferative (Pro) signature separate aGBM samples, pGBM associated with no Ras/Akt activation, and pGBM associated with Ras/Akt activation . Expression levels are color-coded (upregulated transcripts are in red, down regulated transcripts are in green). A bar on the right side is provided to indicate transcripts associated with Mes or Pro signatures. The same aGBM

patient that clustered with the Ras non-active samples (3A) clustered similarly using this gene set.

Figure 2.4: A)- GBM subclasses are distinguished by markers of neural stem cells. Relative to pGBM with negative Akt/Ras scores, aGBM and pGBM with active Ras/Akt show strong expression (validated by qRT-PCR) of the neural stem cells and transit-amplifying markers CD133, dlx2, nestin and MELK. Vimentin, a marker of transit amplifying and astroglial progenitors, is overexpressed in all samples with a mean 3.74 pGBM/aGBM fold expression ratio **B- Validation of YB-1 overexpression in pGBM.** Quantitative RT-PCR done for Y-Box protein 1 (*YB-1)* and *Arha* on pGBM samples validating data obtained by microarray analysis. **C)- Pattern of YB-1 expression in pGBM and normal brain.** Immunohistochemical staining for YB-1 was performed on pGBM (a-b-c) and normal brain (d). Anti-YB-1 C-terminus antibody and staining and scoring of slides were performed as previously described [17]. Representative, nuclear (a), cytoplasmic (b) negative (c) staining are shown with in thumbnail a magnification of cells positive for nuclear or cytoplasmic staining.

Acknowledgments

This work was supported by CIHR and the Penny Cole Foundation (NJ), an NRC Genome Health Initiative grant (AN), the Hungarian Scientific Research Fund (OTKA) Contract No. T-04639, and the National Research and Development Fund (NKFP) Contract No. 1A/002/2004 (PH, MG, LB, ZH). N. Jabado is the recipient of a Chercheur Boursier Award from Fonds de la Recherche en Sante du Quebec. The authors are grateful to Drs R. Rozen and P. Gros for critical reading of the manuscript. This is NRC publication number 47482.

2.7 References

1. Maher, E.A., et al., *Malignant glioma: genetics and biology of a grave matter.* Genes Dev, 2001. **15**(11): p. 1311-33.
2. Holland, E.C., *Gliomagenesis: genetic alterations and mouse models.* Nat Rev Genet, 2001. **2**(2): p. 120-9.
3. Zhu, Y. and L.F. Parada, *The molecular and genetic basis of neurological tumours.* Nat Rev Cancer, 2002. **2**(8): p. 616-26.
4. Packer, R.J., *Primary Central Nervous System Tumors in Children.* Curr Treat Options Neurol, 1999. **1**(5): p. 395-408.
5. Louis, D.N., E.C. Holland, and J.G. Cairncross, *Glioma classification: a molecular reappraisal.* Am J Pathol, 2001. **159**(3): p. 779-86.
6. Mischel, P.S., et al., *Identification of molecular subtypes of glioblastoma by gene expression profiling.* Oncogene, 2003. **22**(15): p. 2361-73.
7. Mischel, P.S., S.F. Nelson, and T.F. Cloughesy, *Molecular analysis of glioblastoma: pathway profiling and its implications for patient therapy.* Cancer Biol Ther, 2003. **2**(3): p. 242-7.
8. Liang, Y., et al., *Gene expression profiling reveals molecularly and clinically distinct subtypes of glioblastoma multiforme.* Proc Natl Acad Sci U S A, 2005. **102**(16): p. 5814-9.
9. Pollack, I.F., et al., *Molecular abnormalities and correlations with tumor response and outcome in glioma patients.* Neuroimaging Clin N Am, 2002. **12**(4): p. 627-39.
10. Rood, B.R. and T.J. Macdonald, *Pediatric high-grade glioma: molecular genetic clues for innovative therapeutic approaches.* J Neurooncol, 2005.
12. Orr, L.C., et al., *Cytogenetics in pediatric low-grade astrocytomas.* Med Pediatr Oncol, 2002. **38**(3): p. 173-7.
13. Rickert, C.H., et al., *Pediatric high-grade astrocytomas show chromosomal imbalances distinct from adult cases.* Am J Pathol, 2001. **158**(4): p. 1525-32.
14. Guha, A., et al., *Proliferation of human malignant astrocytomas is dependent on Ras activation.* Oncogene, 1997. **15**(23): p. 2755-65.
15. Rajasekhar, V.K., et al., *Oncogenic Ras and Akt signaling contribute to glioblastoma formation by differential recruitment of existing mRNAs to polysomes.* Mol Cell, 2003. **12**(4): p. 889-901.
16. Pollack, I.F., et al., *Expression of p53 and prognosis in children with malignant gliomas.* N Engl J Med, 2002. **346**(6): p. 420-7.
17. Sutherland, B.W., et al., *Akt phosphorylates the Y-box binding protein 1 at Ser102 located in the cold shock domain and affects the anchorage-independent growth of breast cancer cells.* Oncogene, 2005. **24**(26): p. 4281-92.
18. Mariani, L., et al., *Identification and validation of P311 as a glioblastoma invasion gene using laser capture microdissection.* Cancer Res, 2001. **61**(10): p. 4190-6.
19. Yim, S.H., et al., *Microarray analysis using amplified mRNA from laser capture microdissection of microscopic hepatocellular precancerous lesions and frozen hepatocellular carcinomas reveals unique and consistent gene expression profiles.* Toxicol Pathol, 2003. **31**(3): p. 295-303.
20. Choe, G., et al., *Analysis of the phosphatidylinositol 3'-kinase signaling pathway in glioblastoma patients in vivo.* Cancer Res, 2003. **63**(11): p. 2742-6.

21. Hu, X., et al., *mTOR promotes survival and astrocytic characteristics induced by Pten/AKT signaling in glioblastoma.* Neoplasia, 2005. **7**(4): p. 356-68.
22. Pollack, I.F., et al., *Age and TP53 mutation frequency in childhood malignant gliomas: results in a multi-institutional cohort.* Cancer Res, 2001. **61**(20): p. 7404-7.
23. Watanabe, H., et al., *Differential somatic CAG repeat instability in variable brain cell lineage in dentatorubral pallidoluysian atrophy (DRPLA): a laser-captured microdissection (LCM)-based analysis.* Hum Genet, 2000. **107**(5): p. 452-7.
24. Emmert-Buck, M.R., et al., *Laser capture microdissection.* Science, 1996. **274**(5289): p. 998-1001.
25. Bonaventure, P., et al., *Nuclei and subnuclei gene expression profiling in mammalian brain.* Brain Res, 2002. **943**(1): p. 38-47.
26. Segal, E., et al., *A module map showing conditional activity of expression modules in cancer.* Nat Genet, 2004. **36**(10): p. 1090-8.
27. Zeeberg, B.R., et al., *GoMiner: a resource for biological interpretation of genomic and proteomic data.* Genome Biol, 2003. **4**(4): p. R28.
28. Pollack, I.F., et al., *The relationship between TP53 mutations and overexpression of p53 and prognosis in malignant gliomas of childhood.* Cancer Res, 1997. **57**(2): p. 304-9.
29. Phillips, H.S., et al., *Molecular subclasses of high-grade glioma predict prognosis, delineate a pattern of disease progression, and resemble stages in neurogenesis.* Cancer Cell, 2006. **9**(3): p. 157-73.
30. Sanai, N., A. Alvarez-Buylla, and M.S. Berger, *Neural stem cells and the origin of gliomas.* N Engl J Med, 2005. **353**(8): p. 811-22.
31. Singh, S.K., et al., *Identification of a cancer stem cell in human brain tumors.* Cancer Res, 2003. **63**(18): p. 5821-8.
32. Phillips, H.S., et al., *Molecular subclasses of high-grade glioma predict prognosis, delineate a pattern of disease progression, and resemble stages in neurogenesis.* Cancer Cell, 2006. **9**(3): p. 157-73.
33. Rajasekhar, V.K., et al., *Oncogenic Ras and Akt signaling contribute to glioblastoma formation by differential recruitment of existing mRNAs to polysomes.* Mol Cell, 2003. **12**(4): p. 889-901.
34. Rich, J.N., et al., *Gene expression profiling and genetic markers in glioblastoma survival.* Cancer Res, 2005. **65**(10): p. 4051-8.
35. Nutt, C.L., et al., *Gene expression-based classification of malignant gliomas correlates better with survival than histological classification.* Cancer Res, 2003. **63**(7): p. 1602-7.
36. Kuwano, M., et al., *The basic and clinical implications of ABC transporters, Y-box-binding protein-1 (YB-1) and angiogenesis-related factors in human malignancies.* Cancer Sci, 2003. **94**(1): p. 9-14.
37. Evdokimova, V., et al., *Akt-Mediated YB-1 Phosphorylation Activates Translation of Silent mRNA Species.* Mol Cell Biol, 2006. **26**(1): p. 277-92.
38. Lu, Z.H., J.T. Books, and T.J. Ley, *YB-1 is important for late-stage embryonic development, optimal cellular stress responses, and the prevention of premature senescence.* Mol Cell Biol, 2005. **25**(11): p. 4625-37.
39. Berquin, I.M., et al., *Y-box-binding protein 1 confers EGF independence to human mammary epithelial cells.* Oncogene, 2005. **24**(19): p. 3177-86.
40. Wu, J., et al., *Disruption of the Y-box binding protein-1 results in suppression of the epidermal growth factor receptor and HER-2.* Cancer Res, 2006. **66**(9): p. 4872-9.

41. Bredel, M., et al., *Inhibition of Ras and related G-proteins as a therapeutic strategy for blocking malignant glioma growth.* Neurosurgery, 1998. **43**(1): p. 124-31; discussion 131-2.
42. Holland, E.C., et al., *Combined activation of Ras and Akt in neural progenitors induces glioblastoma formation in mice.* Nat Genet, 2000. **25**(1): p. 55-7.
43. Parsa, A.T. and E.C. Holland, *Cooperative translational control of gene expression by Ras and Akt in cancer.* Trends Mol Med, 2004. **10**(12): p. 607-13.
44. Kreisberg, J.I., et al., *Phosphorylation of Akt (Ser473) is an excellent predictor of poor clinical outcome in prostate cancer.* Cancer Res, 2004. **64**(15): p. 5232-6.

Chapter 3

Gene expression profiling from formalin-fixed paraffin embedded tumors of pediatric glioblastoma

Takrima Haque[1], Damien Faury[1], Steffen Albrecht[2], Enrique Lopez-Aguilar[3], Péter Hauser[4], Miklós Garami[4], Zoltán Hanzély[5], László Bognár[6], Rolando F. Del Maestro[7], Jeffrey Atkinson[8], Andre Nantel[9], Nada Jabado[1]*.

(Published Manuscript)

Haque, T., D. Faury, et al. (2007). "Gene expression profiling from formalin-fixed paraffin-embedded tumors of pediatric glioblastoma." Clin Cancer Res 13(21): 6284-6292.

[1]Division of Hemato-Oncology, Department of Pediatrics, Montreal Children's Hospital Research Institute, McGill University Health Center, Montreal, Canada.
[2]Department of Pathology, Montreal Children's Hospital, McGill University Health Center, Montreal, Canada.
[3]Oncology Department, Pediatrics Hospital, Centro Medico Nacional Siglo XXI, Mexico City, Mexico
[4]2nd Department of Pediatrics, Faculty of Medicine, Semmelweis University, Budapest, Hungary
[5]Department of Neurosurgery, Medical and Health Science Center, University of Debrecen, Debrecen, Hungary
[6]Division of Neuro-surgery, Division of Pathology, National Institute of Neurosurgery, Budapest, Hungary.
[7]Division of Neuro-Surgery, Montreal Neurological Institute, Brain Tumour Research Centre, McGill University Health Center, Montreal, Canada.
[8]Division of Neuro-Surgery, Montreal Children's Hospital, McGill University Health Center, Montreal, Canada.
[9]Biotechnology Research institute, National Research Council of Canada, Montreal, Canada.

Running title: Gene expression of pediatric glioblastoma from archival fixed tissues.

Key words: pediatric glioblastoma, FFPE samples, DNA microarray, archival tissues, RT-PCR.

* Corresponding author:
Nada Jabado, MD PhD, Montreal Children's Hospital Research Institute, 4060 Ste Catherine West, PT-239, Montreal, Qc, Canada, H3Z 2Z3. Tel: (514) 412 4400 ext 23270; Fax: (514) 412 4331; e-mail: nada.jabado@mcgill.ca

3.1 Abstract

Purpose: Gene expression profiling has proven crucial for understanding the biology of cancer. In rare diseases, including pediatric glioblastoma (pGBM), the lack of readily available fresh frozen (FF) material limits the feasibility of this analysis as well as its validation on independent data sets, a step needed to ensure relevance, mandating the use of alternate RNA sources. To overcome the limitation of material number and to validate results we obtained on FF pGBM, we assessed if we could perform microarrays on RNA extracted from formalin-fixed-paraffin-embedded (FFPE) archival samples from pGBM and control brains, where we had no control on the fixation process.

Experimental Design: RNA from 16 pGBM and 3 control brains was extracted and linearly amplified. Reverse Transcriptase-PCR on housekeeping and formerly identified tumor-associated genes and microarray analysis were performed on this RNA source. Results were validated by immunohistochemistry.

Results: Despite extensive RNA degradation, microarray analysis was possible on 16/19 samples and reproduced the pattern of results obtained on FF pGBM. Gene lists and gene ontology sub-grouping were highly concordant in both sample types. Similar to findings on FF samples, we were able to identify 2 subsets of pGBM based on their association/lack of association with an active Ras pathway.

Conclusions: Archival FFPE tissues are an invaluable resource as they are the most widely available material and often accessible in conjunction with clinical and follow-up data. Gene expression profiling on this material is feasible and may represent a significant advance for understanding the biology of rare human diseases.

3.2 Introduction

In the last decade, gene expression profiling of human cancer has proven valuable in cancer research, providing precious insight into mechanisms and targets involved in oncogenesis in several neoplasms [1, 2]. The applications of microarray and transcript profiling analysis have, however, been limited by the need for fresh frozen (FF) tissues, which allow the extraction of high-quality nucleic acids, and by the limited clinical and outcome data associated with available FF tissues. Even if archiving FF specimens has become a priority, the availability of frozen material and the lack of associated clinical data remain a major issue for rare tumors. On the other side, the collection and storage of archival, formalin-fixed and paraffin-embedded (FFPE) tissue specimens needed to establish diagnosis is a routine practice in pathology laboratories. Moreover, this sample type is often available in conjunction with precious clinical and follow-up data [3]. Extraction of quality RNA for gene expression analysis from FFPE samples has proven a challenge. RNA isolated from this material source is of poorer quality because of the extensive degradation and fragmentation that occurs during the fixation process. There is cross-linkage between the nucleic acids and the proteins that covalently modifies the RNA, making subsequent expression analysis a technical challenge [4]. However, a degree of analysis has been shown to be possible by several groups that showed reliable and reproducible results for RT-PCR and quantitative RT-PCR (qRT-PCR) [5-12]. Multiple gene expression analysis has proven more challenging, with few reports available that mainly address qRT-PCR on multiple gene sets [13-18]. Moreover, for most of the rare retrospective studies available on microarray analysis from FFPE samples, investigators had control on the type of fixative and the process and, for the other studies, the validation of transcript profiles obtained from FF versus this material source has been problematic, based on the difficulty in obtaining matched frozen and fixed samples [13].

Brain tumors are the leading cause of cancer-related mortality in children. Pediatric grade-IV astrocytoma (glioblastoma, pGBM) is a rare and deadly brain tumor [19-22]. It accounts for 15% of all pediatric brain tumors, has a 3-year survival of less than 20%, and is associated with high morbidity [23]. Considerable information is available on adult GBM (aGBM), where this cancer is the most frequent brain tumor [19-21, 24], However, fewer molecular data exist on the mechanisms underlying the development and progression in children, mainly because of the relative lack of frozen samples [25, 26]. We previously generated gene expression profiles on a set of 14 pGBM FF samples using the University Health Network (UHN) Human 19K cDNA microarrays [27]. Results were validated using real-time quantitative PCR and immunohistochemistry and compared to existing data sets on aGBM. The availability of FF pGBM samples is a limiting step to the validation of microarray results on an independent data set from the same tumor. We therefore considered the use of other RNA sources, such as RNA from FFPE samples that are more readily available than FF samples. Our aim was to validate our data on independent data sets, and to see if this archival material, an invaluable resource as they are the most widely available material and are often accessible in conjunction with clinical and long-term follow-up data, can be used for future investigations of expression profiles for other rare tumors, which lack readily available FF material and clinical data.

3.3 Materials and Methods

Sample characteristics and pathological review

A senior neuro-pathologist, Dr S. Albrecht, reviewed all samples included in this study to ensure consistent classification based on contemporary guidelines from the World Health Organization. Only grade IV astrocytomas (GBM) were examined. All samples were obtained with informed consent after approval of the Institutional Review Board of the respective hospitals they were treated in. Seventeen FF samples including 14 pGBM samples and 3 pediatric control brains (CB), and 19 FFPE samples including 16 pGBM and 3 pediatric CB from children aged 3, 5 and 14 years respectively were processed after central review (Table 1). All of the FF and FFPE samples came from distinct individuals (clinical findings summarized in Table 1). All of the 3 CB were obtained from surgical procedures on pediatric patients with epilepsy or congenital malformations and were reviewed by the neuropathologist to ascertain for astrocytic content. Tissues were obtained from the Pediatric Cooperative Human Tissue Network, the London/Ontario Tumor Bank, and from collaborators in Montreal, Hungary, and Mexico. All FFPE blocks were collected more than 3 years prior to RNA extraction and analyses.

RNA extraction following scrape or Laser Capture Microdisection

Seven μm sections from FFPE blocks were collected onto pre-cleaned superfrost® plus slides (VWR Scientific, Missisauga), stored at -70°C and used within 15 days. A representative slide for each sample was stained with hematoxylin and eosin and tumor areas identified by the neuropathologist. Sections were then deparaffinized, stained and dehydrated following manufacturer's instructions (Paradise kit, Arcturus) and as described previously [27, 28]. FF blocks were processed as described previously [27]. For both type of samples, slides were

scraped if the entire section was diagnosed as GBM, otherwise laser capture microdissection (LCM) was performed to extract pure tumor cell populations. Scraped samples were suspended in 25 μl proteinase K and incubated overnight at 50°C. When LCM was needed, it was performed on a PixCell II system (Arcturus Engineering, Mountain View). The laser spot size was set depending on the size of the area to capture (45 to 75mW, pulse duration 650 μs to 10 ms) and 2000 to 2500 GBM cells were captured on CapSure™ HS Caps and processed as per manufacturer's instructions (Arcturus).

RNA extraction and amplification from FFPE and FF tissues; Determination of RNA quality

RNA was extracted from FFPE samples using the Paradise™ Reagent System RNA Extraction/Isolation kit then amplified using the Paradise™ Reagent System RNA Amplification kit (Arcturus). RNA was extracted from FF samples using the PicoPure kit then amplified using the RiboAmp kit (Arcturus). Fidelity of linear amplified RNA (aRNA) has been previously shown [29]; we also validated our material as previously described [30, 31]. After the 1st strand synthesis of the 1st round, the integrity of the starting material was assessed by PCR reaction with β-actin primers. For each sample, the integrity of aRNA was analyzed on an Agilent 2100 Bioanalyzer (Agilent Technologies, Plato Alto, CA) using the RNA 6000 Picochip assay. RNA yield was also measured using Ribogreen RNA Quantitation kit (Molecular Probes) on an LS50 luminescence spectrometer (Perkin-Elmer) and the size of the amplification products checked by loading 2 μl on a formaldehyde agarose gel.

Reverse Transcription and Polymerase Chain Reaction (RT-PCR)

RT-PCR was done in two steps using MMLV-RT (Invitrogen) and random primers. Primers sequences were designed in the 3'end of each gene with the help of Primer3® Software. Primer sequences used for β-Actin, PDGFRβ and Y-Box Protein 1 (YB-1) were as follows: β-Actin: ATCCCCCAAAGTTCACAATG (forward primer) GGCTTTTAGGATGGCAAG (reverse primer); PDGFRβ: ATTGCAGGTTGGCACC

TTA (forward primer) and TGAGTGAGAAGCACCAGGTTT (reverse primer);YB-1: GCCTGGTTTTTCTCAATACGC (forward primer) and ACAGGTGCTTGCAGTTT

GTTG (reverse primer).

Microarray Hybridization

For FF samples, 3-5μg of aRNA was converted to cDNA and compared to the same reference pool of cDNA from aRNA extracted from pediatric control brains. For FFPE samples, cDNA from 10 μg of aRNA extracted from pGBM samples was compared to the same amount from another reference pool of aRNA extracted from 3 other pediatric CB samples. Cy3 or Cy5-labeled cDNA probes from samples and pooled controls were hybridized to Human 19K cDNA spotted arrays (19,008 human genes and ESTs, University Health Network, http://www.microarrays.ca). Slides were scanned and fluorescence intensities were quantified using the QuantArray® software package (Perkin Elmer). Inversion of fluors in distinct cDNA probes were performed (dye swap) to account for non-specific dye associated effects on hybridization and signal detection. We then applied the Lowess scatter smoothing algorithm from the GeneSpring 7.0 software package (Agilent Technologies) to normalize the raw fluorescence data. Sixty-two hybridizations consisting of dye-swap hybridizations of biological

replicates for 31 pediatric samples were analyzed (analysis of several samples was duplicated to assess for reproducibility from 2 different RNA extractions and amplifications). The "Filter on Confidence" and ANOVA (Welch t-test) statistical tools from GeneSpring were used to identify genes with reproducible changes in transcript abundance. In both cases, we applied the Benjamini and Hochberg False Discovery Rate multiple testing correction algorithm. The same software package was used to perform hierarchical clustering and Principal Component Analysis (PCA).

Immunohistochemical Analysis.

Immunohistochemical analyses for phospho-Erk (pErk), Glial Fibrillary Acidic Protein (GFAP, astrocytic marker) and YB-1 were performed and the slides scored as previously described [32, 33]. Slides were counterstained with hematoxylin and mounted. Negative controls (IgG) were included with each batch of sections to confirm the consistency of the analysis. GFAP, a histologically verifiable internal positive control antigen, was used to identify cases in which a lack of immunoreactivity for pErk might indicate problems linked to the labeling of the tissue and thus tissue preservation, rather than a lack of protein phosphorylation. Importantly, all assays were carried out at the same time with the same reagents. The neuro-pathologist, blinded to outcome and histology, evaluated the degree of staining.

3.4 Results

Quantity and quality of amplified RNA obtained from FFPE samples compared to FF samples.

RNA from FF or FFPE samples was extracted after scraping sections or after capture of pure cell populations using LCM (Fig. 3.1A)**.** RNA yield after extraction was higher, as expected based on the number of cells, after scrape, and ranged between 5 to 100ng for FFPE samples and between 10 to 100ng for FF samples (Fig. 3.1B). To determine if the amount of starting material affected the amplification yield, we performed amplifications using a range of 5 to 30ng of starting RNA. For FFPE samples, the total yield of aRNA ranged from 20-40μg after two rounds of amplification, a yield that was not affected by the amount of starting RNA material. For FF samples, the yield after 2 rounds of amplification ranged from 60-200μg and increased with an increase in the amount of starting RNA material (Fig. 3.1B). ARNA from both sample types showed a similar pattern after electrophoretic separation (Fig. 3.1C).

Extensive degradation of nucleic acids may occur during the fixation process. To assess the quality of aRNA extracted from either material source, we used the Agilent Bioanalyzer 2100 Picochip. We obtained sharp 18S and 28S ribosomal RNA peaks from FF tissues, indicative of high quality RNA, in contrast to FFPE tissues where only 18S ribosomal peaks were obtained in combination with a characteristic change in the RNA profile indicative of degradation (data not shown). To further assess if these aRNA from FFPE samples could still be used for microarray analysis, we performed RT-PCR assays using primers designed for the 3' end of genes that included a housekeeping gene, β-actin, and genes we had previously shown to be overexpressed in a subset of frozen pGBM, *PDGFRβ* and *YB-1* [31]. RT-PCR was performed on RNA after extraction and after the first and the second amplification steps. *β-actin* was present in all

samples whereas *PDGFRβ* transcript was seen in some samples at all steps (Fig. 3.1D). Data correlated with previous findings obtained from FF pGBM where *PDGFRβ* was only up-regulated in a number of samples. *YB-1* was also expressed in some samples (Fig. 3.1D). Importantly, results for *YB-1* correlated with the immunohistochemical analysis that was performed in parallel on slides from the same FFPE samples, with samples negative by RT-PCR showing no staining for YB-1 and positive samples showing increased protein expression by immunohistochemistry (Fig. 3.1E).

These results indicate that RNA yield, as well as the quality of extracted RNA, are lower from FFPE samples. However, as previously shown, even if RNA from FFPE samples is degraded, RNA analysis can still be performed on this material source for brain tumors.

Gene expression profiling from FFPE samples

The 28S/18S ratio, as measured with the Bioagilent picochip, was recently shown to lead to a misleading categorization prior to microarray analysis and, therefore, is not a reliable tool for monitoring RNA quality prior to this type of analysis [34]. Based on the rarity of FF samples from pGBM, we chose to perform microarray analysis on aRNA extracted from FFPE pGBM samples to further validate on an independent data set of pGBM gene expression profiles we obtained on 14 FF pGBM samples [27] while investigating if this type of analysis was possible on fixed samples. Samples of aRNA from 16 FFPE pGBM tumors were reverse transcribed, labeled and hybridized to Human 19K cDNA spotted arrays together with a pooled, similarly amplified, reference RNA extracted from 3 FFPE samples from pediatric CB. When hybridizing slides with 5μg of cDNA, few specific spots were seen, in marked contrast to FF samples where the number of high-intensity spots was always satisfactory for high quality hybridizations. We

therefore performed hybridizations using a range of 10, 15 and 20μg of cDNA for the same pGBM sample and control. Optimal results were obtained for 10 μg of amplified cDNA. When compared to arrays obtained from FF samples, the level of background noise was higher on the array slides for FFPE, with a significant lower number of spots for all of the cDNA range. With the higher cDNA concentrations of 15 or 20μg, more background noise was obtained whereas the number of spots showing specific hybridization on the slide did not increase (data not shown). Based on these results we opted to use 10μg of cDNA for each tumor and control, and were able to obtain reliable and reproducible results on 13 of the 16 FFPE pGBM samples.

GeneSpring's "Filter on Confidence" tool identified a list of transcripts with statistically significant changes in abundance in FFPE pGBM samples compared to the pooled controls (Welch t-test, p-value<0.05, multiple testing correction: Benjamini and Hochsberg, false discovery rate of 3.4%). Other statistical algorithms (the Wilcoxon-Mann-Whitney test of Significance Analysis of Microarrays) were tested with similar results. We compared the lists of differentially expressed transcripts between pGBM and control brains obtained by analyzing either FF or FFPE pGBM samples and found 777 transcripts to be differentially expressed in FFPE samples compared to the pooled control and 3647 modulated transcripts in FF samples compared to the FF pooled CB. A 2D-graph and two-dimensional hierarchical clustering organized and visualized the profiles of these differentially regulated transcripts (Y-axis) from each of the 13 FFPE pGBM samples (X-axis, Fig. 3.2B and 3.2C respectively) as compared to those obtained on the previously reported 14 FF pGBM samples [27]. Both the graph representing differentially expressed transcripts between pGBM samples and the pooled controls and the cluster tree of these differentially expressed transcripts show that a significant number of transcripts are lost due to RNA degradation in the FFPE compared to the FF samples. Also, as

shown on the 2D graph, the clustering tree, and the scatter plot graph of all samples from both material sources, transcripts from the FFPE samples show a decreased fold change relative to the CB when compared to the same transcripts from FF samples (Fig. 3.2A). Despite differences in the number of differentially expressed transcripts and in the fold change and the use of different controls, we still found a reasonable correlation of R^2=0.649 between both sample types. Importantly, a similar pattern of gene expression profiles was maintained between FF and FFPE pGBM samples: transcripts that were overexpressed (color coded in red) in the FF samples were also overexpressed in the FFPE, and, conversely, transcripts that were downregulated in both sample types were similar (color coded in green, Fig. 3.2B-3.2C). This indicates that, even if we are losing a number of differentially regulated transcripts in the FFPE samples as compared to the FF samples as well as the extent of the fold change, we are maintaining a similar expression pattern for the significant differentially regulated transcripts in FFPE samples.

Analysis of gene expression profiles from FFPE samples mirrors results obtained from FF samples

We next used Venn diagrams to compare the list of significantly modulated transcripts for both sample sets generated using the p-value cut-off of 0.05. We chose a cut-off of 0.05, as many transcripts were missed by a more stringent p-value and were on the verge of statistical significance. Also, the use of a lower threshold was found to be the most effective method to compare data obtained on different platforms or from different material sources with variable sensitivity for detecting transcripts, including weakly expressed genes [34-38]. We saw an overlap between both gene lists of 606 genes shared by the two subsets of pGBM samples, which gives a significance of overlap of 1.0e-09 according to the Fischer's exact test (Fig. 3.2D). We

analyzed the data set using a module-level view obtained from a 'cancer compendium'[39] and also organized the gene sets using GoMiner, a computer resource that incorporates the hierarchical structure of the Gene Ontology (GO) Consortium[2] to automate a functional categorization of gene lists based on biological processes. Both methods aim to distill a higher-order from a large list of genes. They yielded similar results, showing that modules and GO terms overlapped for the top 15 categories obtained on significantly modulated transcripts from FF and FFPE data sets (Table 3.2)**.** The pediatric CB for the FFPE samples were different from the CB used to profile the FF pGBM samples because of the lack of availability of FFPE blocks from the same FF controls. Therefore the use of different CB could partly account for the lack of complete overlap between both types of samples on gene lists. We had previously determined for FF samples that different control brains had similar if not totally overlapping gene expression profiles (Pearson correlation, r: 0.93). When categorizing the nature of these 171 genes by GO processes, they were mainly grouped into catabolic transcripts. When we looked at the most statistically significant transcripts present in both gene lists, most of the genes that we had validated by qRT-PCR and chose to pursue based on their potential involvement in the oncogenesis of pGBM in FF samples were also present when analyzing significantly modulated transcripts in FFPE samples (Table 3.3).

We have previously shown in FF pGBM samples that there was at least two prognostic subgroups of pGBM that could be molecularly separated based on their association or not with an aberrant Ras active pathway [27]. Ras pathway activation was investigated in FF samples by western blot using phosphorylation-specific antibodies against known Ras effectors including Erk1/2, MEK1/2 and Raf[27]. In FFPE samples, the presence of pErk staining by

immunohistochenistry was associated with Ras activation[32] (Fig 3.3A). To further validate these findings, the same analysis was done on FFPE samples using PCA, a method of data reduction in which the high dimensionality of the data is reduced to 2-3 viewable dimensions representing linear combinations of genes that account for most of the variance of the data set and which allows to visualize similarities within samples. Similarly to our findings in FF pGBM samples[27], PCA separated both sets of FFPE and FF pGBM samples into 2 groups indicating the presence of at least two distinct populations of pGBM (Fig 3.3B). The two pGBM populations segregated by PCA were assocaited with differing Ras activity in samples (Fig. 3.3B). Also, ANOVA testing was able to identify transcripts that could distinguish tumors associated with differing Ras activity in both FF and FFPE pGBM samples (Fig. 3.3C). Despite the loss of a number of differentially expressed transcripts in FFPE samples, a significant degree of correlation is seen between frozen and FFPE as shown by the scatter plot where a linear correlation is seen, even if the graph is slightly skewed due to the difference between the fold change values between the two types of samples.

3.5 Discussion

Validation of data obtained from gene expression profiling on independent data sets is crucial. In rare diseases or tumors, including pGBM, where the lack of readily available FF material and clinical information and the small number of samples limit the analysis and the validation of the data sets, the use of alternate RNA sources including RNA from archival fixed material represents a major breakthrough for validation studies. We show herein that RNA from FFPE samples can be successfully isolated from laser-captured or scraped samples, amplified and used for reliable single or multiple transcript analysis. We performed several RT-PCR

analyses on RNA extracted from the material source for housekeeping and tumor modulated transcripts and validated results on the protein level by immunohistochemical analysis on the same samples for all the 19 FFPE samples included in this study. Importantly, using cDNA arrays, we were able to perform gene expression profiling on this type of material for 13/16 pGBM and 3/3 control brains (84%). Results of expression profiles helped validate the data sets and observations we had previously generated on FF pGBM, even if the number of differentially regulated transcripts and the degree of fold change in transcripts were decreased in FFPE samples.

Several groups showed that the extraction of RNA from fixed samples is possible even if only small targets were being amplified, with an average of 300bp base pair length of RNA extracted from fixed samples[5, 7, 9, 11-13, 40]. These groups further showed the feasibility of single or multiplex transcript analysis, including RT and qRT-PCR, on a limited number of RNA transcripts extracted from fixed tissues. In this study, we were able to extract sufficient quality and quantity of RNA material for microarray analysis. When comparing the spots on the hybridized arrays, FFPE samples produced higher background, possibly due to non-specific hybridizations occurring because of the generally short lengths of the fragmented RNAs. Also, the number of significantly-modulated transcripts was decreased, as previously shown in a study that used cDNA-mediated annealing, selection, extension and ligation (DASL), where the number of differentially regulated transcripts was decreased by 50% in FFPE samples when compared to the FF[41]. However, using the data generated on FFPE samples, we were able to reproduce findings first observed on FF samples. Using PCA, we were able to identify 2 subsets of pGBM in FFPE pGBM samples based on their association or lack of association with an aberrantly active Ras pathway, similar to findings on FF pGBM samples. Analysis of the data set

using GoMiner showed an overlap in biological processes affected in pGBM in both sample types (Table 3.2). The list of differentially regulated transcripts in pGBM compared to the control brains extracted from the FFPE data sets (supplementary gene lists) was concordant with the one obtained in FF samples and included transcripts that were previously identified by other profiling studies on GBM[42, 43].

The lack of total overlap between the transcripts from the two gene lists from both sample types may be due to the use of different sources of material, different fixation procedures and durations and/or different controls. The use of several different sources with different degrees of tissue preservation, the duration of fixation of the specimen and different fixatives can also introduce a bias. It has been suggested that ethanol fixation yield better results than formalin fixation for transcript analysis and correlation to frozen counterparts[44]. Another group also showed that ethanol fixation allowed the recovery of high-quality RNA from micro-dissected cells [18] while other groups showed that Bouin fixation was less detrimental to RNA integrity while preserving tissue architecture and cell morphology. However, all of these groups performed their analysis on samples they manipulated *de novo* under conditions that were optimized for the best results. This is not true for most archival tissues, which are mainly formalin-fixed through the choice of the pathology departments and handled without consideration of future RNA extraction. Therefore, in most retrospective studies, including this one, rare archival tissues are obtained from various sources where the duration of fixation, the type of fixative and the age of the sample are variables that cannot be modified, hence an unavoidable source of variability due to different handling procedures. However, as shown by our results, this variability does not prevent reliable microarray analysis.

In a recently published study, Penland et al profiled 157 archival FFPE samples from colon biopsies and show similar results to this study in term of RNA yield, size and degradation profile[45]. However, only 24% of these FFPE samples yielded reliable microarray data. The authors went to establish a stringent algorithm to obtain a more precise indication of the extent of RNA degradation in a sample prior to hybridization on slides. They indicated that among other criteria, the use of a Taqman assay designed to determine 3'-to-5' ratios in total RNA extracted from a sample increased their success rate from 17% to 48% and the control for the efficiency of labeling further improved their pre-hybridization screening. It is presently difficult to determine why in this study we had a significant success rate in this regard (84%) but, apart of technical factors, this could be due to the autolytic properties of the tissue itself (brain as opposed to colon). One could also consider a bias towards a smaller sample (or specimen) size as in another recent study of 5 FFPE samples colon cancers that use the same RNA extraction, amplification and array platform than Penland et al, the success rate for microarray analysis was 100%[46]. In all, for larger scale studies where the rate limiting aspect is the efficiency of hybridizations and not the small number of samples available, a more thorough screening should be done to optimize the success rate of the hybridization and limit undue work and costs[45].

Despite the numerous challenges faced by the utilization of archival fixed tissues, we show that we are able to reproduce a similar pattern of differential gene expression using FFPE or FF pGBM samples. FF samples are the obvious choice for optimal transcript analysis. However, our data suggest that, in rare tumors and in cases where the lack of clinical data is an issue, the use of archival FFPE samples, the most common type of archival samples, is feasible. In this instance, both the availability of a larger scale of samples and its association to clinical data are assets that

help compensate for lower RNA quality, providing researchers with a valuable source of material that can be used for validation and further investigations in rare diseases.

3.6 Tables and Figures

FFPE pGBM samples	Gender	Age (years)	Ras (IHC)	YB1 (IHC)	Survival from surgery
P1	M	5	pos	pos	D, 7 M
P2	F	7	neg	neg	A, 4Y
P3	F	16	neg	neg	D, 12 M
P4	M	4	pos	pos	D, 3Y
P5	M	14	neg	neg	D, 15 M
P6	F	12	pos	pos	D, 11 M
P7	M	9	pos	pos	D, 14 M
P8	M	14	pos	pos	D, 2.5Y
P9	M	8	pos	pos	D, 9 M
P10	F	8	pos	pos	D, 14 M
P11	F	12	pos	pos	D, 3 Y
P12	F	7	pos	pos	D, 2 M
P13	F	9	pos	pos	D, 36 M
P14	M	4	pos	pos	D, 2Y
P15	M	12	neg	neg	A, 6 Y
P16	F	15	neg	neg	D, 2Y
CB1	M	3	neg	neg	A
CB2	M	5	neg	neg	A
CB3	F	14	neg	neg	A

FF pGBM samples	Gender	Age (years)	Ras (WB)	YB1 (qRT-PCR)	Survival from surgery
FF 1	F	7	neg	1.8	A, 4 Y
FF 2	F	4	pos	3.7	D, 12 M
FF 3	F	10	neg	2	D, 5 M
FF 4	F	14	neg	0.5	A, 6 Y
FF 5	M	14	neg	2.6	A, 6 Y
FF 6	M	14	pos	13.7	D, 1 M
FF 7	F	9	pos	6.7	D, 2 M
FF 8	M	1	pos	10.6	D, 7 M
FF 9	F	11	pos	4	D, 9 M
FF 10	F	13	pos	6.7	D, 14 M
FF 11	M	2	neg	4.6	A, 5 Y
FF 12	F	16	pos	6.5	D, 2 M
FF 13	M	16	pos	8.1	D, 36 M
FF 14	M	13	pos	4.5	D, 11 M

Table 3.1: Characteristics of the patients included in the study.
The diagnosis of pediatric glioblastoma (pGBM) was made according to the WHO criteria. Specific histological findings included regions of necrosis (pseudopalissading necrosis), hypertrophied blood vessels (increased angiogenesis), cells with nuclei highly variable in size and shape with an increased proliferation index. Ras pathway activation was investigated by immunohistochemical staining (IHC) for formalin-fixed paraffin-embedded (FFPE) samples or by western blot analysis (WB) for and fresh frozen (FF) samples for pErk. Y Box protein 1 (YB-1) expression was assessed by quantitative RT-PCR (qRT-PCR, FF samples) or by RT-PCR and IHC (FFPE samples). pos=positive, neg=negative, A= alive, D=died, Y=years, M=months.

	FFPE	FROZEN
1.	Physiological process	Cellular process
2.	Cellular process	Physiological process
3.	Cellular physiological process	Cellular physiological process
4.	Metabolism	Cell communication
5.	Cellular metabolism	Macromolecule metabolism
6.	Primary metabolism	Regulation of biological processes
7.	Macromolecule metabolism	Cellular macromolecule metabolism
8.	Cellular macromolecule metabolism	Protein metabolism
9.	Protein metabolism	Cellular protein metabolism
10.	Cellular protein metabolism	Regulation of cellular process
11.	Localization	Regulation of physiological processes
12.	Establishment of localization	Localization
13.	Organismal physiological process	Establishment of localization
14.	Transport	Regulation of cellular physiological processes
15.	**Regulation of biological process**	Biopolymer metabolism

Table 3.2: Gene ontology classification using Go-miner of the differentially expressed transcripts relative to the pooled control brains of fresh frozen (FF) and formalin-fixed paraffin-embedded (FFPE) pediatric glioblastoma (pGBM) samples. This classification shows that the top15 biological processes affected in pGBM are similar in both sample types.

Table 3.3: List of the top100 differentially expressed transcripts relative to the pooled control brains common to FF and FFPE pGBM.

Common name	Description
sparc	Secreted protein, acidic, cysteine-rich (osteonectin)
rbp1	Retinol binding protein 1, cellular
hla-dpa1	Major histocompatibility complex, class II, DP alpha 1
cfl1	Cofilin 1 (non-muscle)
hla-drb3	Major histocompatibility complex, class II, DR beta 4
col6a1	Collagen, type VI, alpha 1
rpl10	Ribosomal protein L10
hcn3	Hyperpolarization activated cyclic nucleotide-gated potassium channel 3
arhc	Ras homolog gene family, member C
api5	Apoptosis inhibitor 5
timp1	Tissue inhibitor of metalloproteinase 1 (erythroid potentiating activity)
hla-dpb1	Major histocompatibility complex, class II, DP beta 1
s100a6	S100 calcium binding protein A6 (calcyclin)
tcfl1	Transcription factor-like 1
nsep1	**Nuclease sensitive element binding protein 1 (Y Box protein 1)**
serf2	Small EDRK-rich factor 2
cd63	CD63 antigen (melanoma 1 antigen)
chi3l1	Chitinase 3-like 1 (cartilage glycoprotein-39)
myl6	Myosin, light polypeptide 6, alkali, smooth muscle and non-muscle
arha	Ras homolog gene family, member A
gapd	Glyceraldehyde-3-phosphate dehydrogenase
cd99	CD99 antigen
ifi30	Interferon, gamma-inducible protein 30
fn1	Fibronectin 1
rps3	Ribosomal protein S3
tcf8	Transcription factor 8 (represses interleukin 2 expression)
apoc1	Apolipoprotein C-I
rpl10	Ribosomal protein L10
rpl13a	Ribosomal protein L13a
rpl41	Ribosomal protein L41
calu	Calumenin
gns	Glucosamine (N-acetyl)-6-sulfatase (Sanfilippo disease IIID)
rps16	Ribosomal protein S16
rps17	Ribosomal protein S17
hla-dpb1	Major histocompatibility complex, class II, DP beta 1
pabpc4	Poly(A) binding protein, cytoplasmic 4 (inducible form)
cdk4	Cyclin-dependent kinase 4
tm4sf1	Transmembrane 4 superfamily member 1
cd63	CD63 antigen (melanoma 1 antigen)
polr2b	Insulin-like growth factor binding protein 7
sox10	SRY (sex determining region Y)-box 10
rpl13a	Ribosomal protein L13a
eif3s4	Eukaryotic translation initiation factor 3, subunit 4 delta, 44kDa

nrg3	Neuregulin 3
pltp	Phospholipid transfer protein
igkc	HRV Fab N8-VL
h3f3a	H3 histone, family 3B (H3.3B)
mdk	Midkine (neurite growth-promoting factor 2)
rps3	Ribosomal protein S3
col4a2	Collagen, type IV, alpha 2
h2afz	H2A histone family, member Z
ighm	Immunoglobulin lambda constant 2 (Kern-Oz- marker)
arhc	Ras homolog gene family, member C
nnmt	Nicotinamide N-methyltransferase
ighm	Hepatitis B surface antigen antibody variable domain
rpl8	Ribosomal protein L8
eef1g	Eukaryotic translation elongation factor 1 gamma
snrpb	Small nuclear ribonucleoprotein polypeptides B and B1
mect1	Mucoepidermoid carcinoma translocated 1
ncl	Nucleolin
mage-e1	Melanoma antigen family D, 4
xpo1	Exportin 1 (CRM1 homolog, yeast)
ifitm1	Interferon induced transmembrane protein 1 (9-27)
dad1	Defender against cell death 1
plat	Plasminogen activator, tissue
ranbp1	RAN binding protein 1
nme1	Non-metastatic cells 1, protein (NM23A) expressed in
rplp2	Ribosomal protein, large P2
ccnd1	Cyclin D1 (PRAD1: parathyroid adenomatosis 1)
pp1201	H19, imprinted maternally expressed untranslated mRNA
myl6	Myosin, light polypeptide 6, alkali, smooth muscle and non-muscle
igkc	Immunoglobulin kappa constant
fabp7	Fatty acid binding protein 7, brain
canx	Calnexin
pgd	Phosphogluconate dehydrogenase
gapd	Glyceraldehyde-3-phosphate dehydrogenase
s100a10	S100 calcium binding protein A10 (annexin II ligand, calpactin I, light polypeptide (p11))
timp1	Tissue inhibitor of metalloproteinase 1 (erythroid potentiating activity, collagenase inhibitor)
hmgn1	High-mobility group nucleosome binding domain 1
psmb2	Proteasome (prosome, macropain) subunit, beta type, 2
hbb	Hemoglobin, beta
rpl27	Ribosomal protein L27
col4a2	Collagen, type IV, alpha 2
pkm2	Pyruvate kinase, muscle
aebp1	AE binding protein 1
actn4	Actinin, alpha 4
pml	Promyelocytic leukemia
rpl18a	Thioredoxin reductase 1
tubb	Tubulin, beta polypeptide paralog
tubb2	Tubulin, beta, 2
dgkd	Diacylglycerol kinase, delta 130kDa

nedd5	Septin 2
rpn2	Ribophorin II
ercc1	Excision repair cross-complementing rodent repair deficiency, complementation group 1
slc20a1	Solute carrier family 20 (phosphate transporter), member 1
rpl18	Ribosomal protein L18
rps19	Ribosomal protein S19
dusp6	Dual specificity phosphatase 6
polr2l	Polymerase (RNA) II (DNA directed) polypeptide L, 7.6kDa

Table 3.3 Continued

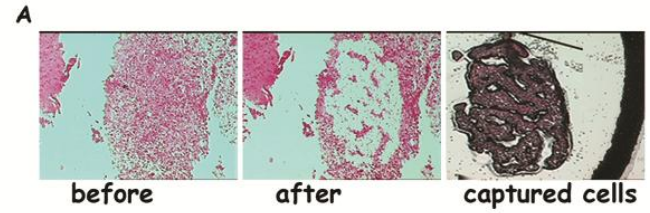

B

	Frozen	FFPE
Extracted RNA by LCM	10-100 ng	0-44 ng
Extracted RNA by Scraping	100-800 ng	100-1000 ng
Amplified RNA	60-200 µg	25-40 µg

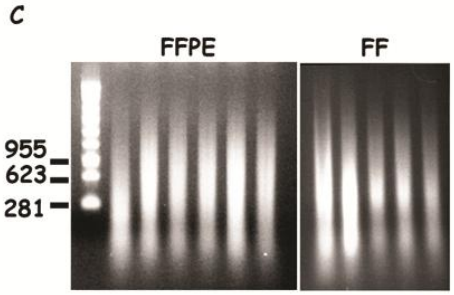

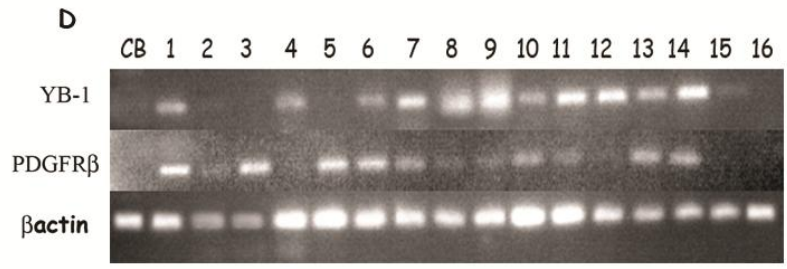

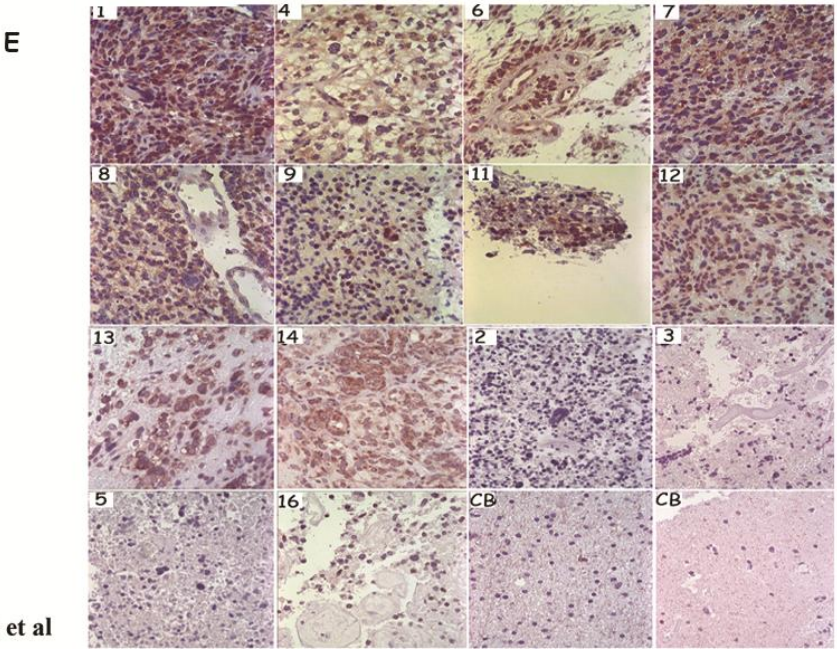

Figure 1, Haque et al

Figure 3.1

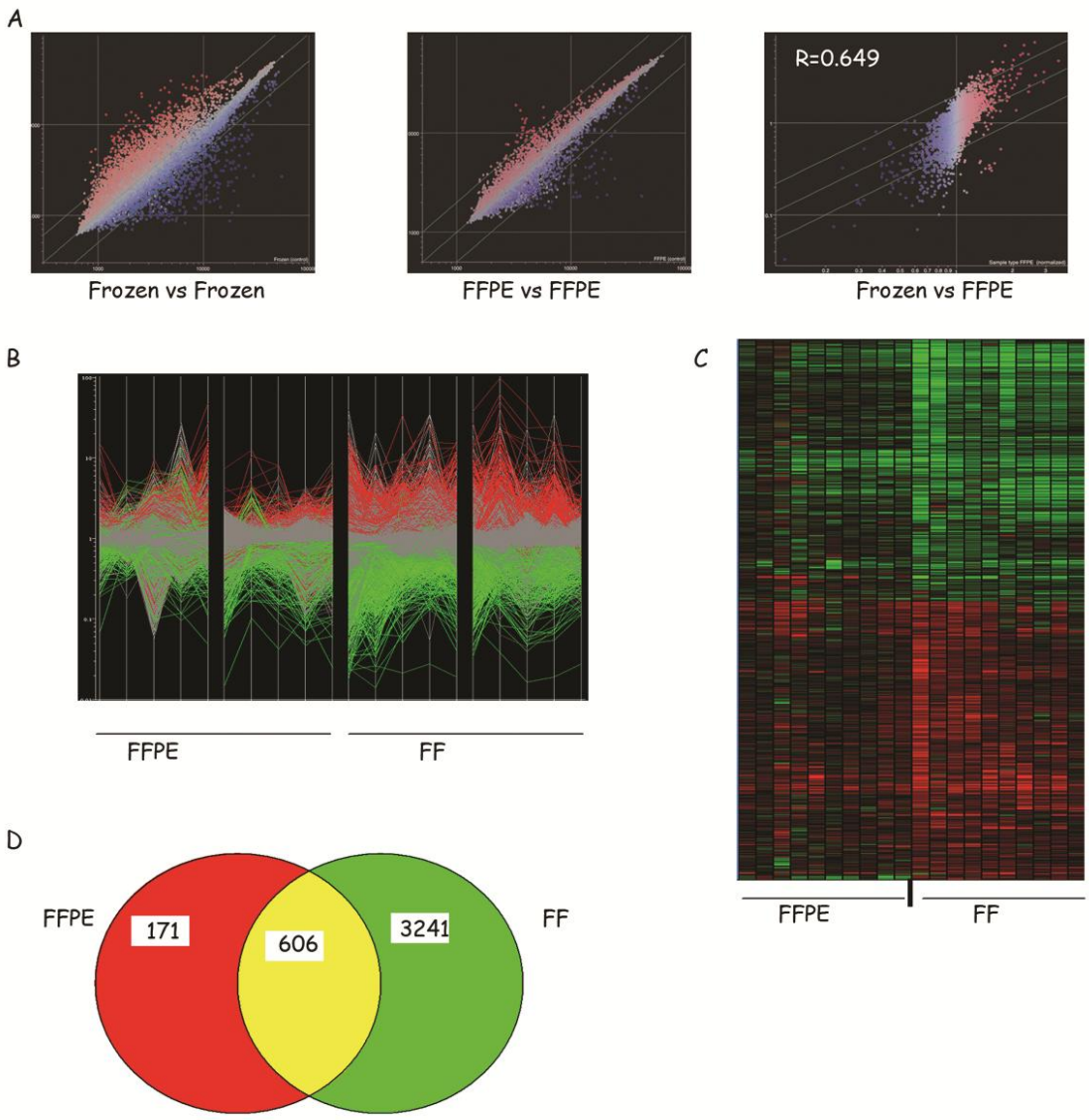
A
R=0.649
Frozen vs Frozen
FFPE vs FFPE
Frozen vs FFPE
B
FFPE
FF
C
FFPE
FF
D
FFPE
171
606
3241
FF

Figure 3.2

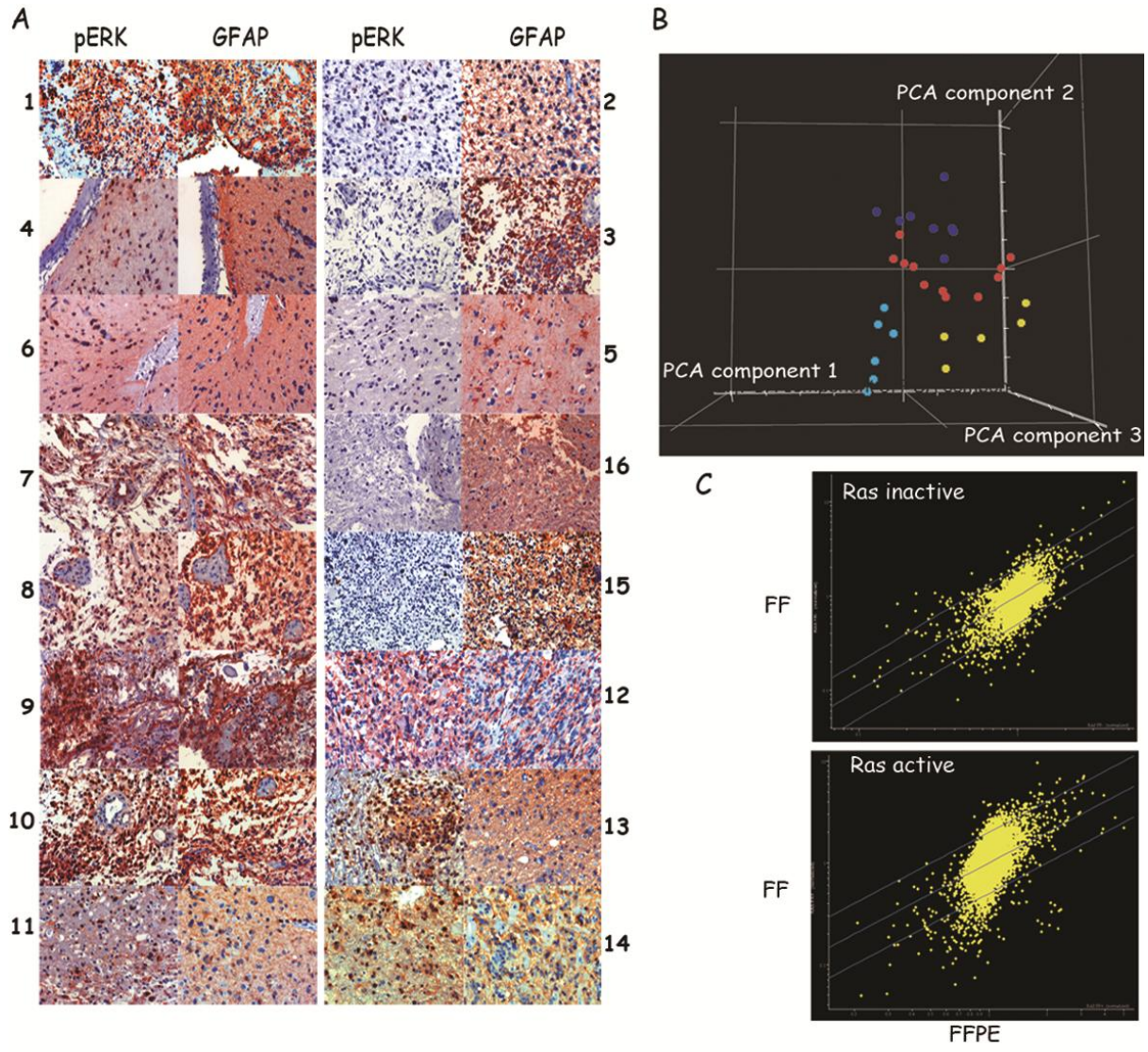
A
pERK
GFAP
pERK
GFAP
1
2
4
3
6
5
7
16
8
15
9
12
10
13
11
14
B
PCA component 2
PCA component 1
PCA component 3
C
Ras inactive
FF
Ras active
FF
FFPE

Figure 3.3

Figure Legends

Figure 3.1: (A). ***Laser Capture Microdissection.*** Formalin-Fixed paraffin embedded (FFPE) pediatric glioblastoma (pGBM) samples were processed for hematoxylin-eosin staining to identify tumour cells. Tumor cells identified by the neuropathologist were captured. Representative images from a pGBM were taken before and after capture from the same section and captured cells are shown. **(B).** ***RNA yield before and after linear amplification in fresh frozen (FF) and FFPE samples***. RNA was extracted from slides after scrape or LCM. Around 5-10 ng of RNA was subjected to 2 rounds of T7 RNA polymerase amplification. RNA yield was higher after scrape and the coefficient of amplification was constantly higher in FF as compared to FFPE samples. ***(C). Electrophoretic separation of amplified RNA (aRNA) from FF and FFPE samples.*** Two μg of aRNA from a representative number of samples from FF and FFPE pGBM samples was subjected to electrophoresis to assess for the presence and the size of the amplified material. The size of aRNA was between 300-600bp and similar in both material sources. ***(D). RT-PCR detection of β-actin YB-1, PDGFR-β gene on RNA extracted from parraffin samples.*** RT-PCR were performed using random primers and starting with 200 ng of amplified RNA. A reference gene (β-actin) was coamplified with PDGFR- β and YB-1 using gene specific primers designed within the 300 last bases of each gene. All 16 pGBM FFPE samples and a Control Brain are shown. β -*actin* is expressed in all samples as expected whereas *PDGFR* β and YB-1 expression are detected only in some samples. *(E).* ***Pattern of YB-1 expression in FFPE pGBM.*** Immunohistochemical staining for YB-1 was performed on 14 pGBM and 2 control brains (CB). Anti-YB-1 C-terminus antibody and staining and scoring of slides were

performed as previously described[47]. Staining confirms results obtained by RT-PCR on the same samples.

Figure 3.2. Gene expression profiling of FFPE samples reproduces the pattern of expression profiles obtained on FF pGBM samples.

(A). Profile similarities between different subgroups of glioblastoma (GBM). Scatter plots comparing the change in transcript abundance between pairs of subgroups of pGBM: FF pGBM (left panel), FFPE (middle panel), FFPE vs FF (right panel). Transcripts colored in red (upregulated) and blue (down-regulated) show a statistical change in abundance between the pair of sub-groups of GBM analyzed relative to the control (Welsh t-test, pvalue cut-off<0.05, multiple testing correction: Benjamini and Hochsberg False Discovery Rate). Log2 intensity scatter plots were generated using raw intensity data, and Pearson correlation coefficients calculated for FF *vs* FFPE samples (left panel), r=0.649; **(B).** Unsupervised hierarchical clustering of the probes with a statistically significant change in transcript abundance (Welsch t-test, p<0.05, Benjamini and Hochsberg) between FF pGBM, FFPE pGBM and the pool of normal brain tissue (X axis) shows a decrease in the number and the fold change of transcript profiles in FFPE samples (probes on the Y axis). Each experimental data point is colored according to the change in fluorescence ratio (more abundant in pGBM colored in red, less abundant colored in green). **(C).** Two dimensional hierarchical clustering of 486 probes that exhibit the highest statistically significant change in transcript abundance between sample pairs in FF samples (Welsch t-test, p<0.05, Benjamini and Hochsberg) (see Sup. Gene lists) shows that the pattern of overexpressed/down-regulated genes is similar in

FFPE samples. Each experimental data point is colored according to the change in fluorescence ratio (more abundant in pGBM colored in red, less abundant colored in green). **(D).** Venn-Diagram of differentially regulated transcripts relative to the pooled CB in FFPE pGBM samples (n=777) and in FF samples (n=3847) (Welch t-test, $p<0.05$) showing a significant overlap (n=606) between both lists of transcripts (supplementary gene lists).

Fig. 3.3: Tumor samples show distinct expression profiles that correlate with Ras pathway activation. (A) Immunohistochemical analyses for pErk, Glial Fibrillary Acidic Protein (GFAP, astrocytic marker) were performed for the 16 pGBM samples included in this study. Samples are numbered as in table 1 and Fig.1D. **(B)-** The 13 FFPE and 14 FF pGBM samples were subjected to a Principal Components Analysis (PCA) based on the expression profile measured on 15,068 individual probes. A three-dimensional plot of PCA components 1, 2 and 3 distinguished the Ras scores of the pediatric tumors irrespective of the nature of the sample source. Samples are color-coded for clarity issues: pGBM samples associated with active Ras pathway in red (FFPE) and dark blue (FF); pGBM samples not associated with active Ras in yellow (FFPE), light blue (FF). Three FFPE samples with an active Ras pathway for which we had enough material were treated in duplicate with separate RNA extraction, amplification and hybridization. They migrated similarly on the PCA graph further confirming the reproducibility of the gene expression analysis on FFPE samples. **(C)** ANOVA identified differentially expressed transcripts in both sample sources based on their association/lack of association with an active Ras pathway. Log2 intensity scatter plots were generated using raw intensity data,

and Pearson correlation coefficients calculated for FF *vs* FFPE samples associated with Ras activation (r=0.651), and pGBM samples not associated with Ras activation (r=0.712).

Acknowledgments

This work was supported by the Canadian Institute of Health Research and the Penny Cole Foundation (NJ), the NRC Genome Health Initiative (AN), the Hungarian Scientific Research Fund (OTKA) Contract No. T-04639, and the National Research and Development Fund (NKFP) Contract No. 1A/002/2004 (PH, MG, LB, ZH). N. Jabado is the recipient of a Chercheur Boursier Award from Fonds de la Recherche en Sante du Quebec. This is NRC publication number 49512.

3.7 References

1. Segal, E., et al., *From signatures to models: understanding cancer using microarrays.* Nat Genet, 2005. **37 Suppl**: p. S38-45.
2. Zeeberg, B.R., et al., *GoMiner: a resource for biological interpretation of genomic and proteomic data.* Genome Biol, 2003. **4**(4): p. R28.
3. Lewis, F., et al., *Unlocking the archive--gene expression in paraffin-embedded tissue.* J Pathol, 2001. **195**(1): p. 66-71.
4. Masuda, N., et al., *Analysis of chemical modification of RNA from formalin-fixed samples and optimization of molecular biology applications for such samples.* Nucleic Acids Res, 1999. **27**(22): p. 4436-43.
5. Jackson, D.P., et al., *Tissue extraction of DNA and RNA and analysis by the polymerase chain reaction.* J Clin Pathol, 1990. **43**(6): p. 499-504.
6. Korbler, T., et al., *A simple method for RNA isolation from formalin-fixed and paraffin-embedded lymphatic tissues.* Exp Mol Pathol, 2003. **74**(3): p. 336-40.
7. Specht, K., et al., *Quantitative gene expression analysis in microdissected archival formalin-fixed and paraffin-embedded tumor tissue.* Am J Pathol, 2001. **158**(2): p. 419-29.
8. Walch, A., et al., *Tissue microdissection techniques in quantitative genome and gene expression analyses.* Histochem Cell Biol, 2001. **115**(4): p. 269-76.
9. Godfrey, T.E., et al., *Quantitative mRNA expression analysis from formalin-fixed, paraffin-embedded tissues using 5' nuclease quantitative reverse transcription-polymerase chain reaction.* J Mol Diagn, 2000. **2**(2): p. 84-91.
10. Finke, J., et al., *An improved strategy and a useful housekeeping gene for RNA analysis from formalin-fixed, paraffin-embedded tissues by PCR.* Biotechniques, 1993. **14**(3): p. 448-53.
11. Stanta, G., S. Bonin, and R. Perin, *RNA extraction from formalin-fixed and paraffin-embedded tissues.* Methods Mol Biol, 1998. **86**: p. 23-6.
12. Stanta, G., S. Bonin, and R. Utrera, *RNA quantitative analysis from fixed and paraffin-embedded tissues.* Methods Mol Biol, 1998. **86**: p. 113-9.
13. Steg, A., et al., *Multiple gene expression analyses in paraffin-embedded tissues by TaqMan low-density array: Application to hedgehog and Wnt pathway analysis in ovarian endometrioid adenocarcinoma.* J Mol Diagn, 2006. **8**(1): p. 76-83.
14. Capodieci, P., et al., *Gene expression profiling in single cells within tissue.* Nat Methods, 2005. **2**(9): p. 663-5.
15. Ma, X.J., et al., *Molecular classification of human cancers using a 92-gene real-time quantitative polymerase chain reaction assay.* Arch Pathol Lab Med, 2006. **130**(4): p. 465-73.
16. Pagedar, N.A., et al., *Gene expression analysis of distinct populations of cells isolated from mouse and human inner ear FFPE tissue using laser capture microdissection--a technical report based on preliminary findings.* Brain Res, 2006. **1091**(1): p. 289-99.
17. Tothill, R.W., et al., *An expression-based site of origin diagnostic method designed for clinical application to cancer of unknown origin.* Cancer Res, 2005. **65**(10): p. 4031-40.

18. Kabbarah, O., et al., *Expression profiling of mouse endometrial cancers microdissected from ethanol-fixed, paraffin-embedded tissues.* Am J Pathol, 2003. **162**(3): p. 755-62.
19. Maher, E.A., et al., *Malignant glioma: genetics and biology of a grave matter.* Genes Dev, 2001. **15**(11): p. 1311-33.
20. Holland, E.C., *Gliomagenesis: genetic alterations and mouse models.* Nat Rev Genet, 2001. **2**(2): p. 120-9.
21. Zhu, Y. and L.F. Parada, *The molecular and genetic basis of neurological tumours.* Nat Rev Cancer, 2002. **2**(8): p. 616-26.
22. Kleihues, P., et al., *The WHO classification of tumors of the nervous system.* J Neuropathol Exp Neurol, 2002. **61**(3): p. 215-25; discussion 226-9.
23. Packer, R.J., *Primary Central Nervous System Tumors in Children.* Curr Treat Options Neurol, 1999. **1**(5): p. 395-408.
24. Louis, D.N., E.C. Holland, and J.G. Cairncross, *Glioma classification: a molecular reappraisal.* Am J Pathol, 2001. **159**(3): p. 779-86.
25. Pollack, I.F., et al., *Molecular abnormalities and correlations with tumor response and outcome in glioma patients.* Neuroimaging Clin N Am, 2002. **12**(4): p. 627-39.
26. Rood, B.R. and T.J. Macdonald, *Pediatric high-grade glioma: molecular genetic clues for innovative therapeutic approaches.* J Neurooncol, 2005.
27. Faury, D., et al., *Molecular profiling identifies prognostic subgroups of pediatric glioblastoma and shows increased YB-1 expression in tumors.* J Clin Oncol, 2007. **25**(10): p. 1196-208.
28. Mariani, L., et al., *Identification and validation of P311 as a glioblastoma invasion gene using laser capture microdissection.* Cancer Res, 2001. **61**(10): p. 4190-6.
29. Aoyagi, K., et al., *A faithful method for PCR-mediated global mRNA amplification and its integration into microarray analysis on laser-captured cells.* Biochem Biophys Res Commun, 2003. **300**(4): p. 915-20.
30. Polacek, D.C., et al., *Fidelity and enhanced sensitivity of differential transcription profiles following linear amplification of nanogram amounts of endothelial mRNA.* Physiol Genomics, 2003. **13**(2): p. 147-56.
31. Faury, D., et al., *Molecular profiling identifies prognostic subgroups of pediatric glioblastoma.* J Clin Oncol, 2006. **In press**.
32. Kreisberg, J.I., et al., *Phosphorylation of Akt (Ser473) is an excellent predictor of poor clinical outcome in prostate cancer.* Cancer Res, 2004. **64**(15): p. 5232-6.
33. Pollack, I.F., et al., *Expression of p53 and prognosis in children with malignant gliomas.* N Engl J Med, 2002. **346**(6): p. 420-7.
34. Copois, V., et al., *Impact of RNA degradation on gene expression profiles: Assessment of different methods to reliably determine RNA quality.* J Biotechnol, 2006.
35. Shi, L., et al., *The MicroArray Quality Control (MAQC) project shows inter- and intraplatform reproducibility of gene expression measurements.* Nat Biotechnol, 2006. **24**(9): p. 1151-61.

36. Patterson, T.A., et al., *Performance comparison of one-color and two-color platforms within the MicroArray Quality Control (MAQC) project.* Nat Biotechnol, 2006. **24**(9): p. 1140-50.
37. Canales, R.D., et al., *Evaluation of DNA microarray results with quantitative gene expression platforms.* Nat Biotechnol, 2006. **24**(9): p. 1115-22.
38. Minor, J.M., *Microarray quality control.* Methods Enzymol, 2006. **411**: p. 233-55.
39. Segal, E., et al., *A module map showing conditional activity of expression modules in cancer.* Nat Genet, 2004. **36**(10): p. 1090-8.
40. Gloghini, A., et al., *RT-PCR analysis of RNA extracted from Bouin-fixed and paraffin-embedded lymphoid tissues.* J Mol Diagn, 2004. **6**(4): p. 290-6.
41. Bibikova, M., et al., *Quantitative gene expression profiling in formalin-fixed, paraffin-embedded tissues using universal bead arrays.* Am J Pathol, 2004. **165**(5): p. 1799-807.
42. Rich, J.N., et al., *Gene expression profiling and genetic markers in glioblastoma survival.* Cancer Res, 2005. **65**(10): p. 4051-8.
43. Shi, Q., et al., *Secreted protein acidic, rich in cysteine (SPARC), mediates cellular survival of gliomas through AKT activation.* J Biol Chem, 2004. **279**(50): p. 52200-9.
44. Karsten, S.L., et al., *An evaluation of tyramide signal amplification and archived fixed and frozen tissue in microarray gene expression analysis.* Nucleic Acids Res, 2002. **30**(2): p. E4.
45. Penland, S.K., et al., *RNA expression analysis of formalin-fixed paraffin-embedded tumors.* Lab Invest, 2007. **87**(4): p. 383-91.
46. Coudry, R.A., et al., *Successful application of microarray technology to microdissected formalin-fixed, paraffin-embedded tissue.* J Mol Diagn, 2007. **9**(1): p. 70-9.
47. Sutherland, B.W., et al., *Akt phosphorylates the Y-box binding protein 1 at Ser102 located in the cold shock domain and affects the anchorage-independent growth of breast cancer cells.* Oncogene, 2005. **24**(26): p. 4281-92.

CHAPTER 4

Pediatric grade III anaplastic astrocytomas are distinct from pediatric Grade IV glioblastomas

(Manuscript in Preparation)

Takrima Haque and Noha Gerges, Damien Faury, Andre Nantel, Nada Jabado

4.1 Abstract

Pediatric high grade astrocytomas (HGAs) comprise grade III and IV neoplasms and are devastating brain tumors. Due to of the paucity of pediatric samples, there are no studies comparing molecular differences between pediatric grade III and IV astrocytomas in children and most published data group grade III and IV tumors together. Our premise is that there are significant molecular differences between grade III (anaplastic) and IV (glioblastoma, GBM) astrocytomas in children based on increased survival and differences in proliferation rate, angiogenesis and necrosis in a tumor between both tumor grades. To this issue, we performed microarray analysis on several HGAs and using principal component analysis (PCA) on the most differentially expressed genes in the dataset, we identify that pediatric grade III and IV astrocytomas segregate into two distinct groups implying they are molecularly distinct. Analysis done using the ingenuity software showed that the mTOR pathway is the most differentially regulated between the two grades and that VEGFc is more upregulated in grade III compared to grade IV astrocytomas. Our findings indicate that anaplastic astrocytomas and GBM in children are distinct molecular entities with potentially distinct molecular

drivers amenable to targeted therapies. Targeting the mTOR pathway may be of therapeutic benefit in anaplastic astrocytomas,

4.2 Introduction

High grade astrocytomas comprise tumors classified as grade III and IV [1, 2]. In children high grade astrocytomas (HGAs) are rare and thus very little molecular data has been available until recently. We showed that pediatric GBM (grade IV astrocytomas) have distinct molecular pathways leading to tumorigenesis compared to adult GBM. In adults, grade III tumors (anaplastic astrocytomas, AA) can develop into grade IV astrocytomas, however in pediatric HGGs, grade III tumors rarely progress into GBMs.

Many studies have shown that molecular categorization of tumors may be better for predicting prognosis and identifying therapeutic targets than histological grading. In adults, several studies have compared gene expression profiles of grade III and IV HGAs [3, 4]. Pathology results indicate that Grade III astrocytomas have more limited angiogenesis and necrosis compared to grade IV tumors. They show improved survival and better therapeutic responses. Microarray expression profiling has identified different molecular subtypes in HGG [1, 5-12]. Some differences in adults show that loss of chromosome 10q is more frequent in GBM than AA [13, 14] also, EGFR amplification is prominent in GBM [15]. The study done by Phillips *et al.* identified 3 subgroups in adult HGG. The groups were designated as proneural, proliferative, and mesenchymal. The proneural subgroups had a slightly better survival advantage over the other two. All grade III tumours were incuded in the proneural subgroup while other GBMs were distributed across the 3 groups [12]. Pediatric HGAs are similar to adult secondary

GBMs since both have PDGFRA amplification but rarely contain EGFR amplification. However, unlike adult secondary GBMs, pediatric HGAs have limited IDH mutations [16]. Due to the paucity of AA tumor samples in children , there haven't been any studies done to compare differences in detail between pediatric grade III and IV astrocytomas and most studies in children group both tumor grades. In the previous two chapters we have shown that grade IV astrocytomas can be divided into by at least 2 subgroups using microarray expression analysis. In this chapter, again using microarray analysis, we show from our results that there are differences between pediatric grade III and IV astrocytomas. A better understanding of molecular subsets of pediatric high grade gliomas may help to identify relevant therapeutic targets.

In our study, we analyzed 6 pediatric grade III astrocytoma tumors by microarray analysis and compared them to our frozen GBM samples analyzed in chapter 2. By Principal component analysis, we found that the grade III and grade IV pediatric astrocytomas clustered separately, suggesting distinct molecular pathways involved in their tumorigensis. Analysis done by ingenuity showed that the mTOR pathway was the pathway most differentially regulated between the two grades.

4.3 Materials and Methods

Characterization of Samples

The tumor set consisted of 14 pediatric GBM and 6 anaplastic astrocytomas. A neuropathologist independently reviewed all the samples to characterize each tumor as WHO grade III or grade IV. The clinical findings of all the patients with GBM and

control brains are published in Faury, et al. 2007. The information on the HGG tumors is described in **table 4.1**.

Tumor cells from each sample were captured using laser microdisection and described previously [11]. RNA was extracted from all the samples and subjected to two rounds of T7-RNA polymerase amplification.

Microarray analysis

RNA from samples were hybridized to human 19K cDNA spotted arrays, scanned and intensity quantified as described previously [11]. The LOWESS scatter smoothing algorithm in the GeneSpring 7.0 software package (Agilent, Santa Clara, CA) normalized the raw fluorescence data. Filter on confidence and analysis of variance (ANOVA) statistical tools in Genespring were used to identify differentially expressed genes. Hierarchal clustering and Principal component analysis (PCA) were also done using Genespring. The statistically significant genes of interest were used for further analysis by Ingenuity Pathway Analysis (Ingenuity Systems, Inc., Redwood City, U.S.A). This software generates functional profiles of the differentially expressed genes and shows different biological processes and pathways involved.

Quantitative Real Time PCR

Forty nanograms of amplified RNA from each tumor sample was converted into cDNA by using the iScript DNA Synthesis Kit (BioRad). Primers sequences were designed in the 3'end of each gene using the Integrated DNA Technologies (IDT) software (http://www.idtdna.com/Scitools/Applications/Primerquest/)

Each reaction was done in triplicate on a Mx3000 Multiplex Quantitative PCR System (Stratagene, Cedar Creek, TX). After 40 cycles of amplification, an additional step

allowing dissociation curve analysis was performed. Specificity of the amplification process was evaluated by dissociation curve analysis. Fold changes were calculated using the standard curve method. Total RNA from 6 pAA samples and 3 pGBM samples were utilized for this reaction. A 10-fold serial dilution of this mixture was used to construct a standard curve for both reference and target genes. Amplification efficiencies (E) were calculated as $E = 10^{(-1/S)}$, where S represents the slope of the standard curve. Only efficiencies within 90% and 110% were accepted. Quantities of target were calculated by plotting the Ct values to the corresponding standard curve. Tumoral quantities were then normalized to an endogenous control (ß-actin). Fold change is given by dividing the normalized target quantity by the value of the calibrator (nontumoral tissue control). The normalized target amount of the calibrator is set to the value 1. Primers for vegfc and PPP2R3A were designed using IDT.

4.4 Results

Grade III gliomas cluster separately from grade IV gliomas

To determine whether grade III astrocytomas are distinct from grade IV astrocytomas, RNA from the 6 grade III astrocytomas were isolated, amplified and hybridized to human 19K cDNA spotted arrays. The same procedure and reference control RNA was used, as was described in the previous chapter. Using Genespring, a list of transcripts statistically different between grade III astrocytoma samples and grade IV astrocytoma samples were compiled. By using Principal component analysis (PCA), as was done on the GBM samples previously, both grades of astrocytomas were separated into two distinct groups. These results are shown in **Figure 4.1**. PCA analysis was able

to cluster all of the anaplastic astrocytomas together and cluster all the GBMs separately. This strongly suggests that both types of astrocytomas are molecularly distinct and may have different molecular pathways leading to tumorigenesis.

Top functions and pathways differentially expressed between grade III and IV astrocytomas

Primary dataset confirms aggressive phenotype of pGBM compared to pAA

Microarray results generated by our laboratory in 2007 [11] were used for further analyses using the IPA software. The gene lists were set up in such a way that normalized pAA data was compared to normalized pGBM data (pAA/pGBM) and then imported into the software. This allowed for clear differences between the two tumor groups to be visualized.

A total of 1291 genes were inputted into the software, however only 606 of those were identifiable by IPA leaving out the last 685 genes. Of the 606, 304 were downregulated, and 302 were upregulated. 429 functions, pathways, and lists were eligible from this analysis. Top biological functions with highly differentially expressed genes included cell death, cellular movement, cell morphology, cell cycle, and cancer to name a few (**Figure 4.2**). Genes with cell death-associated functions are able to aid in apoptosis, and have been highly implicated in cancer. Cellular movement is the integral foundation for tumors to be able to metastasize and so these genes are important in defining tumor grade and aggressiveness. Cell cycle checkpoints are frequently dysregulated in cancers and this was confirmed within our top biological functions. **Table 4.2** highlights differentially expressed genes involved in top biological functions of

interest. Genes with an aggressive role in cancer were downregulated in pAA as compared to pGBM (KRAS, RHOB, SMAD4, ERBB3, DAP).

mTOR pathway is the most differentially regulated between the two grades

Several canonical pathways were different between grade III and IV astrocytomas and one of the more significant ones was the mTOR pathway (**Figure 4.3).** The mTOR pathway is involved in protein synthesis, metabolism, and angiogenic regulation, which makes it an interesting therapeutic target for GBMs. For this reason, we chose to further investigate the dysregulated genes within this pathway to further understand key genetic alterations involved. 5/13 genes from this pathway were downregulated in pAA whereas 8/15 were upregulated in pGBM. Our lab has previously demonstrated the importance of the Akt pathway in pGBM and as the PI3K/Akt pathway is a regulator of the mTOR pathway, these analyses confirm our previous data. We were able to show that pGBM were grouped into 2 subsets based on whether they harbored active or inactive Ras/Akt pathways; patients with the active form had a worse prognosis [11]. This data further highlights the importance of the mTOR pathway and its downstream targets. **Figure 4.4** depicts the IPA-generated mTOR signaling cascade highlighting upregulated (green) and downregulated (red) genes. Of the 13 significantly altered genes highlighted in **Table 4.3**, protein phosphatases involved in the negative regulation of proliferation were found to be overexpressed in pAA when compared to pGBM (PPP2R1B, PPP2R5B). Translational factors (EIF3B, EIF4B) were downregulated, as well as genes involved in cancer progression and poor prognosis (KRAS, RHOB). Interestingly, VEGFc was found overexpressed in pAA. Two other targets were further validated using QRT-PCR. For pAA the QRT-PCR results for VEGFc was 1.55 and 0.34 for PPP2R3A. PKC family

members phosphorylate a wide variety of protein targets and are known to be involved in diverse cellular signaling pathways.

3.5 Discussion

MTOR signaling pathway is deregulated in many cancers including GBM [17]. This pathway is regulated by the PI3K/Akt pathway and plays a role in differentiation, transcription, translation, apoptosis, cell cycle progression, and metabolism [18, 19].

Several tumors show mutations in the mTOR pathway, thus is a potential target to control or abate tumorigenisis. Clinical trials of Rapamycin and its analogs have been ongoing in treatment of a variety of cancers. This made the finding of the mTOR signaling pathway as significantly altered in pAA exciting as it too may be a candidate for targeted gene therapy for this subgroup of patients.

Of the 13 genes found to be dysregulated in this pathway using our gene list, 8 were downregulated whereas 5 were upregulated. We report that genes better known to play roles in more aggressive types of cancer are downregulated in pAA compared to pGBM. These include KRAS and RHOB. We were surprised to find that VEGFc was in fact upregulated in pAA compared to pGBM. The VEGF family of proteins is important signaling proteins involved in both vasculogenesis and angiogenesis. They are also important for proliferation, survival, and growth of tumors. In adults, studies have shown that VEGF proteins are more overexpressed in GBM compared to AA [20]. However, it seems that in this subset of tumors, that VEGFc in particular is more highly expressed in pAA – a finding that we are still trying to decode. VEGFc is upregulated in a number of cancers, such as, breast [21], colorectal [22], and non-small cell lung cancer. It has also

been shown elevated in HGG [23, 24]. However, research surrounding HGG and VEGFc involves adult patients only, and so it might be possible that in pediatrics, the VEGF family of proteins function using different mechanisms. Further work is ongoing in our laboratory to elucidate the reasoning behind this overexpression in pAA.

This is the first report of its kind in the literature where a genetic signature has begun to become elucidated in pAA separately from pGBM. This report of our findings further indicates the dire need for segregation of the HGG in research. These tumors do in fact segregate independently from each other due to different genetic signatures. This data will become valuable in the future development of diagnostic markers that will aid in distinguishing pAA from pGBM histologically. Such acquisition of a set of genetic markers that will distinguish these two types of tumors from one another will not only save precious time, but will also result in preventing misdiagnoses in these patients.

3.6 Tables and Figures

Table 4.1: Characteristics of Samples included in Faury *et al,* 2007 Study			
Grade	**Age**	**Sex**	**Location of tumor**
III	12	F	Temporal occipital
III	13	M	Temporal
III	3	F	Occipital
III	6	F	Pons mesensephalon
III	6	F	Pons
III	17	F	Parietal temporal lobe
IV	7	F	N/A
IV	4	F	N/A
IV	10	F	Left frontal parietal lobe
IV	14	F	Temporal lobe
IV	14	M	Temporal lobe
IV	14	M	Right frontal lobe
IV	9	F	Left temporal parietal
IV	1	M	Hypothalamus
IV	11	F	Ponto-cerebellar
IV	13	F	Brain stem
IV	2	M	Frontal lobe
IV	16	F	Frontal lobe
IV	16	M	Right frontal lobe
IV	13	M	Right frontal lobe

Table 4.1. Characteristics of the pAA and pGBM samples used in the analysis. Six pAA and 14 pGBM samples were used for the analysis.

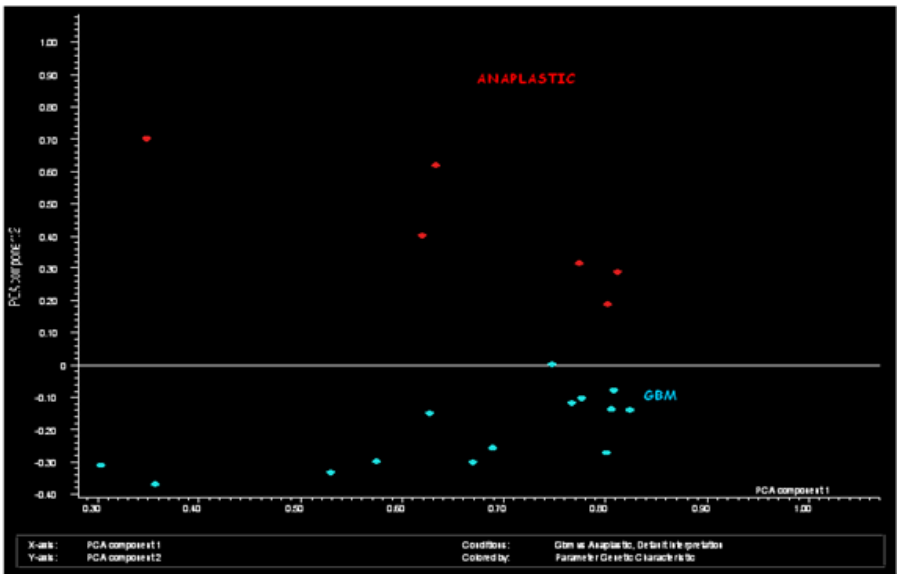

Figure 4.1: PCA analysis from Faury dataset. PCA clearly segregates patients with pAA from those with pGBM. The 14 pGBM and 7 pAA were subjected to a Principal Component Analysis (PCA) based on the expression profile. This two-dimensional plot of PCA resulted in a clear differentiation between pAA (red) and pGBM (blue).

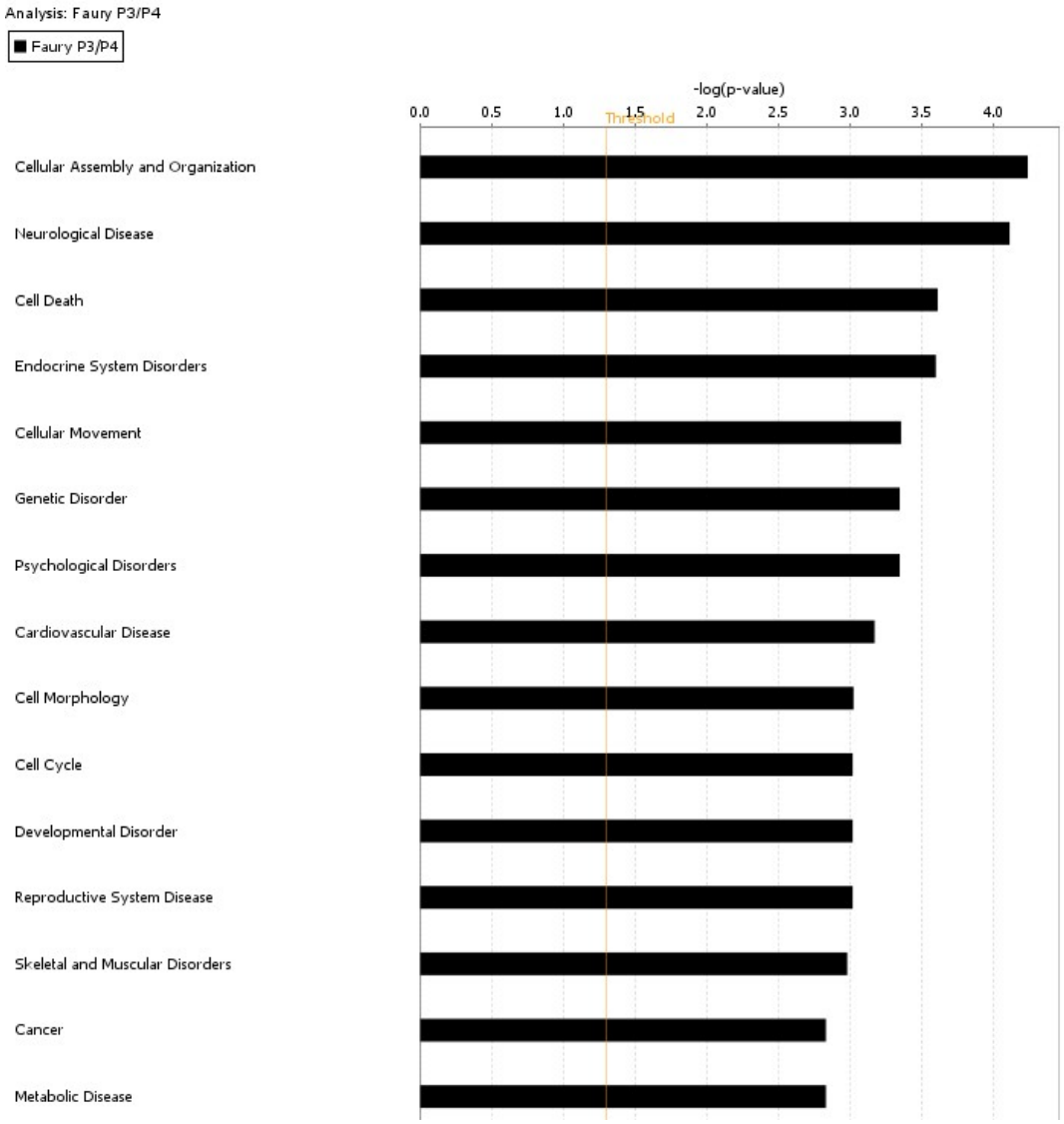

Figure 4.2: Top 15 biological functions associated with a comparison between pediatric anaplastic astrocytomas and pediatric glioblastomas obtained by Ingenuity Pathway Analysis (IPA). Horizontal bar graphs depict biological functions associated with the over- or under-expression of genes in pediatric anaplastic astrocytomas compared to pediatric glioblastomas from the Faury *et al*., 2007 dataset.

Table 4.2: Genes associated with key biological functions involved in pediatric anaplastic astrocytomas compared to pediatric glioblastomas

Function	p-value	Molecules
Cellular Assembly and Organization	$5.74x10^{-5}$ - $3.65x10^{-2}$	ADD1, ADD2, ALS2CL, ANK3, ANXA5, APC, B3GNT1, CD82, CDC42, CRYAB, CTNND1,EPB49, EZR, FLI1, HOOK3, HTT, INA, ITPR1, KRAS, LIMK1, LPAR1, MCAM , MME, PEX16, PLD1, RAB11FIP4, RHOB, RND1, SH2D2A, SMAD4, STX18, TGFBI, TNFSF10, TPR, TRIP10, TTN, UBE2B, VPS18
Neurological Disease	$7.69x10^{-5}$ - $3.09x10^{-2}$	ABCC10, ADCY2, AHI1, AIM1, ALB, ALDH2, ALDH3B1, ANK3, ANO6, ANXA5, APC, APLP1, ARHGDIB, ARPP19, ATG5, ATP6V1C1, ATXN2, B3GNT1, BIRC6, C11ORF41, CAMTA1, CC2D2A, CCBE1, CD36, CD274, CDH8, CDK5RAP2, CDS1, CELF2, CENPF, CEPT1, CGNL1, CLMN, CNP, CNTFR, CRAMP1L, CRBN, CRYAB, CTNNB1, DCHS2, DCLK1, DIABLO, DLG2, DTNBP1, EPHA4, ERBB3, F13A1, FAM114A1, FAM124A, FBXW7, FIG4, GAB2, GABARAPL1, GABRA1, GALNT1, GARNL3, GLT1D1, GNE, GRIN2A, GRM5, HBG2, HIVEP2, HLCS, HMGCR, HPCA, HSPA6, HTT, INA, IRAK4, ITPR1, ITPR2, KCNQ3, KCTD17, KLC1, KRR1, LAMP2, LGI1, LIMK1, LMNB1, LOC150568, LOC440040, LPAR1, LRRC2, LRTOMT, MAP4K4, MBNL2, MED21, METT5D1, MFGE8, MME, MTHFD1L, MTHFR, MTMR6, NDUFS1, NDUFV1, NKAP, NQO1, NR4A2, NRG3, NTRK2, NTRK3, NUMB, OXTR, PAXIP1, PCDH19, PDE4DIP, PDIA3, PDLIM5, PEX16, PHACTR2, PHF21A, PLCB1, PPP1R14C, PPP1R9B, PPP3CC, PRDM2, PRKCB, PSAP, PTCD3, PTGS1, PVALB, RAB13, RAB11FIP4, RERGL, RFX4, RHOB, RHOBTB3, ROD1, RPH3A, RPL31, RPL13A, RPS6KA5, SCN2B, SCN3B, SEC24A, SHROOM2, SLC16A1, SLC1A2, SND1, SNTG1, SOX9, SSBP3, SURF6, SUSD1, SYNGR1, SYT7, TARBP1, TASP1, TEAD3, TF, TIAM1, TLE4, TMEM209, TMEM55A, TRIM10, TRIM27, TRIM32, TRPM1, TSHZ2, UBXN4, WDR7, WDR25, ZCCHC4, ZKSCAN1, ZMYND8, ZNF3, ZNF551

Cell Death	$2.44x10^{-4}$ - $4.72x10^{-2}$	AAK1, ALB, ALDH2, ALDH3B1, APC, ARG2, ATG5, ATXN2, BAG1, BFAR, CD36, CD47, CD82, CD274, CDC42, CRYAB, CTCF, CTNNB1, DAP, DIABLO, EMP2, ERBB3, EZR, FBXO32, FLI1, FXR1, GULP1, GNE, HTT, IAPP, IL15RA, ITPR1, ITPR2, KRAS, LAMP2, LMNB1, LPAR1, LSP1, MAP2K6, MSR1, MTMR6, MYB, NDUFS1, NQO1, NR4A2, NTRK2, OGFOD1, PCBP2, PECAM1, PLD1, PRDM2, PRKCB, PTGER3, PTGS1, RAD23B, RASSF2, RHOB, SCN3B, SOX9, STAT5B, TASP1, TF, TGFA, TIAM1, TNFSF10, TRIM27, TRIM32, UBE2B, VEGFC, YY1, ZAC, ZEB1
Cellular Movement	$4.39x10^{-4}$ - $4.71x10^{-2}$	ALB, ALPP, APC, ARHGDIB, B3GNT1, BDKRB1, CD36, CD47, CD82, CDC42, CTNNB1, ERBB3, EREG, EZR, GAB2, HMGCR, HOXD10, ITPR1, LIMK1, LPAR1, LSP1 MAP4K4, MYH10, NUMB, PECAM1, PLD1, PPBP, PRKCB, RASGRP1, RHOB, SH2D2A, SMAD4, TEK, TIAM1, TNFSF10, TPR, VEGFC
Cell Morphology	$9.42x10^{-4}$ - $4.37x10^{-2}$	ADRBK1, ANK3, APC, ATG5, CDC42, CTNND1, EZR, F2RL2, FBXW7, GABARAPL1, HTT, KRAS, LAMA4, LIMK1, LSP1, PECAM1, PLA2G12A, PLD1, RASGRF1, RHOB, SMAD4, SOX9, TIAM1, TNFSF10, TPR, TTN, VEGFC
Cell Cycle	$9.56x10^{-4}$ - $4.25x10^{-2}$	AMACR, APC, CDC42, CENPF, CKS1B, CTNND1, ERBB3, KRAS, LIMK1, MAP2K6, MYB, SMAD4, SOX9, TGFA, TRIM21, TXNL4B, VPS18
Cancer	$1.47x10^{-3}$ - $4.52x10^{-2}$	ABCA8, AIM1, ALB, AMACR, ANK3 , ANXA5, APC, ARG2, BAG1, BAT1, BDKRB1, CALD1, CD36, CD82, CD274, CDC42, CDC73, CENPF, CNP, CTNNB1, CTNND1, DCLK1, DLG2, EPHA4, ERBB3, EREG, EZR, FBXW7, FECH, GABRA1, GRIN2A, HMGCR, IFIT1, IL15RA, KIAA0892, KRAS ,LAMA4, LEFTY2, LGI1, LPAR1, LSP1, MAP4K4, MBNL2, MCAM, MME, MTHFD1L, MTHFR, MTMR6, MYH10, NPAS2, NQO1, NTRK2, PECAM1, PEX11A , PLD1, PPP2R1B, PRDM2, PRKCB, PTGS1, PVRL4, RNF160, RPL13A, SEC63, SLC16A1, SMAD4, SOX9, SPIRE2, SRRM2, SSBP3, SSTR1, STAT5B, STX3, SYNGR1, TASP1, TEK, TMBIM4, TNFSF10, TRIM10, TRIM32, UBE2B, VEGFC, ZEB1

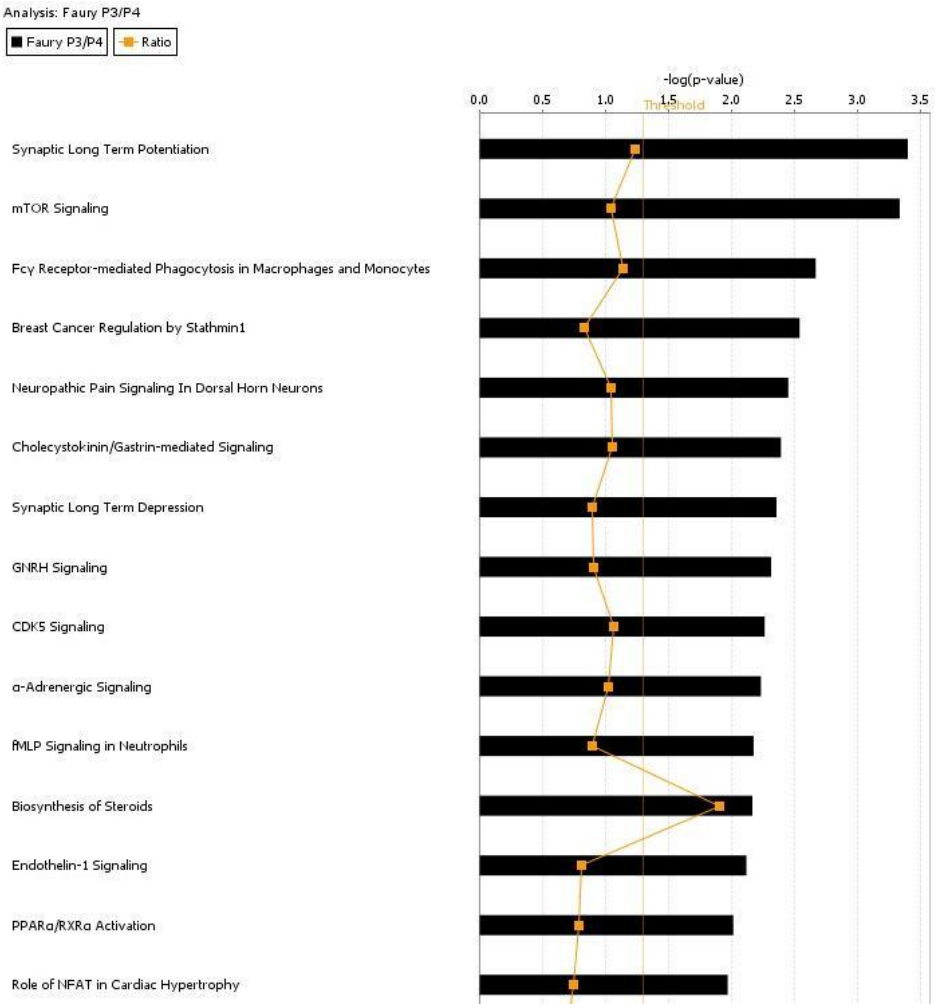

Figure 4.3: Top 15 canonical pathways involved with the over- or under-expression of genes in pediatric anaplastic astrocytomas compared to pediatric glioblastomas generated by IPA. Horizontal bar graphs depict canonical pathways differentially altered due to the over- or under-expression of genes in pediatric anaplastic astrocytomas compared to pediatric glioblastomas from the Faury *et al*., 2007 dataset.

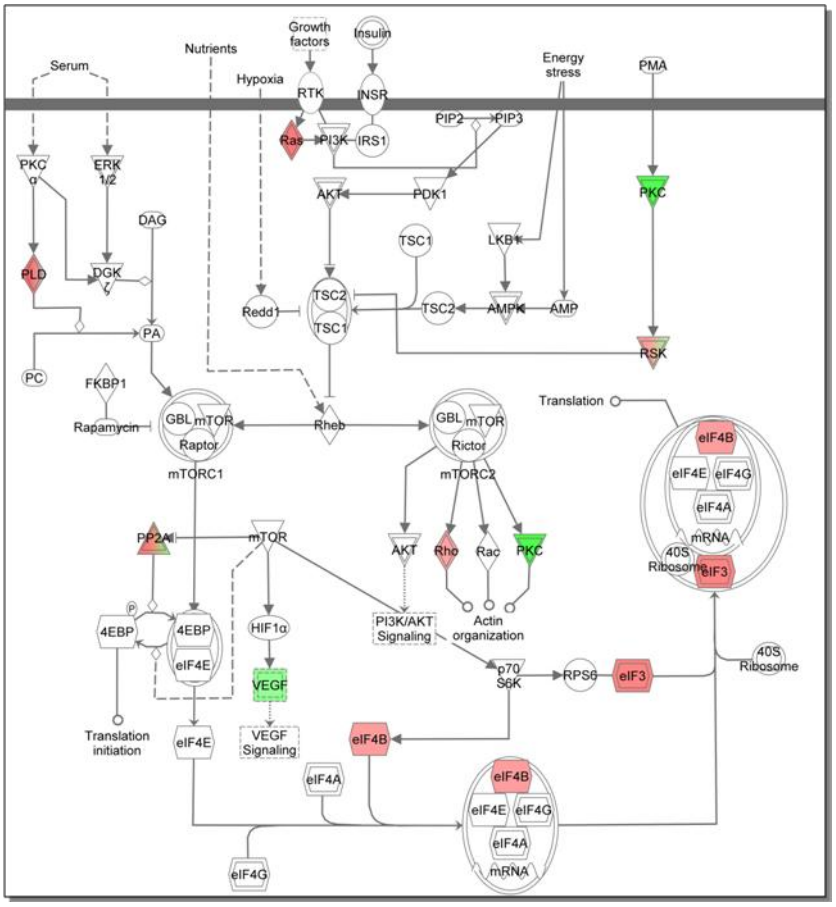

Figure 4.4: IPA-generated mTOR pathway. IPA-generated mTOR pathway depicting over- and under-expressed genes within the Faury dataset. Over-expressed genes in pAA compared to pGBM are highlighted in green and under-expressed genes are highlighted in red.

Table 4.3: List of differentially expressed genes within the mTOR pathway.

Gene	Fold change
PLD1	-2.062
GPLD1	-2.018
PPP2R3A	-1.831
KRAS	-1.812
EIF3B	-1.662
RPS6KA4	-1.341
EIF4B	-1.325
RHOB	-1.250
RPS6KA5	+1.360
PPP2R1B	+1.412
VEGFC	+1.638
PPP2R5B	+1.807
PRKCB	+2.723

3.7 References

1. Dreyfuss, J.M., M.D. Johnson, and P.J. Park, *Meta-analysis of glioblastoma multiforme versus anaplastic astrocytoma identifies robust gene markers.* Mol Cancer, 2009. **8**: p. 71.
2. Louis, D.N., et al., *The 2007 WHO classification of tumours of the central nervous system.* Acta Neuropathol, 2007. **114**(2): p. 97-109.
3. Toedt, G., et al., *Molecular signatures classify astrocytic gliomas by IDH1 mutation status.* Int J Cancer, 2011. **128**(5): p. 1095-103.
4. Holland, H., et al., *WHO grade-specific comparative genomic hybridization pattern of astrocytoma - a meta-analysis.* Pathol Res Pract, 2010. **206**(10): p. 663-8.
5. Liang, Y., et al., *Gene expression profiling reveals molecularly and clinically distinct subtypes of glioblastoma multiforme.* Proc Natl Acad Sci U S A, 2005. **102**(16): p. 5814-9.
6. Freije, W.A., et al., *Gene expression profiling of gliomas strongly predicts survival.* Cancer Res, 2004. **64**(18): p. 6503-10.
7. Nutt, C.L., et al., *Gene expression-based classification of malignant gliomas correlates better with survival than histological classification.* Cancer Res, 2003. **63**(7): p. 1602-7.
8. Verhaak, R.G., et al., *Integrated genomic analysis identifies clinically relevant subtypes of glioblastoma characterized by abnormalities in PDGFRA, IDH1, EGFR, and NF1.* Cancer Cell, 2010. **17**(1): p. 98-110.
9. Petalidis, L.P., et al., *Improved grading and survival prediction of human astrocytic brain tumors by artificial neural network analysis of gene expression microarray data.* Mol Cancer Ther, 2008. **7**(5): p. 1013-24.
10. Godard, S., et al., *Classification of human astrocytic gliomas on the basis of gene expression: a correlated group of genes with angiogenic activity emerges as a strong predictor of subtypes.* Cancer Res, 2003. **63**(20): p. 6613-25.
11. Faury, D., et al., *Molecular profiling identifies prognostic subgroups of pediatric glioblastoma and shows increased YB-1 expression in tumors.* J Clin Oncol, 2007. **25**(10): p. 1196-208.
12. Phillips, H.S., et al., *Molecular subclasses of high-grade glioma predict prognosis, delineate a pattern of disease progression, and resemble stages in neurogenesis.* Cancer Cell, 2006. **9**(3): p. 157-73.
13. Schmidt, M.C., et al., *Impact of genotype and morphology on the prognosis of glioblastoma.* J Neuropathol Exp Neurol, 2002. **61**(4): p. 321-8.
14. Smith, J.S., et al., *PTEN mutation, EGFR amplification, and outcome in patients with anaplastic astrocytoma and glioblastoma multiforme.* J Natl Cancer Inst, 2001. **93**(16): p. 1246-56.
15. Nobusawa, S., et al., *IDH1 mutations as molecular signature and predictive factor of secondary glioblastomas.* Clin Cancer Res, 2009. **15**(19): p. 6002-7.
16. Paugh, B.S., et al., *Integrated molecular genetic profiling of pediatric high-grade gliomas reveals key differences with the adult disease.* J Clin Oncol, 2010. **28**(18): p. 3061-8.

17. Gulati, N., et al., *Involvement of mTORC1 and mTORC2 in regulation of glioblastoma multiforme growth and motility.* Int J Oncol, 2009. **35**(4): p. 731-40.
18. Sunayama, J., et al., *Crosstalk between the PI3K/mTOR and MEK/ERK pathways involved in the maintenance of self-renewal and tumorigenicity of glioblastoma stem-like cells.* Stem Cells, 2010. **28**(11): p. 1930-9.
19. Sunayama, J., et al., *Dual blocking of mTor and PI3K elicits a prodifferentiation effect on glioblastoma stem-like cells.* Neuro Oncol, 2010. **12**(12): p. 1205-19.
20. Zhou, Y.H., et al., *The expression of PAX6, PTEN, vascular endothelial growth factor, and epidermal growth factor receptor in gliomas: relationship to tumor grade and survival.* Clin Cancer Res, 2003. **9**(9): p. 3369-75.
21. Raica, M., et al., *Lymphatic microvessel density, VEGF-C, and VEGFR-3 expression in different molecular types of breast cancer.* Anticancer Res, 2011. **31**(5): p. 1757-64.
22. Du, B., et al., *Metastasis-associated protein 1 induces VEGF-C and facilitates lymphangiogenesis in colorectal cancer.* World J Gastroenterol, 2011. **17**(9): p. 1219-26.
23. Grau, S.J., et al., *Expression of VEGFR3 in glioma endothelium correlates with tumor grade.* J Neurooncol, 2007. **82**(2): p. 141-50.
24. Fountzilas, G., et al., *Post-operative combined radiation and chemotherapy with temozolomide and irinotecan in patients with high-grade astrocytic tumors. A phase II study with biomarker evaluation.* Anticancer Res, 2006. **26**(6C): p. 4675-86.

Chapter 5

Determination of the role of SNX3 in the endosomal trafficking of receptor tyrosine kinases (RTKs) including the epidermal growth factor receptor (EGFR)

(Manuscript in preparation)

Takrima Haque, Dong-Anh Khuong-Quang, Damien Faury, Brian Meehan, Janusz Rak, Nada Jabado

5.1 Abstract

Pediatric glioblastomas (pGBM) have dismal prognosis and, unlike adult GBM (aGBM), little is known about molecular events driving oncogenesis in children. We previously established in primary pGBM samples that there are at least two subtypes of pGBM, both molecularly distinct from aGBM, one was associated with Ras/Akt-activation and a poor prognosis and the other with no obvious Ras/Akt activation and a better outcome [1]. Aberrant Ras activation in GBM is driven by upstream events including aberrant signaling through receptor tyrosine kinases (RTKs) which are amplified, mutated, or rearranged in a large proportion of aGBM. However, unlike primary aGBM, which harbour amplification of *EGFR* in ~50% of tumors, pGBM show no genetic amplification/mutation of RTKs [2-4]. Data from our microarray analysis identified *Sorting Nexin 3 (SNX3*) as one of the genes to be exclusively overexpressed in the pGBM subset associated with Ras activation. SNX3 belongs to a family of proteins involved in the regulation of intracellular trafficking of membrane receptors. It is

associated with early endosomes through a novel motif (PX domain) following its interaction with phosphatidylinositol-3-phosphate [5-7]. We show that over expression of SNX3 sustains EGFR and MET signaling. Using immunofluorescence imaging, we identify in primary aGBM and pGBM cell lines overexpressing SNX3 delayed EGFR degradation and prolonged signaling of EGF-EGFR complexes from within the endosomes. Delay in receptor tyrosine kinase (RTK) degradation by SNX3 overexpression induced increased proliferation, anchorage independent growth *in vitro* and lastly tumor formation and growth in a heterotopic xenograft mouse model *in vivo*. Our data suggest that deregulation of endocytic trafficking by SNX3 overexpression reproduces genetic amplification/alteration of RTK. As this phenomenon concerns multiple RTKs, their sustained and combined co-activation could decrease the efficiency of targeting therapy against a single receptor currently seen in clinical trials for GBM.

5.2 Introduction:

Activated receptors, such as receptor tyrosine kinases are rapidly internalized and transported via sorting endosomes where sorting decisions are made. Some activated receptors are recycled and others are degraded [8, 9]. Signalling receptors that need to be down-regulated, such as, EGFR, are destined to degradation. This occurs by inward budding of the endosomal lumen to form a multivesicular body, which eventually matures and fuses with lysosomes, leading to degradation [10-15]. In cancer, RTKs evade degradation by overexpression and/or amplification at the gene level or at the post-translational level (delayed recycling/increased stability of the protein) [16, 17].

PGBM is a grade IV astrocytic brain tumor, where EGFR is deregulated. In children, it is a rare tumor, however it causes high mortality and morbidity. Significantly more information is available in literature about aGBMs compared to pGBMs. In both aGBM and pGBM, EGFR is overexpressed. In adults, EGFR is amplified at the gene level and also a mutant form of EGFR is found that is constitutively active. In pGBM, EGFR is overexpressed but amplification is rare and the mutant form is not seen. Therefore, factors involved in the post-translational level may contribute to the increased EGFR activity in pediatric GBM [4, 18, 19].

Previously, microarray analyses were done on several pGBM samples [1, 20] and SNX3 was found to be overexpressed in a subset of pGBM. Members of the sorting nexin family have roles in different aspects of endosomal sorting. This family consists of 30 mammalian members and many are involved in the regulation of endosomal intracellular trafficking of membrane receptors [5, 21]. SNX1 and SNX16 have shown to increase the rate of EGFR degradation while SNX5 and SNX3 were shown to delay EGFR degradation [7, 22-24]. SNXs are characterized by the presence of a phox homology (PX) domain, with limited conservation between family members. The PX domain has different binding affinities for phosphatidylinositol phosphates (PtdInsPs) [5]. The PX domain of SNX3 binds directly and selectively to Phosphatidylinositol (3,4,5)-trisphosphate (PIP3), a product of active PI3K. This interaction is required for SNX3 localization to early endosomes. A study conducted by Xu et al, showed that overexpression of SNX3 in cells, lead to swelling of the endosomal compartments and inhibited transport of internalized transferrin receptors [7]. These SNX3-induced expanded membranous structures contained markers of sorting, recycling and late

endosomes, indicating mixing of the three endosomal compartments. Important to our study, SNX3 seemed to delay EGFR degradation with internalized EGF/EGFR complexes being retained in the swollen structures rather than being targeted to the lysosome for degradation. This may partly account for one of the reasons for overexpression of RTKs in pGBM. Exactly how SNX3 functions is still unclear. We hypothesized that SNX3 delays/prevents endosomal degradation of RTKs including EGFR which are trapped within early endosomes and prolongs signalling. Thus the sustained co-activation of multiple RTKs could decrease the efficiency of targeting therapy against a single receptor such as EGFR.

5.3 Materials and Methods:

Cells, Antibodies and Reagents

SNX3 expression vector and SNX3 antibody used in immunohistochemistry were a generous gift from Wanjin Hong, Singapore. SF188, SJ-G2, U87, U251 cell line were generous gifts from Dr Del Maestro (MNI, McGill University). Dulbecco's modified eagle's medium (DMEM) and bovine calf serum were purchased from Hyclone (Logan, UT). TGFα and EGF were purchased from Sigma-Aldrch, HGF, anti-Mek, anti-perk, anti-akt, anti-myc were purchased from Cell Signalling. Anti-SNX3, used for western blots, was purchased from Santa Cruz Biotechnology (Santa Cruz). Anti-EEA1 and Anti-LAMP1 were also purchase from Santa Cruz Biotechnology (Santa Cruz). Rhodamine tagged EGF (EGF-Rh) was purchased from molecular probes, Invitrogen. SNX3 SiRNA was purchased from Invitrogen. ^{3}Thymidine was purchased from PerkinElmer.

RT-PCR

RT-PCR was done in two steps using MMLV-RT (Invitrogen) and random primers. Primers sequences were designed in the 3'end of each gene with the help of Primer3® Software.

Stable SNX3 overexpression in SF188, SJ-G2, NHA and U251 cell lines.

All cells were maintained in 5% CO_2 at 37ºC in DMEM (SF188 was maintained in MEM). Cell lines were transfected using liposome-mediated Lipofectamine transfection (Invitrogen, CA), using the manufacturer's protocol at a ratio of 1µg plasmid DNA to 6µl Lipofectamine. SNX3 overexpressed clones were selected with geneticin.

Western blot and kinetics

For EGF and MET stimulation, cells were serum starved overnight and stimulated for specific time periods with 50ng/mL of each of either EGF, TGFα or HGF. After stimulation of indicted time points, cells were washed once with PBS, lysed and scraped with lysis buffer containing protease and phosphatase inhibitors. Supernatant was obtained after centrifugation at 12, 000 g for 10 minutes at 4ºC. Proteins were solubilised in 6X Laemli buffer and separated in 10% SDS-PAGE and transferred to PVDF membranes. Blocking was done in TBST buffer (10mM Tris-HCl, pH 7.6, 150mM NaCl, 0.1% Tween 20) containing 5% skim milk. Membranes were incubated with different antibodies overnight, washed and incubated with horseradish peroxidise-linked secondary antibody for 1h in room temperature, washed in TBST solution and developed by horseradish peroxidise-dependent chemiluminescence (ECL) (GE Healthcare). Membranes were scanned.

Immunofluorescence

Cells were cultured in 12-well cell culture plate containing 18 mm diameter coverslips to 60-70% confluency. Cells were starved with serum free medium overnight, washed once with PBS and incubated 2h at 4ºC in medium containing 20 ng/mL rhodamine conjugated EGF. The cells were then incubated at 37ºC for indicated times, washed once with PBS and fixed with 4% paraformaldehyde for 20 min. Fixed cells were blocked with 2% BSA and incubated with LAMP1 or EEA1 overnight, then incubated with secondary antibodies (Alexa 488, Cy3, or Alexa 594) for 30 min. Coverslips were fixed onto slides using ProLong Gold Antifade (Invitrogen) and visualized with Zeiss and by confocal microscopy.

Proliferation assays

Cells were harvested and 10 000 cells were seeded in 5 different 24 well plates for 5 different consecutive days. Cells were incubated at 37ºC for indicated times (1 to 5 days). For each time point (designated well for each day), cells were incubated with 1 μCi of ^{3}Thymadine/well overnight at 37ºC. Cells were washed with PBS and incubated at 4ºC for 30 min with TCA, then treated with 0.5N NaOH/0.5% SDS and transferred to scintillation vials containing 4mL scintillation fluid, and counted with a β-counter.

Soft Agar assays

Soft agar colony formation was done in 6 well plates containing a base layer of 1% agar and 15 000 cells were added with a top layer of 0.6% agar and incubated at 37ºC for 3 to 4 weeks. The numbers of colonies were counted.

SNX3 silencing

Transient SNX3 silencing was done using the manufacturer's protocol (Invitrogen). After 2 days of siRNA incubation cells were lysed and proteins were isolated for immunoblot assays.

In Vivo injections

SCID mice or NOD-SCID mice were used and subcutaneous injection of 10 million SF188 cells or 1 million of U87 cells was done. Monitoring twice a week, mice were sacrificed when tumor largest dimension was over 18mm.

5.4 Results:

1. Validation of microarray results for SNX3.

The microarray results for SNX3 were validated by quantitative real time PCR. **Table 5.1** shows the RT-PCR validation for some of the samples with the genespring values. Also an independent data set of tissue microarrays (TMA) of 180 High grade astrocytomas (HGA) were done (collaboration with Dr Pfister, Germany and Dr Siegel, Mcgill) (Data not shown). These results furthered showed SNX3 to be overexpressed in pGBM.

Using genespring, the software for microarray data analysis we used at the time, a mean value fold change of 2.9 of SNX3 was found in samples associated with Ras/Akt activation when compared to samples without Ras/Akt activation and the control brain. Looking at each sample individually, a value of less than 1.4 fold change was found for all the samples with inactive Ras/Akt pathways and a value of 2.2 to 3.1 fold change was found for all the samples with active Ras/Akt pathways. We also looked into other SNXs

in our microarray data. The summarized p-fold values of the different SNXs on the microarray chip are represented in **Table 5.2**. Only two of the SNXs showed differential regulation as compared to the normal brain in samples associated with Ras/Akt activation. They included, SNX3 (2.9 fold change) and SNX27 (1.72 fold change), which were upregulated in these samples. SNX27 was found to traffic G-protein-gated potassium (Kir3) channels and has a PDZ domain and not related to EGFR trafficking and thus we did not pursue this SNX any further [25].

Levels of SNX3 were also evaluated using RT-PCR in the different pGBM samples. The primers used were forward TGCGTCTTGTTTGCTTCTTG and reverse TCCTCCAGGCTTGTAATACCC. **Figure 5.1a** shows the RT-PCR results we obtained. Lanes 2, 7, 10, 12, 13, 15, and 16 represents samples with SNX3 overexpression by microarray analysis. Samples 3, 4, 8, and 9 had SNX3 downregulated by microarray. Samples that showed SNX3 overexpression by RT-PCR and microarray analysis also coincided with samples associated with Ras/Akt activation. RT-PCR was also done on the FFPE samples, however, based on RNA degradation in samples; it was hard to assess SNX3 status in samples (**Figure 5.1b**).

2. Overexpressing SNX3 in SF188 and SJ-G2:

To assess *in vitro* and *in vivo* effects of modulating SNX3 expression in astrocytomas and astrocytes, we used pediatric GBM primary cell lines SF188 and SJ-G2 and adult GBM cell lines U87 and U251. The use of multiple cell lines was to avoid a clone effect and use of U87 and U251 was to overcome the poor tumorigenic potential *in vivo* of the pediatric GBM cell lines and speed tumour formation in nude mice (U87 and

U251 are highly tumorigenic in this model). (*Also, the use of highly aggressive GBM cell lines does not fully address the role of SNX3 in oncogenesis as all lines available have constitutively active PI3K, and/or EGFR amplification, and/or alterations in the cell cycle, which impact their behavior and growth independently from SNX3. To address this issue and work in close to physiological conditions for future work we elected to also use telomeRase immortalized astrocytes (NHA), which mimic as much as possible normal astrocytes, to assess the effects of SNX3 expression and AKT activation).* We stably overexpressed myc-tagged human SNX3 cDNA or a myc-empty vector. We also stably silenced SNX3 expression in these cell lines.

Characterization of Cell lines: Initially we looked into the basal level of SNX3 protein and mRNA in the different cell lines since we were interested in overexpressing SNX3 in a cell line that had a lower level of SNX3. The cell lines in the lab were characterized to see if there were differences in the RNA and protein levels of SNX3. We also compared the basal level of EGFR in these cell lines. The basal levels of SNX3 and EGFR mRNA was assessed by RT-PCR as shown in **Figures 5.2.** No differences were seen at the mRNA levels between the cell lines. The basal level of SNX3 and EGFR protein was seen by western blot, **Figure 5.3** and by Immunofluorescence **Figure 5.4.** Again SNX3 levels were similar at the protein level between the cell lines. Our results indicate that basal SNX3 and EGFR protein and mRNA levels are similar within the different cell lines except for U251 which has a EGFR genomic amplification. We characterized the cell lines we used for EGFR, p53 mutational status, PTEN loss and AKT pathway activation. SF188 has a PTEN deletion and SJ-G2 does not; both cell lines have mutated p53 and no EGFR amplification (**Figure 5.3)**.

Generation of Stable Clones: Several stable clones in the pGBM cell lines, SF188 and SJ-G2 were isolated and characterized using immunofluorescence images and western blot analysis of total protein lysates as shown in **Figure 5.5**. From the western blots, a larger number of stable clones were generated for SF188 compared to SJ-G2, therefore for this cell line two clones were used for subsequent studies, clones 4 and 6. Clone 4 had a higher SNX3 overexpression than clone 6. Clone 3 was used for SJ-G2. *Other SNX3 overexpressed clones in NHA, U87 and U251 (adult GBM cell lines and immortalized astrocytes) were generated by Dongh- Anh Khuong-Quang.*

3. SNX3 Overexpression Delays EGF Degradation in SF188 Cells.

EGFR endosomal trafficking through early and late endosomes in was studied by immunofluorescence. It was seen that after EGFR activation its transit from the early to late endosome was delayed in SNX3 overexpressed SF188 cells compared to EV cells. SNX3 clone 6 and empty vector (EV) transfectants of SF188 cells were incubated for 1 hour on ice with Rhodamine tagged EGF (EGF-Rh, red) followed by incubation at 37°C for 0, 15 min, 30 min, 2h or 4 hours to follow the kinetics of EGFR transport from early to late endosomes by co-staining with EEA1 (early endosomal marker, green), or Lamp1 (late endosomal marker, green). Merged immunofluorescence and confocal images (overlay, co-localization in yellow) are shown in **figure 5.6 and 5.7**, respectively. Internalization of EGF occurred normally in all cells. Its subsequent delivery to the lysosome was significantly delayed in SNX3-induced structures in the transfectants as compared to the EV control. This indicates a delay in EGF degradation in SNX3

transfectant cells with persistent staining up to 4 hours as compared to an early decrease in EV cells**.**

4. Increased EGFR expression and prolonged signaling in pGBM cell line SNX3 transfectants.

EGF binds to EGF receptor and it is usually quickly delivered via endosomes to the lysosome for degradation. In our studies we have found that endosomal trafficking of EGFR for degradation was affected by SNX3 overexpression. To study the effect of SNX3 on EGFR degradation, stable clones were stimulated with EGF or TGF α for 0 to 6h, as shown in **figure 5.8**, cells were lysed and analyzed by western blotting. The western blot bands were quantitated and values were plotted on a graph and the levels of the protein were normalized to Akt or β-actin levels used as a loading control. The graphs shown are means of 3 independent experiments. EGFR expression level and Ras pathway activation was assessed in 2 clones overexpressing c-mycSNX3 from the parental cell line SF188 and in one clone from SJ-G2. Ras activation is increased and more sustained as shown by prolonged and higher levels of the downstream effectors, p-Erk and pMek. For SJ-G2 transfectants, an increased and sustained activation of the Ras pathway is also observed as shown in **figure 5.9**. These results suggest that SNX3 delays EGFR degradation prolonging their signaling from within early endosomes and thus sustaining RAS activation in cells.

5. SNX3 overexpression prolongs signaling by MET activation.

Sorting nexins may be involved in trafficking of several receptors and are not necessarily specific to one. From the paper published by Xu et al. it was shown that SNX3 was also involved in the recycling of TfR. From our results we found that SNX3 is involved in the trafficking of EGFR. Therefore we were interested in seeing if SNX3 modulates the trafficking of other RTKs. We used MET as another candidate RTK since it has been shown to be involved in gliomagenesis [26, 27]. We activated MET using HGF, its known ligand. **Figure 5.10** shows a western blot of SF188 EV and clone 4 activated by HGF for 6h. Again, as seen previously, there is a sustained level of p-Erk and p-Mek in the SNX3 overexpressed clone, indicating that SNX3 may also be involved in the trafficking of MET. (*Experiments performed by Dong Anh Khuong-Quang showed sustained JNK activation in SNX3 overexpressed in U87 cell lines*).

6. SNX3 overexpression causes more proliferation in SF188 cells.

To examine the effects of SNX3 overexpression on proliferation, SF188 clones and empty vector cells were treated with ^{3}thymidine and its uptake was tested over a 4 day period. These results are summarized in **figure 5.11.** The data shown are representative of three separate experiments. From the results, higher proliferation was observed for both SNX3 overexpressing clones compared to EV cells. All three samples had a steady rate of proliferation over the 4 day period. Starting at day 2 both SNX3 overexpressing clones proliferated at a much higher rate than the empty vector clone. Also, between the two SNX3 overexpressing clones, a higher proliferation was seen for

clone 4 compared to clone 6. This can be due to the higher SNX3 expression seen in clone 4 as shown earlier.

7. SNX3 overexpression causes increased colony formation in soft agar.

To further evaluate the effects of SNX3 on tumorigenesis, soft agar assays on both SF188 clones and on EV were done to examine the effects of SNX3 on anchorage dependent growth. Cells were grown in soft agar over 14 days and we found that SNX3 overexpression did have an effect on colony formation in both clones, shown in **figure 5.12a**. More so in clone 4, which may be due to its higher SNX3 expression compared to clone 6. The number of colonies was similar in both cases; however the size of the colonies seen in clone 4 was much larger. These results suggest that SNX3 overexpression can cause anchorage independent growth in soft agar. Similar results were obtained by Dong Anh Quang, where more colonies were formed in SNX3 overexpressed U87 cell line (aGBM) (data not shown).

9. Tumour Growth *in vivo*

(*This part of the project is being performed in collaboration with the group of Dr. J. Rak. The mice experiments were performed by Dong-Anh Khuong-Quang and Damien Faury*). SF188 overexpressing SNX3, in parallel with wild type cells and cells transfected with an empty vector were injected in xenograft nude-mouse model. Preliminary results show that the SNX3 overexpressed SF188 cells are able to cause

increased tumour formation and tumour size compared to mice injected with EV (data not shown).

5. Silencing SNX3 in cells causes reduces EGFR signaling.

In order to determine if we can reverse the effects of SNX3 we first transiently silenced SNX3 in SF188 cells. We tested 3 different siRNA's to observe if we can transiently silence SNX3 at the protein and mRNA levels. As shown in **figure 5.13a** and **5.13b**, SNX3 is silenced both at the mRNA and protein levels tested by RT-PCR and western blotting. **Figure 5.14** shows transiently silenced SNX3 and control SF188 cells activated with EGF over a 6h period. The western blot indicates a decrease in MAPK signaling in SNX3 silenced cells compared to control cells. Also a decrease in EGFR is observed in SNX3 silenced cells over a 6h period. Showing an increase in EGFR degradation in SNX3 silenced SF188 cells. The graphs shown are means of 3 independent experiments. Significant values are obtained for lower pERK levels in silenced cells. (* stastistical value of at least $p<0.05$ is achieved) Therefore, the results confirmed that we were able to reverse the effects of SNX3 overexpression by transiently silencing it in SF188.

5.5 Discussion

We report here that SNX3 delays endosomal degradation of EGFR in glioblastoma cell lines. We have shown that overexpressing SNX3 in glioblastoma cell lines prolonged EGFR and MET signaling. Sorting nexins have recently been identified as an important regulator in endosomal targeting of several mediators, including receptor

tyrosine kinases. SNX1 was first discovered to associate with EGFR and regulate lysosomal degradation [9]. SNX16 was another sorting nexin involved in EGFR lysosomal targeting [22]. In this study, we demonstrated that SNX3 delays endosomal degradation of EGFR. Other SNXs have been responsible for trafficking one or several RTKs. For example SNX2 and SNX4 have been associated with trafficking of EGFR and PDGFR [6]. SNX15 was described to slow the internalization and degradation of PDGFR and delays the post-translational processing of the pro-receptors for insulin and HGF [28].

Our results indicate SNX3 delays endosomal recycling of EGFR and MET. This leads to sustained activation of the MAPK and the JNK pathways in SNX3 transfectant cells compared to the EV, which in turn translates in increased growth advantage (proliferation, soft agar). These effects were observed in SF188, U251 and U87 cell lines. SF188 is poorly tumorigenic in vivo and very few tumors are seen in SCID or NOD-SCID mice even with high number of cells injected in the soft pad. In two SF188 clones overexpressing SNX3 we observed tumour formation (6/10 mice injected, 2 separate experiments) and metastasis of cells to the peritoneum, liver and lungs (3/10). Only one out of 10 injected mice with the Myc control empty vector developed a tumour. These tumours replicated GBM on pathology and were all positive for the Myc-tag. Interestingly, some had a very angiogenic phenotype. On an independent study done in collaboration with Dr C. Hawkins, Sickkids/Toronto, a set of tissue microarrays (TMA) of 180 high grade astrocytomas (HGA) were shown to have SNX3 overexpressed.

Our results indicate that SNX3 sustains signalling of at least two activated RTKs, EGFR and MET. One group identified SNX3 to be a mediator necessary for lithium-

induced neurite outgrowth [29]. Another study has shown that SNX3 is involved in the transport of surface internalized anti-Tfr antibody from the early to recycling antibody [7]. Also recently, SNX3 has been shown as a part of an alternative retromer pathway that recycles Wnt-binding protein Wntless (WIs) [30]. In future, work will need to be done to see if SNX3 is involved in the trafficking of other mediators that may be responsible for tumoregensis in GBMs.

SNXs contain a PX domain which interacts directly with PtdIns. SNX3 has been shown to interact with PtdIns(3)P [7]. However, we still have to determine if this interaction is essential for sustained EGFR signalling. Our preliminary data (data not shown) showed that treatment with LY294002, a PtdIns(3)P inhibitor, on SNX3 overexpressed pGBM cell line SF188 did not decrease EGFR signalling. This may suggest that maybe the C-terminal region of SNX3 may have a role in EGFR trafficking. The study done by Mizutani *et al* has shown that the C-terminus as well as the PX domain of SNX3 is responsible for neurite outgrowth [29].

Other studies have shown that more than one SNX can work cooperatively to achieve the same goal [21, 31-33]. Another report suggests that SNXs can play antagonistic roles in regulating endosomal trafficking of EGFR [24]. In our work we still have to determine if other SNXs are also involved in pGBM tumorigencity or if there are any other SNXs that are upregulated after SNX3 is silenced.

In conclusion, EGFR is frequently overexpressed in cancer and also has become a model protein for understanding mechanisms of endocytosis and degradation of RTKs [14]. In our study, we have shown for the first time SNX3 to promote proliferation in cell lines and tumor growth *in vivo*.

5.6 Tables and Figures

Sample	QRT-PCR of SNX3	SNX3 level shown by Genespring
4	**0.682102**	**0.888**
9	**0.139989**	**0.537**
10	**1.168425**	**1.62**
13	**3.95**	**2.201**
8	**0.119547**	**0.599**
a	**2.587548**	**3.721**
5	**1.896149**	**3.171**
control	**1**	**1**

Table 5.1: SNX3 mRNA quantitative results confirmed by QRT-PCR for some of the frozen pGBM samples. Column 1 shows SNX3 mRNA levels by QRT-PCR and the 2nd column shows the SNX3 p-fold value obtained by genespring. Sample numbers corresponds to the numbers on the gel in **Figure 5.1a. (**Sample "*a"* was a GBM sample that was not run on the gel)

SNX	P-Fold Value
SNX3	1.56
SNX 27	1.34
SNX 17	1.3
SNX 2	1.26
SNX 4	1.14
SNX12	1.06
SNX14	1.06
SNX15	1.02
SNX13	1.01
SNX 11	0.99
SNX1	0.96
SNX6	0.9
SNX8	0.91
SNX 9	0.82
SNX 10	0.69

Snxs found in the list of genes upregulated in RAS+ve

SNX 3 2.9 fold change

SNX 27 1.72 fold change

Table 5.2: Several SNXs are shown to be differentially expressed in pediatric GBMs compared to normal. Table on the left shows the SNXs found on the microarray chip and p-fold values of pGBM compared to normal. On the Right, shows P fold values of SNX3 and SNX27 comparing Ras associated samples and samples not showing Ras activation in pGBM.

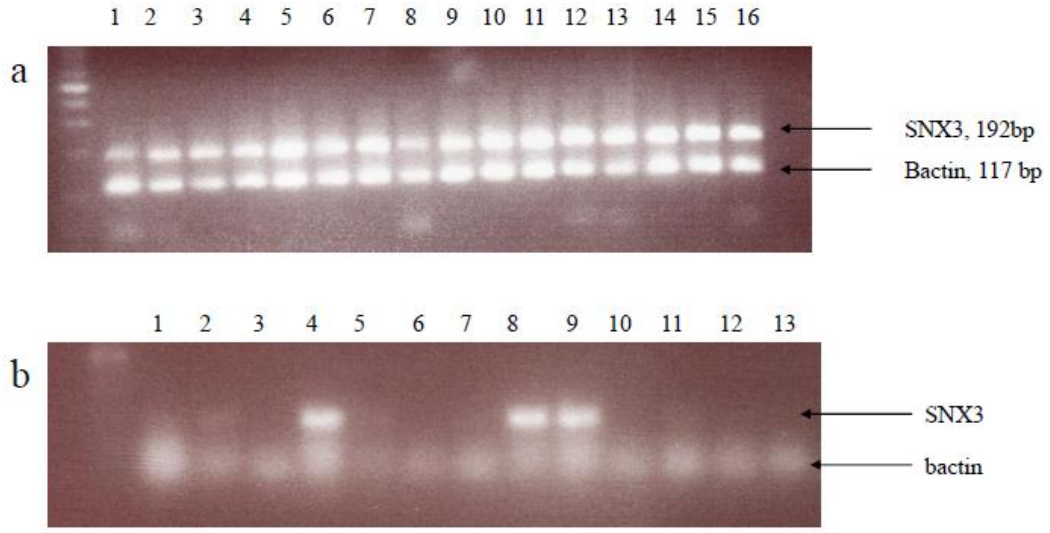

Figure 5.1: RT-PCR of SNX3 of different pGBM samples studied by microarray analysis. **1a** are mRNA obtained from frozen samples. Lane 1 represents control sample 783 and lane 2-16 are samples different frozen GBM samples used in chapter 2 and 3. **1b** are mRNA from FFPE samples. The lanes in 1b from 1-12 are FFPE GBM samples and lane 13 is control. These were samples used in chapter 3. B-actin was used as a control.

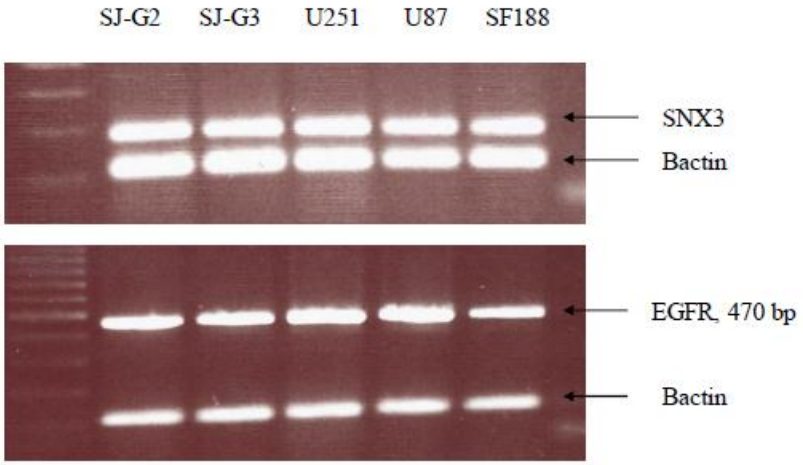

Figure 5.2: mRNA levels of SNX3 and EGFR in different cell lines. RT-PCR of SJ-G2, SJ-G3, U251, U87, and SF188 cell lines were done to see mRNA levels of SNX3 (top gel) and EGFR (bottom gel). B-actin was used as a control.

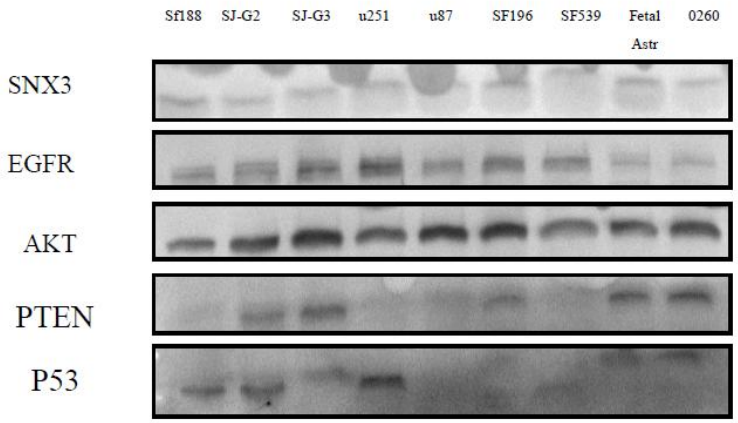

Figure 5.3: Characterization of SNX3, EGFR, AKT, PTEN, and P53 levels in different cell lines. Protein levels of SNX3, EGFR, AKT, PTEN, and P53 in different cell lines shown by western blot. Akt was used as a loading control.

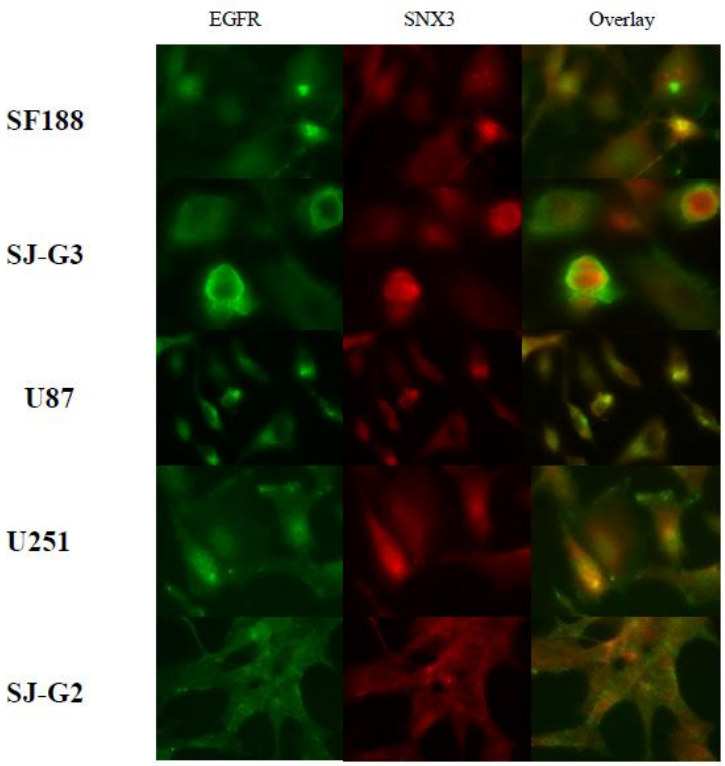

Figure 5.4: Levels of SNX3 and EGFR protein was assessed by immunofluorescence imaging. SNX3 and EGFR levels in different cell lines, SF188, SJ-G3, U87, U251, SJ-G2 are shown. SNX3 stained red and EGFR stained green, the last column shows an overlay of SNX3 and EGFR.

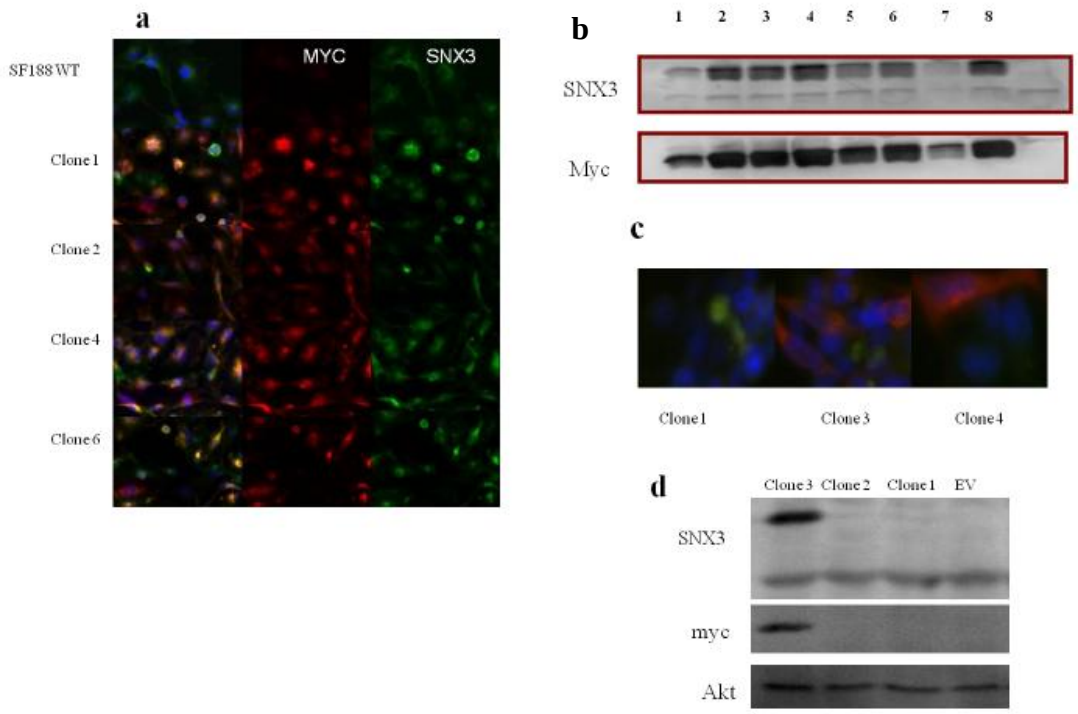

Figure 5.5: Stable SNX3 overexpressed transfectants in SF188 and SJ-G2 cell lines. **5.5a** shows immunofluorescene staining of some of the SNX3 overexpressed clones in SF188 stained with SNX3 and MYC and **5.5b** shows western blot analysis of these clones with SNX3 and MYC. The bottom band in SNX3 western blot represents endogenous SNXs in the samples and the upper band represents the overespressed SNX3 tagged with MYC. **5.5c** shows different clones generated overexpressing SNX3 in SJ-G2 cell line and **5.5d** shows western blot analysis of these clones.

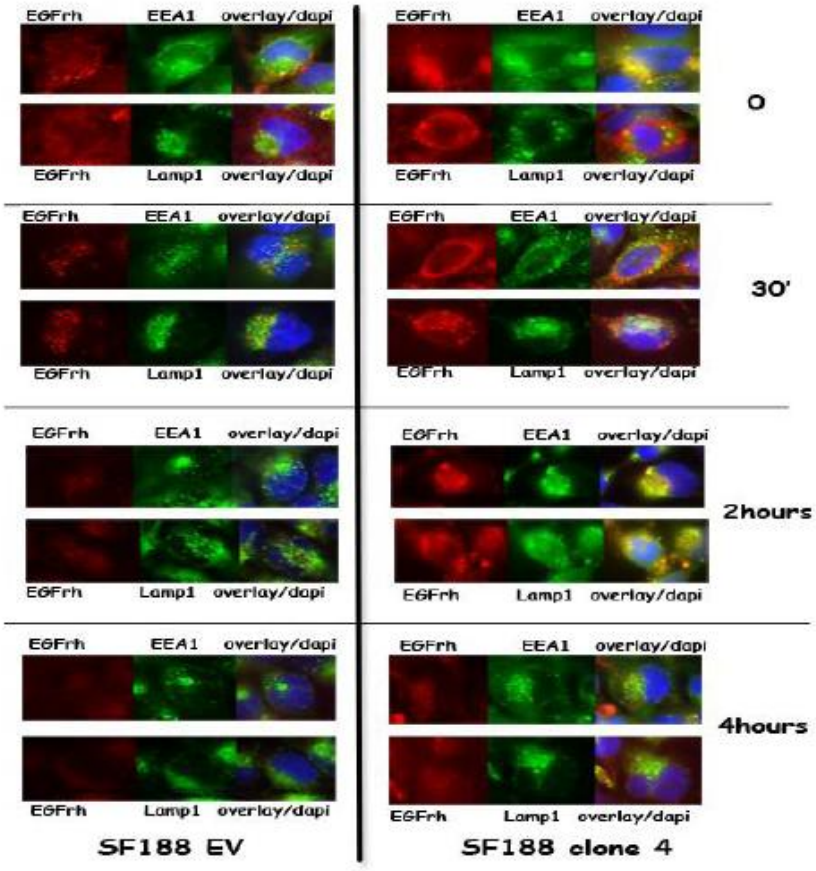

Figure 5.6: Endosomal trafficking of EGFR in SF188 SNX3 overexpressed cells and control by immunofluorescence. Stable SF188 clone 4 and EV transfected SF188 cells were activated by rhodamine tagged EGF and followed for up to 4h, at each time point, cells were fixed and co-stained with either EEA1 or Lamp1. Immunofluorescence images were taken for clone 4 and EV at indicated times. EGFrh was tagged red and EEA1 and LAMP1 green.

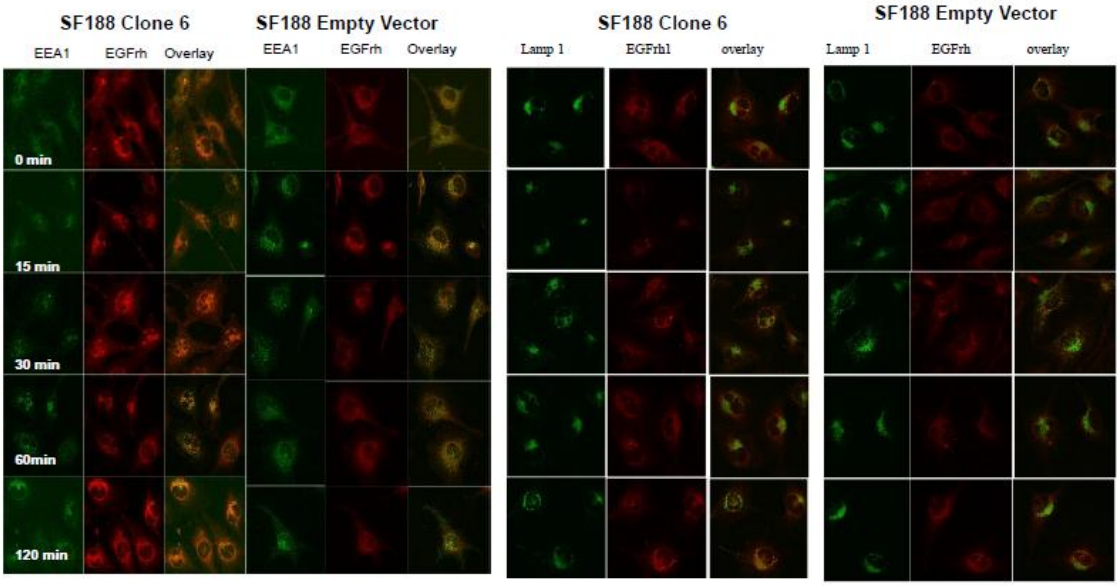

Figure 5.7: Endosomal trafficking of EGFR in SF188 SNX3 overexpressed cells and control by confocal microscopy. Stable SF188 clone 6 and SF188 EV were activated using rhodamine tagged EGF and co-stained with either EEA1 or LAMP1 at different time points. Confocal images were taken for indicated times over a 2h period.

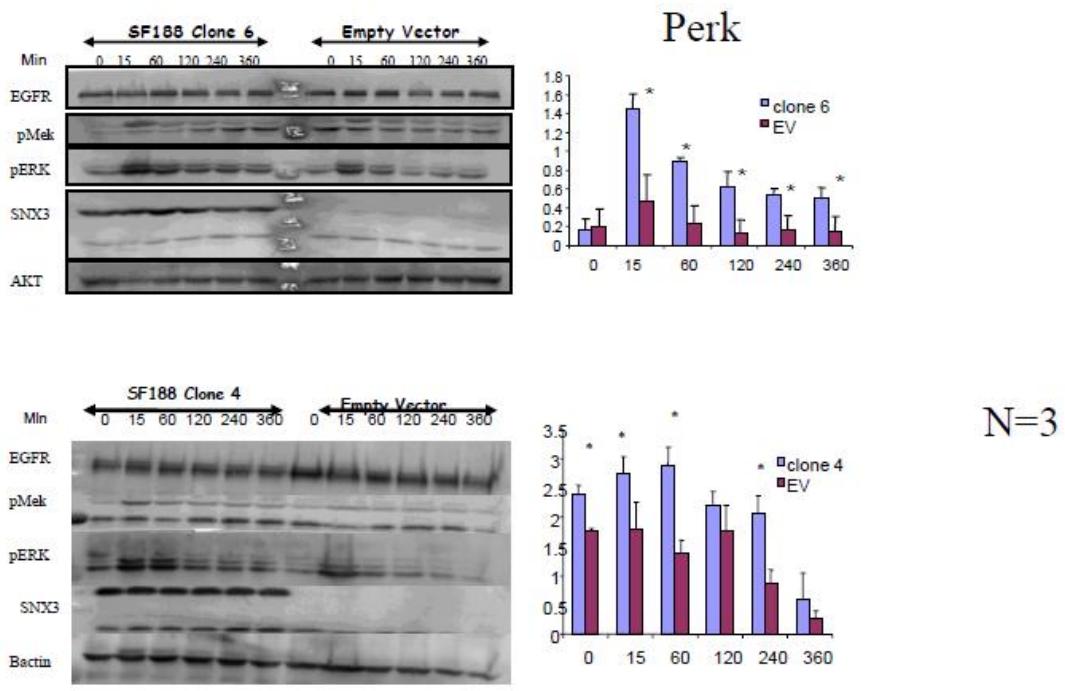

Figure 5.8: Overexpresssion of SNX3 sustains EGFR signaling in SF188 cells. Western blot analysis of EGFR signalling of stable SF188 SNX3 overexpressed and SF188 EV clones were activated with TGF α over a 6h period. Cells were lysed at indicated times and proteins were extracted for western blot analysis. The levels of pErk, pMek, EGFR, and SNX3 were shown by western blot. B-actin or Akt were used as loading controls. Upper band in SNX3 represents SNX3 overexpression. Upper blot represents activation of clone 6 and lower blot clone 4. For both blots pErk was measured quantitatively using 3 independent experiments. (* stastistical value of at least $p<0.05$ is achieved).

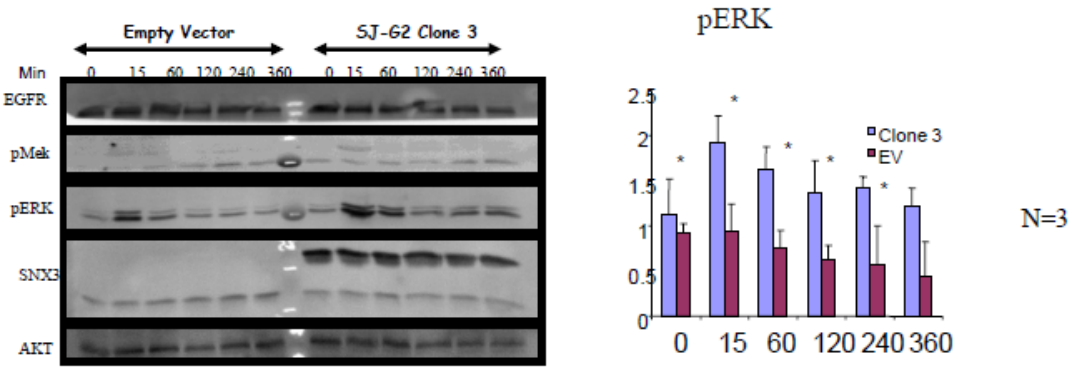

Figure 5.9: Overexpresssion of SNX3 sustains EGFR signaling in SJ-G2 cells. Stable SJ-G2 clone was activated by TGFα over a 6h period and protein was extracted from lysed cells at indicated times. Levels of pMek, pErk, and EGFR were analyzed by western blot. Level of pErk was quantitated from blots using 3 independent experiments. (* stastistical value of at least $p<0.05$ is achieved). B-actin was used as a loading control.

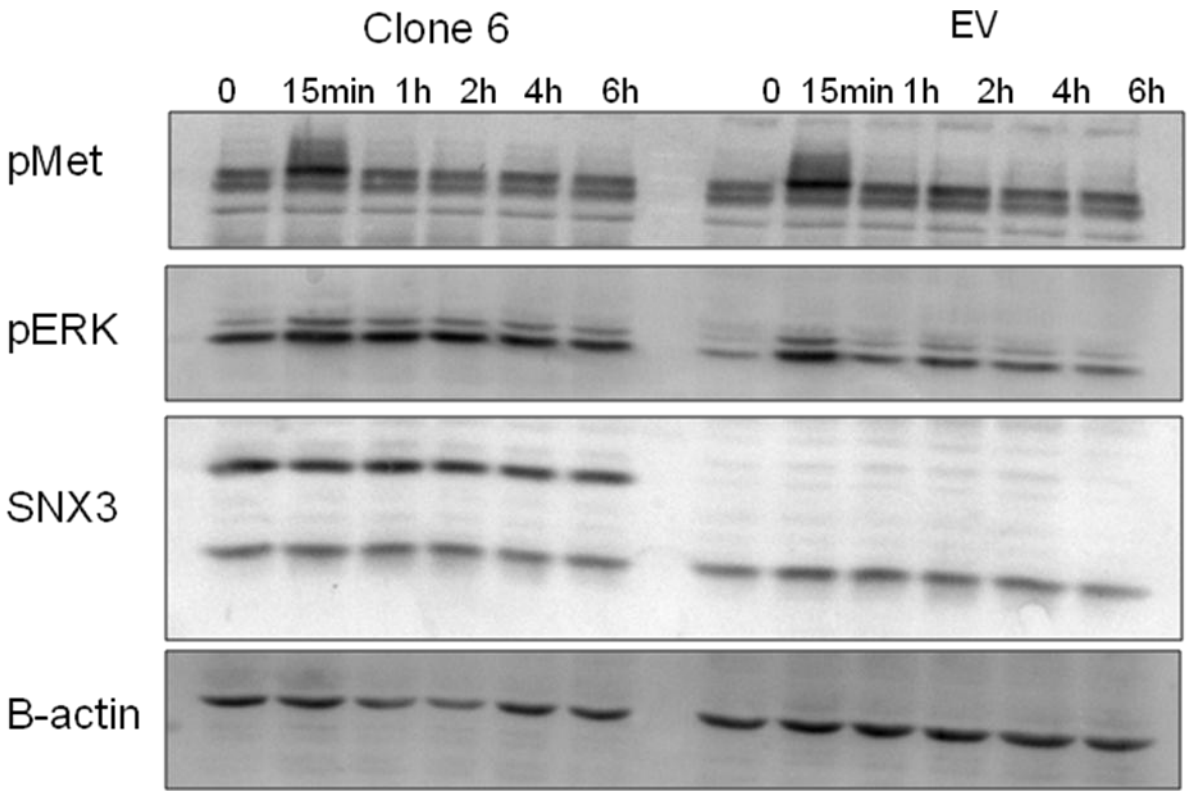

Figure 5.10: Overexpresssion of SNX3 sustains MET signaling in SF188 cells. Stable SNX3 overexpresing SF188 clone 6 and EV were activated with HGF over a 6h period to see downstream effects of MET signaling. Cells were lysed and protein was extracted at indicated times and the levels of pERK and pMET were analyzed by western blot. B-actin was used as a loading control.

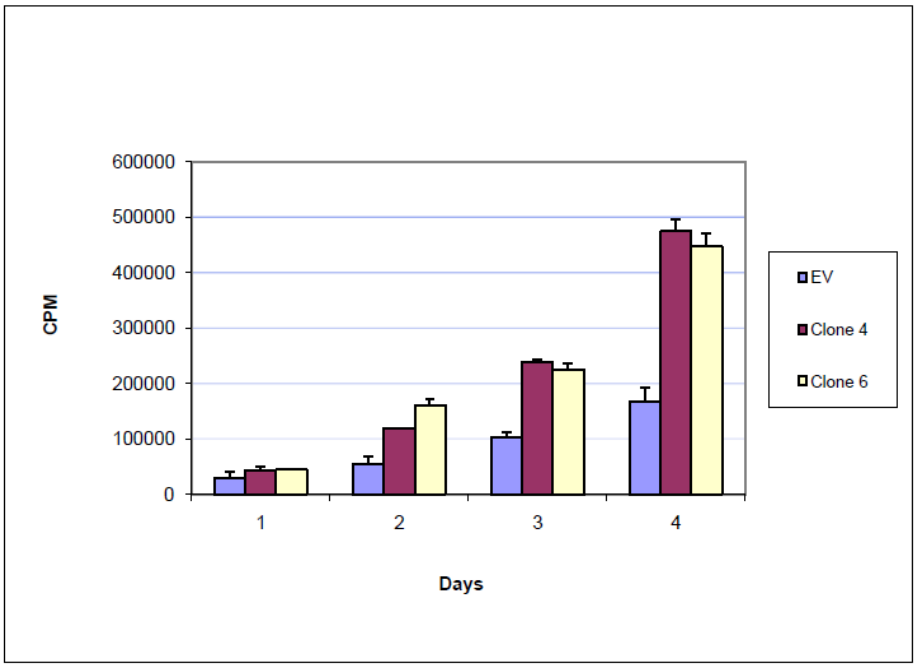

Figure 5.11: SNX3 overexpression increases proliferation in SF188 cells. Proliferation assays using ^{3}thymidine uptake was done on stable SF188 clones over a four day period. Data shown are average values of three separate experiments.

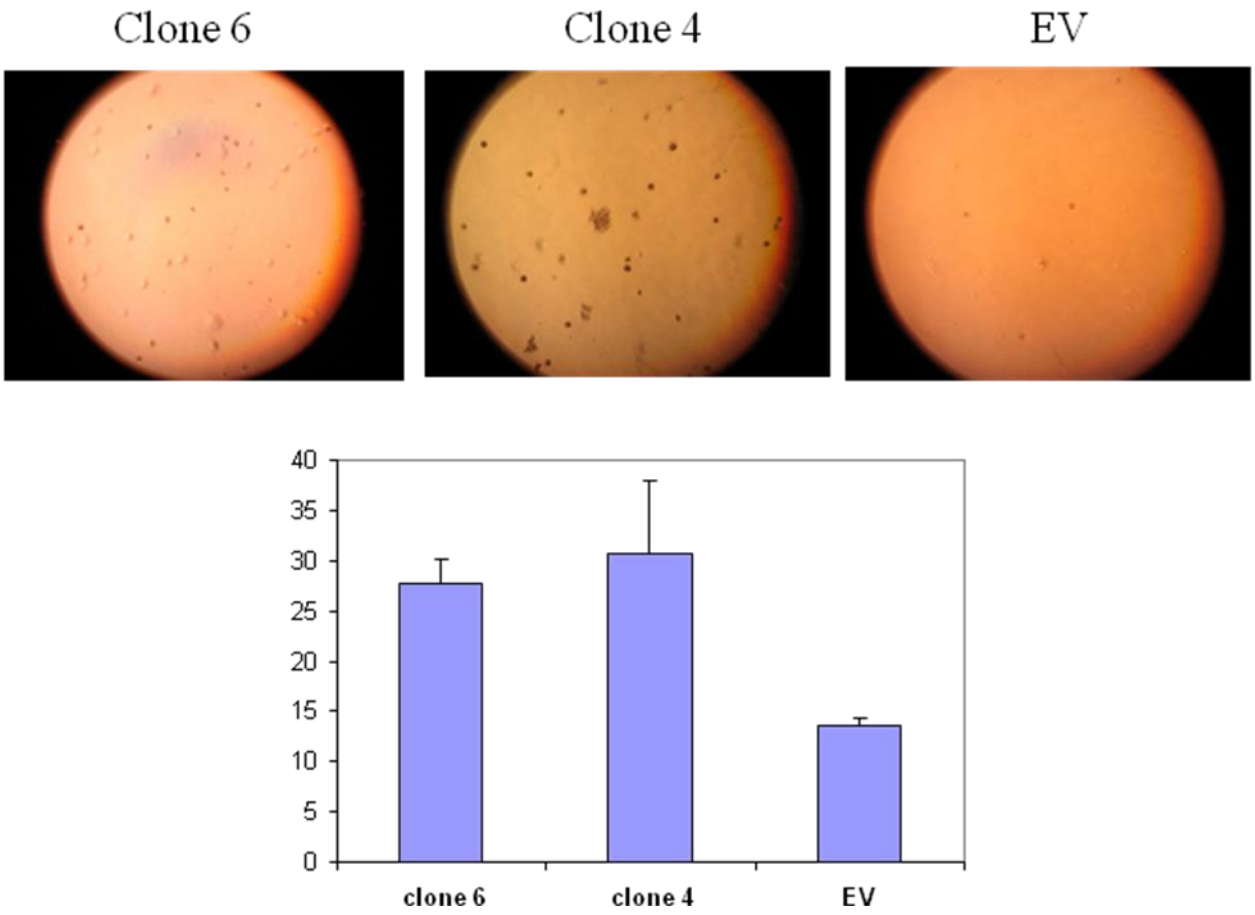

Figure 5.12: SNX3 overexpression in SF188 cells increases colony formation in soft agar. SF188 clones 4, 6 and EV were grown in soft agar to see anchorage dependant growth. Upper image shows representations of soft agar plates with colonies. Bottom graph represents average colony counts for each clone. Y-Axis on the graph represents the average colony count for 3 different experiments. Cells were grown for 3 to 4 weeks.

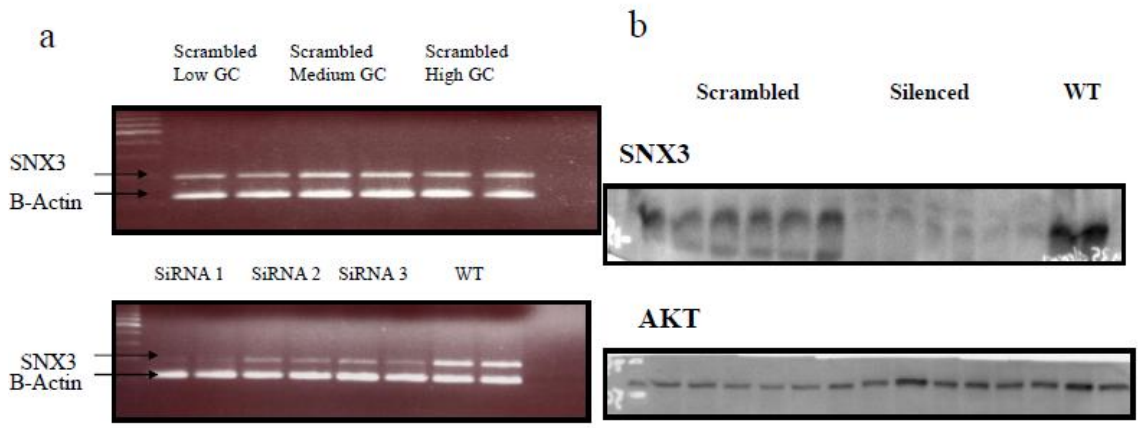

Figure 5.13: SNX3 transiently silenced using commercially available siRNA. 3 different siRNA were tested and we were able to silence SNX3 in the mRNA (a) and protein (b) level using all 3 siRNAs in SF188 cells.

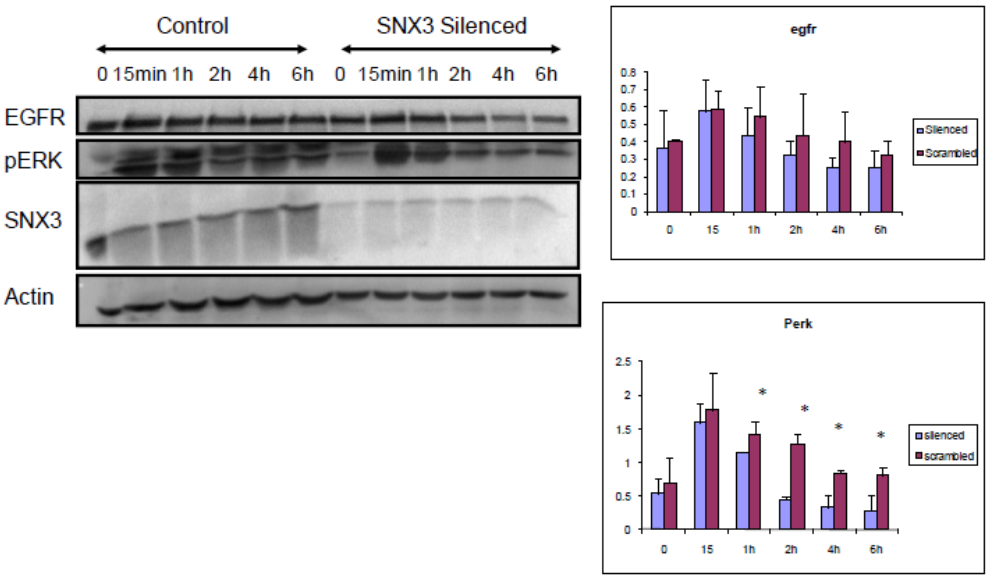

Figure 5.14: SNX3 silencing in SF188 cells decreases downstream EGFR signaling. Transiently silenced clones were activated by TGFα for up to 4h and levels of perk and EGFR was analyzed by western blot. EGFR and pErk levels were quantitated by averaging 3 independent experiments.

5.7 References

1. Faury, D., et al., *Molecular profiling identifies prognostic subgroups of pediatric glioblastoma and shows increased YB-1 expression in tumors.* J Clin Oncol, 2007. **25**(10): p. 1196-208.
2. Maher, E.A., et al., *Malignant glioma: genetics and biology of a grave matter.* Genes Dev, 2001. **15**(11): p. 1311-33.
3. Hagerstrand, D., et al., *PI3K/PTEN/Akt pathway status affects the sensitivity of high-grade glioma cell cultures to the insulin-like growth factor-1 receptor inhibitor NVP-AEW541.* Neuro Oncol, 2010. **12**(9): p. 967-75.
4. Nakamura, M., et al., *Molecular pathogenesis of pediatric astrocytic tumors.* Neuro Oncol, 2007. **9**(2): p. 113-23.
5. Seet, L.F. and W. Hong, *The Phox (PX) domain proteins and membrane traffic.* Biochim Biophys Acta, 2006. **1761**(8): p. 878-96.
6. Haft, C.R., et al., *Identification of a family of sorting nexin molecules and characterization of their association with receptors.* Mol Cell Biol, 1998. **18**(12): p. 7278-87.
7. Xu, Y., et al., *SNX3 regulates endosomal function through its PX-domain-mediated interaction with PtdIns(3)P.* Nat Cell Biol, 2001. **3**(7): p. 658-66.
8. Haglund, K., P.P. Di Fiore, and I. Dikic, *Distinct monoubiquitin signals in receptor endocytosis.* Trends Biochem Sci, 2003. **28**(11): p. 598-603.
9. Kurten, R.C., *Sorting motifs in receptor trafficking.* Adv Drug Deliv Rev, 2003. **55**(11): p. 1405-19.
10. Roepstorff, K., et al., *Differential effects of EGFR ligands on endocytic sorting of the receptor.* Traffic, 2009. **10**(8): p. 1115-27.
11. Balbis, A., et al., *Compartmentalization of signaling-competent epidermal growth factor receptors in endosomes.* Endocrinology, 2007. **148**(6): p. 2944-54.
12. Dikic, I., *Mechanisms controlling EGF receptor endocytosis and degradation.* Biochem Soc Trans, 2003. **31**(Pt 6): p. 1178-81.
13. Wiley, H.S. and P.M. Burke, *Regulation of receptor tyrosine kinase signaling by endocytic trafficking.* Traffic, 2001. **2**(1): p. 12-8.
14. Madshus, I.H. and E. Stang, *Internalization and intracellular sorting of the EGF receptor: a model for understanding the mechanisms of receptor trafficking.* J Cell Sci, 2009. **122**(Pt 19): p. 3433-9.
15. Resat, H., et al., *An integrated model of epidermal growth factor receptor trafficking and signal transduction.* Biophys J, 2003. **85**(2): p. 730-43.
16. McShane, M.P. and M. Zerial, *Survival of the weakest: signaling aided by endosomes.* J Cell Biol, 2008. **182**(5): p. 823-5.
17. Mosesson, Y., G.B. Mills, and Y. Yarden, *Derailed endocytosis: an emerging feature of cancer.* Nat Rev Cancer, 2008. **8**(11): p. 835-50.
18. Pytel, P., *Spectrum of pediatric gliomas: implications for the development of future therapies.* Expert Rev Anticancer Ther, 2007. **7**(12 Suppl): p. S51-60.

19. Paugh, B.S., et al., *Integrated molecular genetic profiling of pediatric high-grade gliomas reveals key differences with the adult disease.* J Clin Oncol, 2010. **28**(18): p. 3061-8.
20. Haque, T., et al., *Gene expression profiling from formalin-fixed paraffin-embedded tumors of pediatric glioblastoma.* Clin Cancer Res, 2007. **13**(21): p. 6284-92.
21. Carlton, J.G. and P.J. Cullen, *Sorting nexins.* Curr Biol, 2005. **15**(20): p. R819-20.
22. Choi, J.H., et al., *Sorting nexin 16 regulates EGF receptor trafficking by phosphatidylinositol-3-phosphate interaction with the Phox domain.* J Cell Sci, 2004. **117**(Pt 18): p. 4209-18.
23. Gullapalli, A., et al., *An essential role for SNX1 in lysosomal sorting of protease-activated receptor-1: evidence for retromer-, Hrs-, and Tsg101-independent functions of sorting nexins.* Mol Biol Cell, 2006. **17**(3): p. 1228-38.
24. Liu, H., et al., *Inhibitory regulation of EGF receptor degradation by sorting nexin 5.* Biochem Biophys Res Commun, 2006. **342**(2): p. 537-46.
25. Rincon, E., et al., *Proteomics identification of sorting nexin 27 as a diacylglycerol kinase zeta-associated protein: new diacylglycerol kinase roles in endocytic recycling.* Mol Cell Proteomics, 2007. **6**(6): p. 1073-87.
26. Cecchi, F., D.C. Rabe, and D.P. Bottaro, *Targeting the HGF/Met signalling pathway in cancer.* Eur J Cancer, 2010. **46**(7): p. 1260-70.
27. Li, Y., et al., *Interactions between PTEN and the c-Met pathway in glioblastoma and implications for therapy.* Mol Cancer Ther, 2009. **8**(2): p. 376-85.
28. Phillips, S.A., et al., *Identification and characterization of SNX15, a novel sorting nexin involved in protein trafficking.* J Biol Chem, 2001. **276**(7): p. 5074-84.
29. Mizutani, R., et al., *Sorting nexin 3, a protein upregulated by lithium, contains a novel phosphatidylinositol-binding sequence and mediates neurite outgrowth in N1E-115 cells.* Cell Signal, 2009. **21**(11): p. 1586-94.
30. Harterink, M., et al., *A SNX3-dependent retromer pathway mediates retrograde transport of the Wnt sorting receptor Wntless and is required for Wnt secretion.* Nat Cell Biol, 2011. **13**(8): p. 914-23.
31. Carlton, J., et al., *Sorting nexins--unifying trends and new perspectives.* Traffic, 2005. **6**(2): p. 75-82.
32. Kerr, M.C., et al., *Visualisation of macropinosome maturation by the recruitment of sorting nexins.* J Cell Sci, 2006. **119**(Pt 19): p. 3967-80.
33. Griffin, C.T., J. Trejo, and T. Magnuson, *Genetic evidence for a mammalian retromer complex containing sorting nexins 1 and 2.* Proc Natl Acad Sci U S A, 2005. **102**(42): p. 15173-7.

Chapter 6

General Conclusion

6.1 Chapters 2 and 3

In our lab we have generated data that clearly shows a difference in the molecular signature between adult and pediatric GBM. We have also found that within pGBM there are two subsets with differing Ras/Akt pathway activation. These results were confirmed by two independent studies using frozen samples and FFPE samples. Although I did not perform several of the experiments using the frozen samples, the results I obtained from the FFPE samples confirmed the findings of clearly defined two pediatric subsets in pGBM. These results also helped demonstrate that even though FFPE samples are not as reliable as frozen samples for microarray analysis, in tumours with scarce frozen material such as pediatric GBM, they are valuable to confirm data obtained from frozen samples.

Also over the years improvements have been made in the analysis of RNA in formalin- fixed samples where the RNA is segmented. One of these new techniques was launched by Illumina called cDNA-mediated Annealing, Selection, extension, and Ligation (DASL) assay. Many researchers have extracted RNA from FFPE samples to study gene expression signatures [1, 2]. Re-doing these gene expression analysis using newer techniques with our FFPE samples will increase our sample size with better

microarray results and hence give us even more insight in the genetic signature of pediatric GBMs.

6.2 Chapter 4

We have also found that within pHGA, there are differences in their differentially expressed genes based on grade and across the lifespan (grade III and IV, adult and pediatric). This was one of the first studies done to separate pediatric grade III and IV astrocytomas, as most studies combine the two types of tumors since they are both quite rare [3]. Several studies have been done comparing adult grade III and IV astrocytomas but not pediatric ones [4-6]. From our results we found that the mTOR pathway is most differentially regulated between the two grades and VEGFc is more upregulated in grade III compared to grade IV. However, there were many limitations in this study, most importantly the small sample size for grade III tumors. Interestingly, grade III tumours in children do not carry the mutations in the histone 3 variant 3 we uncovered in 35% of pGBM, independently confirming our findings that these are distinct molecular/genetic disorders. Also, we attempted in doing a meta-analysis comparing our samples with data from published papers. This proved difficult since a lot of publications use Affymetrix expression arrays whereas our dataset was derived from an Agilent platform. For future work, it would be important to increase the sample size from grade III tumours and if possible to re-do the analysis using an Affymetrix platform.

6.3 Chapter 5

One of the key mediators in driving oncogenesis in several cancers is RTK signaling including EGFR. EGFR plays a major role in neural stem cell proliferation and survival. Its signaling activates major oncogenes such as Ras and Akt [7, 8]. In pGBM, EGFR gene is not amplified, however the transcript and the protein are overexpressed [3, 9]. This project aimed to study mechanisms that can potentially increase EGFR expression at the protein level. Through gene list generated from our microarray analysis, SNX3 was chosen as a candidate gene due to its function in delaying EGF degradation [10]. The other candidate gene that was mentioned in chapter 1 was YB-1. Work on this gene was continued by other members of the lab and my project only focused on SNX3. From our results, overexpressing SNX3, seemed to delay EGFR degradation and sustain signaling in several GBM cell lines. Also, SNX3 overexpression increased proliferation and colony formation in soft agar. It was presumed that SNX3 will have a general effect on membrane receptor trafficking. Continuation of this work may uncover a detailed mechanism of tumorigenesis that disrupts physiological trafficking of membrane receptors and potentially further shed light as to how in pediatric GBM, EGFR and other RTKs are overexpressed in the absence of the genetic abnormalities seen in adult GBM. Presently in the lab, several studies are being continued with SNX3. Most importantly, *in vivo* work is being done where SNX3 is overexpressed in NOD/SKID mice. Promising results are seen where the SNX3 overexpressed mice are forming tumors faster than mice injected with EV cells. Also work is being done using EGFR and MET inhibitors on SNX3 overexpressed clones to

see if there are any effects on the MAPK signaling pathway and on decreasing mouse tumors.

This was one of the earliest studies done to show that derailed receptor trafficking in cells can lead to sustain receptor signaling and tumor growth *in vitro* and *in vivo*. The sorting nexin family is a relatively newly found family and several studies have described SNXs to be involved in various aspects of protein trafficking [11, 12]. We have shown here that overexpression of SNXs can be linked to cancer. Our focus was only on SNX3, however it would be interesting to see if other SNX members can also be involved in cancer. Previously, it has been shown that SNXs can work synergistically or antagonistically with other members [13] For future work it would be interesting to see if any other SNXs are upregulated by silencing SNX3 in cell lines and *in vivo*. Continuation of this work may lead to potential therapeutic targets specific to pGBM or other cancers. Several SNXs have shown to be involved in trafficking various RTKs. From our work we have shown that overexpressing SNX3 sustains signaling of both MET and EGFR. Therefore, by targeting one effector we may be able to stop signaling from multiple RTKs. This thesis introduced a new potential target for cancer that may open up the possibilities of new research directions leading towards receptor trafficking and its link to cancer.

6.4 Contributions to original knowledge

This PhD project provided novel and new discoveries in different aspects regarding pediatric high grade astrocytomas. Chapters 2 and 3 describe the first reports of gene expression profiling in pGBM and at least two subtypes of pGBM were found. This was the first study to show that one subset of pGBM is associated with Ras/Akt activation and the other subset is not associated with Ras/Akt activation, which had a slightly better survival advantage over the other subgroup. Chapter 4 is one of the earliest studies done to show that there are distinct differences within grade III and IV pediatric high grade astrocytomas. This was the first time that it has been shown that the mTOR pathway is the most differentially regulated between the two high grade pediatric astrocytomas. Lastly, in chapter 5 we have shown for the first time, SNX3 to promote proliferation and tumor growth in cell lines and *in vivo*. It is the first report to show that SNX3 is upregulated in a subset of pGBM that is associated with Ras and Akt activation and that deregulated endocytosis and membrane trafficking can mimic genetic amplification of an oncogene.

6.5 References

1. April, C., et al., *Whole-genome gene expression profiling of formalin-fixed, paraffin-embedded tissue samples.* PLoS One, 2009. **4**(12): p. e8162.
2. Abramovitz, M., et al., *Molecular characterisation of formalin-fixed paraffin-embedded (FFPE) breast tumour specimens using a custom 512-gene breast cancer bead array-based platform.* Br J Cancer, 2011. **105**(10): p. 1574-81.
3. Paugh, B.S., et al., *Integrated molecular genetic profiling of pediatric high-grade gliomas reveals key differences with the adult disease.* J Clin Oncol, 2010. **28**(18): p. 3061-8.
4. Phillips, H.S., et al., *Molecular subclasses of high-grade glioma predict prognosis, delineate a pattern of disease progression, and resemble stages in neurogenesis.* Cancer Cell, 2006. **9**(3): p. 157-73.
5. Gulati, S., et al., *Overexpression of c-erbB2 is a negative prognostic factor in anaplastic astrocytomas.* Diagn Pathol, 2010. **5**: p. 18.
6. Furnari, F.B., et al., *Malignant astrocytic glioma: genetics, biology, and paths to treatment.* Genes Dev, 2007. **21**(21): p. 2683-710.
7. Layfield, L.J., et al., *Epidermal growth factor receptor gene amplification and protein expression in glioblastoma multiforme: prognostic significance and relationship to other prognostic factors.* Appl Immunohistochem Mol Morphol, 2006. **14**(1): p. 91-6.
8. Roepstorff, K., et al., *Endocytic downregulation of ErbB receptors: mechanisms and relevance in cancer.* Histochem Cell Biol, 2008. **129**(5): p. 563-78.
9. Hargrave, D., *Paediatric high and low grade glioma: the impact of tumour biology on current and future therapy.* Br J Neurosurg, 2009. **23**(4): p. 351-63.
10. Xu, Y., et al., *SNX3 regulates endosomal function through its PX-domain-mediated interaction with PtdIns(3)P.* Nat Cell Biol, 2001. **3**(7): p. 658-66.
11. van Weering, J.R., P. Verkade, and P.J. Cullen, *SNX-BAR proteins in phosphoinositide-mediated, tubular-based endosomal sorting.* Semin Cell Dev Biol, 2010. **21**(4): p. 371-80.
12. Xu, Y., et al., *The Phox homology (PX) domain, a new player in phosphoinositide signalling.* Biochem J, 2001. **360**(Pt 3): p. 513-30.
13. Liu, H., et al., *Inhibitory regulation of EGF receptor degradation by sorting nexin 5.* Biochem Biophys Res Commun, 2006. **342**(2): p. 537-46.

GENERAL REFERENCES

(2008). "Comprehensive genomic characterization defines human glioblastoma genes and core pathways." Nature 455(7216): 1061-1068.

Abounader, R. (2009). "Interactions between PTEN and receptor tyrosine kinase pathways and their implications for glioma therapy." Expert Rev Anticancer Ther 9(2): 235-245.

Aoyagi, K., T. Tatsuta, et al. (2003). "A faithful method for PCR-mediated global mRNA amplification and its integration into microarray analysis on laser-captured cells." Biochem Biophys Res Commun 300(4): 915-920.

Baker, S. J. and P. J. McKinnon (2004). "Tumour-suppressor function in the nervous system." Nat Rev Cancer 4(3): 184-196.

Balbis, A., A. Parmar, et al. (2007). "Compartmentalization of signaling-competent epidermal growth factor receptors in endosomes." Endocrinology 148(6): 2944-2954.

Baldys, A. and J. R. Raymond (2009). "Critical role of ESCRT machinery in EGFR recycling." Biochemistry 48(40): 9321-9323.

Berquin, I. M., B. Pang, et al. (2005). "Y-box-binding protein 1 confers EGF independence to human mammary epithelial cells." Oncogene 24(19): 3177-3186.

Bibikova, M., D. Talantov, et al. (2004). "Quantitative gene expression profiling in formalin-fixed, paraffin-embedded tissues using universal bead arrays." Am J Pathol 165(5): 1799-1807.

Bonaventure, P., H. Guo, et al. (2002). "Nuclei and subnuclei gene expression profiling in mammalian brain." Brain Res 943(1): 38-47.

Bonifacino, J. S. and J. H. Hurley (2008). "Retromer." Curr Opin Cell Biol 20(4): 427-436.

Bouffet, E., U. Tabori, et al. (2010). "Possibilities of new therapeutic strategies in brain tumors." Cancer Treat Rev 36(4): 335-341.

Braun, V., A. Wong, et al. (2010). "Sorting nexin 3 (SNX3) is a component of a tubular endosomal network induced by Salmonella and involved in maturation of the Salmonella-containing vacuole." Cell Microbiol 12(9): 1352-1367.

Bredel, M., C. Bredel, et al. (2005). "High-resolution genome-wide mapping of genetic alterations in human glial brain tumors." Cancer Res 65(10): 4088-4096.

Bredel, M., D. M. Scholtens, et al. (2009). "A network model of a cooperative genetic landscape in brain tumors." Jama 302(3): 261-275.

Bredel, M., I. F. Pollack, et al. (1998). "Inhibition of Ras and related G-proteins as a therapeutic strategy for blocking malignant glioma growth." Neurosurgery 43(1): 124-131; discussion 131-122.

Brennan, C., H. Momota, et al. (2009). "Glioblastoma subclasses can be defined by activity among signal transduction pathways and associated genomic alterations." PLoS One 4(11): e7752.

Broniscer, A. (2006). "Past, present, and future strategies in the treatment of high-grade glioma in children." Cancer Invest 24(1): 77-81.

Broniscer, A., S. J. Baker, et al. (2007). "Clinical and molecular characteristics of malignant transformation of low-grade glioma in children." J Clin Oncol 25(6): 682-689.

Canales, R. D., Y. Luo, et al. (2006). "Evaluation of DNA microarray results with quantitative gene expression platforms." Nat Biotechnol 24(9): 1115-1122.

Capodieci, P., M. Donovan, et al. (2005). "Gene expression profiling in single cells within tissue." Nat Methods 2(9): 663-665.

Carlton, J. G. and P. J. Cullen (2005). "Sorting nexins." Curr Biol 15(20): R819-820.

Carlton, J., M. Bujny, et al. (2005). "Sorting nexins--unifying trends and new perspectives." Traffic 6(2): 75-82.

Carro, M. S., W. K. Lim, et al. "The transcriptional network for mesenchymal transformation of brain tumours." Nature 463(7279): 318-325.

Cerami, E., E. Demir, et al. (2010). "Automated network analysis identifies core pathways in glioblastoma." PLoS One 5(2): e8918.

Choe, G., S. Horvath, et al. (2003). "Analysis of the phosphatidylinositol 3'-kinase signaling pathway in glioblastoma patients in vivo." Cancer Res 63(11): 2742-2746.

Choi, J. H., W. P. Hong, et al. (2004). "Sorting nexin 16 regulates EGF receptor trafficking by phosphatidylinositol-3-phosphate interaction with the Phox domain." J Cell Sci 117(Pt 18): 4209-4218.

Copois, V., F. Bibeau, et al. (2006). "Impact of RNA degradation on gene expression profiles: Assessment of different methods to reliably determine RNA quality." J Biotechnol.

Coudry, R. A., S. I. Meireles, et al. (2007). "Successful application of microarray technology to microdissected formalin-fixed, paraffin-embedded tissue." J Mol Diagn 9(1): 70-79.

Dikic, I. (2003). "Mechanisms controlling EGF receptor endocytosis and degradation." Biochem Soc Trans 31(Pt 6): 1178-1181.

Dirks, P. B. (2006). "Cancer: stem cells and brain tumours." Nature 444(7120): 687-688.

Donson, A. M., S. O. Addo-Yobo, et al. (2006). "MGMT promoter methylation correlates with survival benefit and sensitivity to temozolomide in pediatric glioblastoma." Pediatr Blood Cancer.

Dreyfuss, J. M., M. D. Johnson, et al. (2009). "Meta-analysis of glioblastoma multiforme versus anaplastic astrocytoma identifies robust gene markers." Mol Cancer 8: 71.

Du, B., Z. Y. Yang, et al. (2011). "Metastasis-associated protein 1 induces VEGF-C and facilitates lymphangiogenesis in colorectal cancer." World J Gastroenterol 17(9): 1219-1226.

Emmert-Buck, M. R., R. F. Bonner, et al. (1996). "Laser capture microdissection." Science 274(5289): 998-1001.

Endersby, R. and S. J. Baker (2008). "PTEN signaling in brain: neuropathology and tumorigenesis." Oncogene 27(41): 5416-5430.

Evdokimova, V., P. Ruzanov, et al. (2006). "Akt-Mediated YB-1 Phosphorylation Activates Translation of Silent mRNA Species." Mol Cell Biol 26(1): 277-292.

Faury, D., A. Nantel, et al. (2007). "Molecular profiling identifies prognostic subgroups of pediatric glioblastoma and shows increased YB-1 expression in tumors." J Clin Oncol 25(10): 1196-1208.

Feng, J., S. T. Kim, et al. (2011). "An integrated analysis of germline and somatic, genetic and epigenetic alterations at 9p21.3 in glioblastoma." Cancer.

Finke, J., R. Fritzen, et al. (1993). "An improved strategy and a useful housekeeping gene for RNA analysis from formalin-fixed, paraffin-embedded tissues by PCR." Biotechniques 14(3): 448-453.

Finlay, J. L., J. M. Boyett, et al. (1995). "Randomized phase III trial in childhood high-grade astrocytoma comparing vincristine, lomustine, and prednisone with the eight-drugs-in-1-day regimen. Childrens Cancer Group." J Clin Oncol 13(1): 112-123.

Fischer, I. and K. Aldape "Molecular tools: biology, prognosis, and therapeutic triage." Neuroimaging Clin N Am 20(3): 273-282.

Fisher, P. G., T. Tihan, et al. (2008). "Outcome analysis of childhood low-grade astrocytomas." Pediatr Blood Cancer 51(2): 245-250.

Fountzilas, G., G. Karkavelas, et al. (2006). "Post-operative combined radiation and chemotherapy with temozolomide and irinotecan in patients with high-grade astrocytic tumors. A phase II study with biomarker evaluation." Anticancer Res 26(6C): 4675-4686.

Freije, W. A., F. E. Castro-Vargas, et al. (2004). "Gene expression profiling of gliomas strongly predicts survival." Cancer Res 64(18): 6503-6510.

Furnari, F. B., T. Fenton, et al. (2007). "Malignant astrocytic glioma: genetics, biology, and paths to treatment." Genes Dev 21(21): 2683-2710.

Gajjar, A., R. A. Sanford, et al. (1997). "Low-grade astrocytoma: a decade of experience at St. Jude Children's Research Hospital." J Clin Oncol 15(8): 2792-2799.

Gilbertson, R. J. and J. N. Rich (2007). "Making a tumour's bed: glioblastoma stem cells and the vascular niche." Nat Rev Cancer 7(10): 733-736.

Gloghini, A., B. Canal, et al. (2004). "RT-PCR analysis of RNA extracted from Bouin-fixed and paraffin-embedded lymphoid tissues." J Mol Diagn 6(4): 290-296.

Godard, S., G. Getz, et al. (2003). "Classification of human astrocytic gliomas on the basis of gene expression: a correlated group of genes with angiogenic activity emerges as a strong predictor of subtypes." Cancer Res 63(20): 6613-6625.

Godfrey, T. E., S. H. Kim, et al. (2000). "Quantitative mRNA expression analysis from formalin-fixed, paraffin-embedded tissues using 5' nuclease quantitative reverse transcription-polymerase chain reaction." J Mol Diagn 2(2): 84-91.

Grau, S. J., F. Trillsch, et al. (2007). "Expression of VEGFR3 in glioma endothelium correlates with tumor grade." J Neurooncol 82(2): 141-150.

Griffin, C. T., J. Trejo, et al. (2005). "Genetic evidence for a mammalian retromer complex containing sorting nexins 1 and 2." Proc Natl Acad Sci U S A 102(42): 15173-15177.

Guha, A., M. M. Feldkamp, et al. (1997). "Proliferation of human malignant astrocytomas is dependent on Ras activation." Oncogene 15(23): 2755-2765.

Gulati, N., M. Karsy, et al. (2009). "Involvement of mTORC1 and mTORC2 in regulation of glioblastoma multiforme growth and motility." Int J Oncol 35(4): 731-740.

Gulati, S., B. Ytterhus, et al. (2010). "Overexpression of c-erbB2 is a negative prognostic factor in anaplastic astrocytomas." Diagn Pathol 5: 18.

Gullapalli, A., B. L. Wolfe, et al. (2006). "An essential role for SNX1 in lysosomal sorting of protease-activated receptor-1: evidence for retromer-, Hrs-, and Tsg101-independent functions of sorting nexins." Mol Biol Cell 17(3): 1228-1238.

Haft, C. R., M. de la Luz Sierra, et al. (1998). "Identification of a family of sorting nexin molecules and characterization of their association with receptors." Mol Cell Biol 18(12): 7278-7287.

Haglund, K., P. P. Di Fiore, et al. (2003). "Distinct monoubiquitin signals in receptor endocytosis." Trends Biochem Sci 28(11): 598-603.

Halatsch, M. E., E. Gehrke, et al. (2003). "EGFR but not PDGFR-beta expression correlates to the antiproliferative effect of growth factor withdrawal in glioblastoma multiforme cell lines." Anticancer Res 23(3B): 2315-2320.

Haque, T., D. Faury, et al. (2007). "Gene expression profiling from formalin-fixed paraffin-embedded tumors of pediatric glioblastoma." Clin Cancer Res 13(21): 6284-6292.

Hargrave, D. (2009). "Paediatric high and low grade glioma: the impact of tumour biology on current and future therapy." Br J Neurosurg 23(4): 351-363.

Harterink, M., F. Port, et al. (2011). "A SNX3-dependent retromer pathway mediates retrograde transport of the Wnt sorting receptor Wntless and is required for Wnt secretion." Nat Cell Biol 13(8): 914-923.

Hegi, M. E., A. C. Diserens, et al. (2005). "MGMT gene silencing and benefit from temozolomide in glioblastoma." N Engl J Med 352(10): 997-1003.

Hoffmann, S., A. Burchert, et al. (2007). "Differential effects of cetuximab and AEE 788 on epidermal growth factor receptor (EGF-R) and vascular endothelial growth factor receptor (VEGF-R) in thyroid cancer cell lines." Endocrine 31(2): 105-113.

Holland, E. C. (2001). "Gliomagenesis: genetic alterations and mouse models." Nat Rev Genet 2(2): 120-129.

Holland, E. C., J. Celestino, et al. (2000). "Combined activation of Ras and Akt in neural progenitors induces glioblastoma formation in mice." Nat Genet 25(1): 55-57.

Holland, H., T. Koschny, et al. (2010). "WHO grade-specific comparative genomic hybridization pattern of astrocytoma - a meta-analysis." Pathol Res Pract 206(10): 663-668.

Huang, H., S. Colella, et al. (2000). "Gene expression profiling of low-grade diffuse astrocytomas by cDNA arrays." Cancer Res 60(24): 6868-6874.

Huang, P. H., A. M. Xu, et al. (2009). "Oncogenic EGFR signaling networks in glioma." Sci Signal 2(87): re6.

Huang, P. H., W. K. Cavenee, et al. (2007). "Uncovering therapeutic targets for glioblastoma: a systems biology approach." Cell Cycle 6(22): 2750-2754.

Huang, Z., L. Cheng, et al. (2010). "Cancer stem cells in glioblastoma--molecular signaling and therapeutic targeting." Protein Cell 1(7): 638-655.

Ishii, N., M. Tada, et al. (1999). "Cells with TP53 mutations in low grade astrocytic tumors evolve clonally to malignancy and are an unfavorable prognostic factor." Oncogene 18(43): 5870-5878.

Jackson, D. P., F. A. Lewis, et al. (1990). "Tissue extraction of DNA and RNA and analysis by the polymerase chain reaction." J Clin Pathol 43(6): 499-504.

Kabbarah, O., K. Pinto, et al. (2003). "Expression profiling of mouse endometrial cancers microdissected from ethanol-fixed, paraffin-embedded tissues." Am J Pathol 162(3): 755-762.

Karsten, S. L., V. M. Van Deerlin, et al. (2002). "An evaluation of tyramide signal amplification and archived fixed and frozen tissue in microarray gene expression analysis." Nucleic Acids Res 30(2): E4.

Kato, H., S. Kato, et al. (2000). "Functional evaluation of p53 and PTEN gene mutations in gliomas." Clin Cancer Res 6(10): 3937-3943.

Kerr, M. C., M. R. Lindsay, et al. (2006). "Visualisation of macropinosome maturation by the recruitment of sorting nexins." J Cell Sci 119(Pt 19): 3967-3980.

Kirisits, A., D. Pils, et al. (2007). "Epidermal growth factor receptor degradation: an alternative view of oncogenic pathways." Int J Biochem Cell Biol 39(12): 2173-2182.

Kleihues, P., D. N. Louis, et al. (2002). "The WHO classification of tumors of the nervous system." J Neuropathol Exp Neurol 61(3): 215-225; discussion 226-219.

Korbler, T., M. Grskovic, et al. (2003). "A simple method for RNA isolation from formalin-fixed and paraffin-embedded lymphatic tissues." Exp Mol Pathol 74(3): 336-340.

Kotliarov, Y., M. E. Steed, et al. (2006). "High-resolution Global Genomic Survey of 178 Gliomas Reveals Novel Regions of Copy Number Alteration and Allelic Imbalances." Cancer Res 66(19): 9428-9436.

Kreisberg, J. I., S. N. Malik, et al. (2004). "Phosphorylation of Akt (Ser473) is an excellent predictor of poor clinical outcome in prostate cancer." Cancer Res 64(15): 5232-5236.

Kurten, R. C. (2003). "Sorting motifs in receptor trafficking." Adv Drug Deliv Rev 55(11): 1405-1419.

Kuwano, M., T. Uchiumi, et al. (2003). "The basic and clinical implications of ABC transporters, Y-box-binding protein-1 (YB-1) and angiogenesis-related factors in human malignancies." Cancer Sci 94(1): 9-14.

Lai, A. Z., J. V. Abella, et al. (2009). "Crosstalk in Met receptor oncogenesis." Trends Cell Biol 19(10): 542-551.

Layfield, L. J., C. Willmore, et al. (2006). "Epidermal growth factor receptor gene amplification and protein expression in glioblastoma multiforme: prognostic significance and relationship to other prognostic factors." Appl Immunohistochem Mol Morphol 14(1): 91-96.

Lewis, F., N. J. Maughan, et al. (2001). "Unlocking the archive--gene expression in paraffin-embedded tissue." J Pathol 195(1): 66-71.

Li, Y., F. Guessous, et al. (2009). "Interactions between PTEN and the c-Met pathway in glioblastoma and implications for therapy." Mol Cancer Ther 8(2): 376-385.

Liang, Y., M. Diehn, et al. (2005). "Gene expression profiling reveals molecularly and clinically distinct subtypes of glioblastoma multiforme." Proc Natl Acad Sci U S A 102(16): 5814-5819.

Liu, H., Z. Q. Liu, et al. (2006). "Inhibitory regulation of EGF receptor degradation by sorting nexin 5." Biochem Biophys Res Commun 342(2): 537-546.

Louis, D. N., E. C. Holland, et al. (2001). "Glioma classification: a molecular reappraisal." Am J Pathol 159(3): 779-786.

Louis, D. N., H. Ohgaki, et al. (2007). "The 2007 WHO classification of tumours of the central nervous system." Acta Neuropathol 114(2): 97-109.

Lu, Z. H., J. T. Books, et al. (2005). "YB-1 is important for late-stage embryonic development, optimal cellular stress responses, and the prevention of premature senescence." Mol Cell Biol 25(11): 4625-4637.

Ma, X. J., R. Patel, et al. (2006). "Molecular classification of human cancers using a 92-gene real-time quantitative polymerase chain reaction assay." Arch Pathol Lab Med 130(4): 465-473.

Madshus, I. H. and E. Stang (2009). "Internalization and intracellular sorting of the EGF receptor: a model for understanding the mechanisms of receptor trafficking." J Cell Sci 122(Pt 19): 3433-3439.

Maher, E. A., C. Brennan, et al. (2006). "Marked genomic differences characterize primary and secondary glioblastoma subtypes and identify two distinct molecular and clinical secondary glioblastoma entities." Cancer Res 66(23): 11502-11513.

Maher, E. A., F. B. Furnari, et al. (2001). "Malignant glioma: genetics and biology of a grave matter." Genes Dev 15(11): 1311-1333.

Mariani, L., W. S. McDonough, et al. (2001). "Identification and validation of P311 as a glioblastoma invasion gene using laser capture microdissection." Cancer Res 61(10): 4190-4196.

Masuda, N., T. Ohnishi, et al. (1999). "Analysis of chemical modification of RNA from formalin-fixed samples and optimization of molecular biology applications for such samples." Nucleic Acids Res 27(22): 4436-4443.

McBride, S. M., D. A. Perez, et al. (2010). "Activation of PI3K/mTOR pathway occurs in most adult low-grade gliomas and predicts patient survival." J Neurooncol 97(1): 33-40.

McShane, M. P. and M. Zerial (2008). "Survival of the weakest: signaling aided by endosomes." J Cell Biol 182(5): 823-825.

Mellinghoff, I. K., M. Y. Wang, et al. (2005). "Molecular determinants of the response of glioblastomas to EGFR kinase inhibitors." N Engl J Med 353(19): 2012-2024.

Merchant, T. E., I. F. Pollack, et al. (2010). "Brain tumors across the age spectrum: biology, therapy, and late effects." Semin Radiat Oncol 20(1): 58-66.

Minor, J. M. (2006). "Microarray quality control." Methods Enzymol 411: 233-255.

Mischel, P. S. and T. F. Cloughesy (2003). "Targeted molecular therapy of GBM." Brain Pathol 13(1): 52-61.

Mischel, P. S., R. Shai, et al. (2003). "Identification of molecular subtypes of glioblastoma by gene expression profiling." Oncogene 22(15): 2361-2373.

Mischel, P. S., S. F. Nelson, et al. (2003). "Molecular analysis of glioblastoma: pathway profiling and its implications for patient therapy." Cancer Biol Ther 2(3): 242-247.

Mizutani, R., J. Yamauchi, et al. (2009). "Sorting nexin 3, a protein upregulated by lithium, contains a novel phosphatidylinositol-binding sequence and mediates neurite outgrowth in N1E-115 cells." Cell Signal 21(11): 1586-1594.

Mosesson, Y., G. B. Mills, et al. (2008). "Derailed endocytosis: an emerging feature of cancer." Nat Rev Cancer 8(11): 835-850.

Mueller, K. L., L. A. Hunter, et al. (2008). "Met and c-Src cooperate to compensate for loss of epidermal growth factor receptor kinase activity in breast cancer cells." Cancer Res 68(9): 3314-3322.

Mueller, S. and S. Chang (2009). "Pediatric brain tumors: current treatment strategies and future therapeutic approaches." Neurotherapeutics 6(3): 570-586.

Nakamura, M., K. Shimada, et al. (2007). "Molecular pathogenesis of pediatric astrocytic tumors." Neuro Oncol 9(2): 113-123.

Nicholas, M. K. (2007). "Glioblastoma multiforme: evidence-based approach to therapy." Expert Rev Anticancer Ther 7(12 Suppl): S23-27.

Nobusawa, S., T. Watanabe, et al. (2009). "IDH1 mutations as molecular signature and predictive factor of secondary glioblastomas." Clin Cancer Res 15(19): 6002-6007.

Noushmehr, H., D. J. Weisenberger, et al. "Identification of a CpG island methylator phenotype that defines a distinct subgroup of glioma." Cancer Cell 17(5): 510-522.

Nutt, C. L., D. R. Mani, et al. (2003). "Gene expression-based classification of malignant gliomas correlates better with survival than histological classification." Cancer Res 63(7): 1602-1607.

Ohgaki, H. and P. Kleihues (2007). "Genetic pathways to primary and secondary glioblastoma." Am J Pathol 170(5): 1445-1453.

Orr, L. C., J. Fleitz, et al. (2002). "Cytogenetics in pediatric low-grade astrocytomas." Med Pediatr Oncol 38(3): 173-177.

Packer, R. J. (1999). "Primary Central Nervous System Tumors in Children." Curr Treat Options Neurol 1(5): 395-408.

Pagedar, N. A., W. Wang, et al. (2006). "Gene expression analysis of distinct populations of cells isolated from mouse and human inner ear FFPE tissue using laser capture microdissection--a technical report based on preliminary findings." Brain Res 1091(1): 289-299.

Parsa, A. T. and E. C. Holland (2004). "Cooperative translational control of gene expression by Ras and Akt in cancer." Trends Mol Med 10(12): 607-613.

Parsons, D. W., S. Jones, et al. (2008). "An integrated genomic analysis of human glioblastoma multiforme." Science 321(5897): 1807-1812.

Patterson, T. A., E. K. Lobenhofer, et al. (2006). "Performance comparison of one-color and two-color platforms within the MicroArray Quality Control (MAQC) project." Nat Biotechnol 24(9): 1140-1150.

Paugh, B. S., C. Qu, et al. (2010). "Integrated molecular genetic profiling of pediatric high-grade gliomas reveals key differences with the adult disease." J Clin Oncol 28(18): 3061-3068.

Penland, S. K., T. O. Keku, et al. (2007). "RNA expression analysis of formalin-fixed paraffin-embedded tumors." Lab Invest 87(4): 383-391.

Petalidis, L. P., A. Oulas, et al. (2008). "Improved grading and survival prediction of human astrocytic brain tumors by artificial neural network analysis of gene expression microarray data." Mol Cancer Ther 7(5): 1013-1024.

Phillips, H. S., S. Kharbanda, et al. (2006). "Molecular subclasses of high-grade glioma predict prognosis, delineate a pattern of disease progression, and resemble stages in neurogenesis." Cancer Cell 9(3): 157-173.

Phillips, S. A., V. A. Barr, et al. (2001). "Identification and characterization of SNX15, a novel sorting nexin involved in protein trafficking." J Biol Chem 276(7): 5074-5084.

Pochampalli, M. R., R. M. el Bejjani, et al. (2007). "MUC1 is a novel regulator of ErbB1 receptor trafficking." Oncogene 26(12): 1693-1701.

Polacek, D. C., A. G. Passerini, et al. (2003). "Fidelity and enhanced sensitivity of differential transcription profiles following linear amplification of nanogram amounts of endothelial mRNA." Physiol Genomics 13(2): 147-156.

Pollack, I. F. (1999). "Pediatric brain tumors." Semin Surg Oncol 16(2): 73-90.

Pollack, I. F. (1999). "The role of surgery in pediatric gliomas." J Neurooncol 42(3): 271-288.

Pollack, I. F., R. L. Hamilton, et al. (1997). "The relationship between TP53 mutations and overexpression of p53 and prognosis in malignant gliomas of childhood." Cancer Res 57(2): 304-309.

Pollack, I. F., R. L. Hamilton, et al. (2002). "Molecular abnormalities and correlations with tumor response and outcome in glioma patients." Neuroimaging Clin N Am 12(4): 627-639.

Pollack, I. F., R. L. Hamilton, et al. (2006). "Rarity of PTEN deletions and EGFR amplification in malignant gliomas of childhood: results from the Children's Cancer Group 945 cohort." J Neurosurg 105(5 Suppl): 418-424.

Pollack, I. F., R. L. Hamilton, et al. (2011). "IDH1 mutations are common in malignant gliomas arising in adolescents: a report from the Children's Oncology Group." Childs Nerv Syst 27(1): 87-94.

Pollack, I. F., S. D. Finkelstein, et al. (2001). "Age and TP53 mutation frequency in childhood malignant gliomas: results in a multi-institutional cohort." Cancer Res 61(20): 7404-7407.

Pollack, I. F., S. D. Finkelstein, et al. (2002). "Expression of p53 and prognosis in children with malignant gliomas." N Engl J Med 346(6): 420-427.

Pons, V., P. P. Luyet, et al. (2008). "Hrs and SNX3 functions in sorting and membrane invagination within multivesicular bodies." PLoS Biol 6(9): e214.

Puli, S., A. Jain, et al. (2010). "Effect of combination treatment of rapamycin and isoflavones on mTOR pathway in human glioblastoma (U87) cells." Neurochem Res 35(7): 986-993.

Purow, B. and D. Schiff (2009). "Advances in the genetics of glioblastoma: are we reaching critical mass?" Nat Rev Neurol 5(8): 419-426.

Pytel, P. (2007). "Spectrum of pediatric gliomas: implications for the development of future therapies." Expert Rev Anticancer Ther 7(12 Suppl): S51-60.

Qu, H., K. Jacob, et al. (2008). "Genome–wide profiling using Single Nucleotide Polymorphism Arrays identifies distinct chromosomal imbalances in Pediatric and Adult High-Grade Astrocytomas. ." Cancer research submitted.

Raica, M., A. M. Cimpean, et al. (2011). "Lymphatic microvessel density, VEGF-C, and VEGFR-3 expression in different molecular types of breast cancer." Anticancer Res 31(5): 1757-1764.

Rajasekhar, V. K., A. Viale, et al. (2003). "Oncogenic Ras and Akt signaling contribute to glioblastoma formation by differential recruitment of existing mRNAs to polysomes." Mol Cell 12(4): 889-901.

Reznik, T. E., Y. Sang, et al. (2008). "Transcription-dependent epidermal growth factor receptor activation by hepatocyte growth factor." Mol Cancer Res 6(1): 139-150.

Rich, J. N., C. Hans, et al. (2005). "Gene expression profiling and genetic markers in glioblastoma survival." Cancer Res 65(10): 4051-4058.

Rickert, C. H., R. Strater, et al. (2001). "Pediatric high-grade astrocytomas show chromosomal imbalances distinct from adult cases." Am J Pathol 158(4): 1525-1532.

Rickman, D. S., M. P. Bobek, et al. (2001). "Distinctive molecular profiles of high-grade and low-grade gliomas based on oligonucleotide microarray analysis." Cancer Res 61(18): 6885-6891.

Roepstorff, K., L. Grovdal, et al. (2008). "Endocytic downregulation of ErbB receptors: mechanisms and relevance in cancer." Histochem Cell Biol 129(5): 563-578.

Roepstorff, K., M. V. Grandal, et al. (2009). "Differential effects of EGFR ligands on endocytic sorting of the receptor." Traffic 10(8): 1115-1127.

Rood, B. R. and T. J. Macdonald (2005). "Pediatric high-grade glioma: molecular genetic clues for innovative therapeutic approaches." J Neurooncol.

Rutka, J. T., J. S. Kuo, et al. (2004). "Advances in the treatment of pediatric brain tumors." Expert Rev Neurother 4(5): 879-893.

Sanai, N., A. Alvarez-Buylla, et al. (2005). "Neural stem cells and the origin of gliomas." N Engl J Med 353(8): 811-822.

Sansal, I. and W. R. Sellers (2004). "The biology and clinical relevance of the PTEN tumor suppressor pathway." J Clin Oncol 22(14): 2954-2963.

Saran, F. (2002). "Recent advances in paediatric neuro-oncology." Curr Opin Neurol 15(6): 671-677.

Schmidt, M. C., S. Antweiler, et al. (2002). "Impact of genotype and morphology on the prognosis of glioblastoma." J Neuropathol Exp Neurol 61(4): 321-328.

Seet, L. F. and W. Hong (2006). "The Phox (PX) domain proteins and membrane traffic." Biochim Biophys Acta 1761(8): 878-896.

Segal, E., N. Friedman, et al. (2004). "A module map showing conditional activity of expression modules in cancer." Nat Genet 36(10): 1090-1098.

Segal, E., N. Friedman, et al. (2005). "From signatures to models: understanding cancer using microarrays." Nat Genet 37 Suppl: S38-45.

Shi, L., L. H. Reid, et al. (2006). "The MicroArray Quality Control (MAQC) project shows inter- and intraplatform reproducibility of gene expression measurements." Nat Biotechnol 24(9): 1151-1161.

Singh, S. K., I. D. Clarke, et al. (2003). "Identification of a cancer stem cell in human brain tumors." Cancer Res 63(18): 5821-5828.

Smith, J. S., I. Tachibana, et al. (2001). "PTEN mutation, EGFR amplification, and outcome in patients with anaplastic astrocytoma and glioblastoma multiforme." J Natl Cancer Inst 93(16): 1246-1256.

Specht, K., T. Richter, et al. (2001). "Quantitative gene expression analysis in microdissected archival formalin-fixed and paraffin-embedded tumor tissue." Am J Pathol 158(2): 419-429.

Stanta, G., S. Bonin, et al. (1998). "RNA extraction from formalin-fixed and paraffin-embedded tissues." Methods Mol Biol 86: 23-26.

Steg, A., W. Wang, et al. (2006). "Multiple gene expression analyses in paraffin-embedded tissues by TaqMan low-density array: Application to hedgehog and Wnt pathway analysis in ovarian endometrioid adenocarcinoma." J Mol Diagn 8(1): 76-83.

Stommel, J. M., A. C. Kimmelman, et al. (2007). "Coactivation of receptor tyrosine kinases affects the response of tumor cells to targeted therapies." Science 318(5848): 287-290.

Sul, J. and H. A. Fine (2010). "Malignant gliomas: new translational therapies." Mt Sinai J Med 77(6): 655-666.

Sunayama, J., A. Sato, et al. (2010). "Dual blocking of mTor and PI3K elicits a prodifferentiation effect on glioblastoma stem-like cells." Neuro Oncol 12(12): 1205-1219.

Sunayama, J., K. Matsuda, et al. (2010). "Crosstalk between the PI3K/mTOR and MEK/ERK pathways involved in the maintenance of self-renewal and tumorigenicity of glioblastoma stem-like cells." Stem Cells 28(11): 1930-1939.

Sutherland, B. W., J. Kucab, et al. (2005). "Akt phosphorylates the Y-box binding protein 1 at Ser102 located in the cold shock domain and affects the anchorage-independent growth of breast cancer cells." Oncogene 24(26): 4281-4292.

Toedt, G., S. Barbus, et al. (2011). "Molecular signatures classify astrocytic gliomas by IDH1 mutation status." Int J Cancer 128(5): 1095-1103.

Tothill, R. W., A. Kowalczyk, et al. (2005). "An expression-based site of origin diagnostic method designed for clinical application to cancer of unknown origin." Cancer Res 65(10): 4031-4040.

Tso, C. L., W. A. Freije, et al. (2006). "Distinct transcription profiles of primary and secondary glioblastoma subgroups." Cancer Res 66(1): 159-167.

van Weering, J. R., P. Verkade, et al. (2010). "SNX-BAR proteins in phosphoinositide-mediated, tubular-based endosomal sorting." Semin Cell Dev Biol 21(4): 371-380.

Verhaak, R. G., K. A. Hoadley, et al. (2010). "Integrated genomic analysis identifies clinically relevant subtypes of glioblastoma characterized by abnormalities in PDGFRA, IDH1, EGFR, and NF1." Cancer Cell 17(1): 98-110.

Walch, A., K. Specht, et al. (2001). "Tissue microdissection techniques in quantitative genome and gene expression analyses." Histochem Cell Biol 115(4): 269-276.

Wang, R., K. Chadalavada, et al. (2010). "Glioblastoma stem-like cells give rise to tumour endothelium." Nature 468(7325): 829-833.

Watanabe, H., F. Tanaka, et al. (2000). "Differential somatic CAG repeat instability in variable brain cell lineage in dentatorubral pallidoluysian atrophy (DRPLA): a laser-captured microdissection (LCM)-based analysis." Hum Genet 107(5): 452-457.

Weller, M., J. Felsberg, et al. (2009). "Molecular predictors of progression-free and overall survival in patients with newly diagnosed glioblastoma: a prospective translational study of the German Glioma Network." J Clin Oncol 27(34): 5743-5750.

Wiley, H. S. and P. M. Burke (2001). "Regulation of receptor tyrosine kinase signaling by endocytic trafficking." Traffic 2(1): 12-18.

Worby, C. A. and J. E. Dixon (2002). "Sorting out the cellular functions of sorting nexins." Nat Rev Mol Cell Biol 3(12): 919-931.

Wu, J., C. Lee, et al. (2006). "Disruption of the Y-box binding protein-1 results in suppression of the epidermal growth factor receptor and HER-2." Cancer Res 66(9): 4872-4879.

Xu, Y., H. Hortsman, et al. (2001). "SNX3 regulates endosomal function through its PX-domain-mediated interaction with PtdIns(3)P." Nat Cell Biol 3(7): 658-666.

Xu, Y., L. F. Seet, et al. (2001). "The Phox homology (PX) domain, a new player in phosphoinositide signalling." Biochem J 360(Pt 3): 513-530.

Yan, H., D. W. Parsons, et al. (2009). "IDH1 and IDH2 mutations in gliomas." N Engl J Med 360(8): 765-773.

Yim, S. H., J. M. Ward, et al. (2003). "Microarray analysis using amplified mRNA from laser capture microdissection of microscopic hepatocellular precancerous lesions and frozen hepatocellular carcinomas reveals unique and consistent gene expression profiles." Toxicol Pathol 31(3): 295-303.

Zeeberg, B. R., W. Feng, et al. (2003). "GoMiner: a resource for biological interpretation of genomic and proteomic data." Genome Biol 4(4): R28.

Zheng, H., H. Ying, et al. (2008). "p53 and Pten control neural and glioma stem/progenitor cell renewal and differentiation." Nature 455(7216): 1129-1133.

Zhong, Q., C. S. Lazar, et al. (2002). "Endosomal localization and function of sorting nexin 1." Proc Natl Acad Sci U S A 99(10): 6767-6772.

Zhou, Y. H., F. Tan, et al. (2003). "The expression of PAX6, PTEN, vascular endothelial growth factor, and epidermal growth factor receptor in gliomas: relationship to tumor grade and survival." Clin Cancer Res 9(9): 3369-3375.

Zhu, Y. and L. F. Parada (2002). "The molecular and genetic basis of neurological tumours." Nat Rev Cancer 2(8): 616-626.